# STRUCTURE-FUNCTION ANALYSIS OF THE β SUBUNIT OF NEURONAL NICOTINIC ACETYLCHOLINE RECEPTORS

Thesis by

Antonio Figl

In Partial Fulfillment of the Requirements for the Degree of

Doctor of Philosophy

California Institute of Technology

Pasadena, California

1996

(Submitted June 14, 1995)

# Acknowledgments

My deepest thanks I extend toward all postdocs in the Lester-Davidson lab, especially Bruce Cohen for being a good friend and collaborator in the past, present and future; Mike Quick for his unique wit and being able to keep me going when nothing else could; Craig Doupnik for always listening and (more importantly) explaining.

Moreover, I thank Cesar Labarca for teaching me the little I know about life, liberty and molecular biology;

the many wonderful people in the Lester lab for being who they are: Purnima, Linda, John, Haiyun, Jennifer, Beth, Al, Markus, Mary, Janis, Mark, Nael, Stefan and whoever else I may have forgotten. It would not have been the same without you!

Many special thanks to Henry Lester who finally threw up his hands and let me graduate.

I also would like to acknowledge everyone else who made a difference in my life during my extended tenure at Caltech; thank you.

## ABSTRACT

Nicotinic receptors belong to the superfamily of ligand-gated ion channels. Since evidence was rapidly accumulating implicating the non-α subunits in ligand-binding events, we decided to investigate eventual contributions of the neuronal β subunit to these events by performing a series of increasingly detailed experiments on a series of chimeric β subunits. In the first set of experiments, we constructed a variety of chimeric β subunits consisting of $NH_2$-terminal neuronal β4 sequences and COOH-terminal β2 sequences and expressed them with the α3 subunit in *Xenopus* oocytes. The results showed that (*a*) two residues in the extracellular domain of chimeric β4•β2 subunits (108β2Phe↔β4Val, 110β2Ser↔β4Thr) account for much of the relative cytisine sensitivity; and (*b*) four extracellular residues of chimeric β4•β2 subunits (112β2Ala↔β4Val, 113β2Val↔β4Ile and 115β2Ser↔β4Arg, 116β2Tyr↔β4Ser) account for most of the relative tetramethylammonium sensitivity.

Encouraged by the above results, we continued our experiments with additional chimeras of the β2 and β4 neuronal nicotinic subunits to locate regions that contribute to differences between the acetylcholine dose-response relationships of α3β2 and α3β4 receptors. Substitutions within the first 120 residues convert the $EC_{50}$ for ACh from one wild-type value to the other, suggesting that amino acids within the first 120 residues of β2 and the corresponding region of β4 contribute to an agonist binding site that bridges the α and β subunits in neuronal nicotinic receptors.

Since the $EC_{50}$ phenotypes caused by the β2 and β4 subunits could be due to a difference in gating or binding properties, we attempted to unravel this question by performing voltage-jump relaxations for the series of neuronal nicotinic acetylcholine receptors we constructed previously. The chimeric β4/β2 subunits showed a transition in the concentration dependence of the relaxation rate constants in the region between residues 94 and 109, analogous to our previous observation with steady-state dose-response relationships. The data reinforce previous conclusions that the region between residues 94 and 109 on the β subunit plays a role in binding agonist but also show that other regions of the receptor control gating kinetics subsequent to the binding step.

# Table of Contents

# INTRODUCTION

## *General Remarks*

Acetylcholine receptors exist in two classes: metabotropic (linked to a G-protein pathway) and ionotropic (binding site and ion channel are part of the same protein). The latter class can be further subdivided into muscle-like receptors (reviewed in Changeux , Benoit, Bessis, Cartaud, Devillers-Thiery, Fontaine, Galzi, Klarsfled, and Laufer, 1990; Changeux, Devillers-Thiery, Galzi, and Bertrand, 1992a; Changeux, Galzi, Devillers-Thiery, and Bertrand, 1992c; Changeux, 1993; Karlin, 1993) and neuronal receptors (reviewed in Deneris, Connolly, Rogers, and Duvoisin, 1991; Role, 1992; Sargent, 1993). This project will deal with the latter group of receptors.

To date, a variety of neuronal-specific nicotinic acetylcholine receptors (nAChRs) have been cloned and characterized (Role, 1992). Muscle receptors require two alpha, and one each of beta, gamma (or epsilon in adult tissues) and delta subunits to form functional pentameric channels. The neuronal receptors exist in a variety of forms. At present the list consists of eight separate genes encoding alpha-like subunits and three beta-like subunits mostly cloned from rodents or chicks. $\alpha 2$, $\alpha 3$ and $\alpha 4$ (Boulter, Evans, Goldman, Martin, Treco, Heinemann, and Patrick, 1986; Boulter, Connolly, Deneris, Goldman, Heinemann, and Patrick, 1987) require co-expression with beta subunits (Deneris, Connolly, Boulter, Wada, Wada, Swanson, Patrick, and Heinemann, 1988;

Deneris, Boulter, Swanson, Patrick, and Heinemann, 1989; Duvoisin, Deneris, Patrick, and Heinemann, 1989) to form functional channels in *Xenopus* oocytes. α5, although present *in vivo* (Conroy, Vernallis, and Berg, 1992), has not been fully characterized since it does not form functional channels when co-injected with the beta subunits. α6 and β3's functions have not been elucidated yet. α7, α8 and α9 (Couturier, Bertrand, Matter, Hernandez, Bertrand, Millar, Valera, Barkas, and Ballivet, 1990; Elgoyhen, Johnson, Boulter, Vetter, and Heinemann, 1994) all can form homomeric channels in *Xenopus* oocytes.

These nAChRs are found in the central and peripheral nervous systems. In the brain, radioactive agonists have mapped nicotinic sites in the cerebral cortex, hypothalamus, hippocampus, interpeduncular nucleus and superior culliculus (Clarke, Schwartz, Paul, Pert, and Pert, 1985). Antibody staining for specific subunits has found β2 subunit distribution throughout the brain (Swanson, Simmons, Whiting, and Lindstrom, 1987), and α7 distribution to vary somewhat from that of β2 and correspond largely to α-bungarotoxin (α-Btx) sites (Britto, Hamassakibritto, Ferro, Keyser, Karten, and Lindstrom, 1992). Northern blots and *in situ* hybridization were able to map the distribution of several subunits within the CNS (Seguela, Wadiche, Dineley-Miller, Dani, and Patrick, 1993). The α4 subunit seems to be expressed strongly in many areas, α2 and α3 are both expressed to a lesser degree in the rat brain (Seguela et al., 1993). The β2 subunit is also detected strongly, overlapping largely with α4 expression (Deneris et al., 1988). β4 expression seems to be limited to the medial habenula (Duvoisin et al., 1989),

although low levels can be detected in many more areas (Dineley-Miller and Patrick, 1992).

Distribution of neuronal genes at the single-cell level in peripheral nervous system neurons has yielded complex results. Chick E11 sympathetic neurons express a wide variety of neuronal genes, including α3, α5, α7 and β4 (Devay, Qu, and Role, 1994). Rat chromaffin cells express a similar spectrum of subunits, including low levels of β2 (Lambolez, Audinat, Bochet, Crepel, and Rossier, 1992). In individual intracardiac parasympathetic neurons, determined by RT-single cell PCR, the view is even messier. Expression appears to vary among individual neurons. Some express two subunits (e.g., α3 and β4), whereas others express a complex pattern of genes (e.g., α2, α3, α4, α7 and β2 or α3, α7, β2, β3 and β4) (Corriveau and Berg, 1993).

Pharmacologically, different combinations of subunits, when expressed in frog oocytes, yield unique agonist sensitivities (Luetje and Patrick, 1991) as well as sensitivities to neurotoxins (Luetje, Wada, Rogers, Abramson, Tsuji, Heinemann, and Patrick, 1990). It is perhaps surprising to note that the beta subunit appears to have as much effect as the alpha subunit in determining agonist potencies.

## *Structure-function Work*

It is no exaggeration to claim that the muscle nAChR is the most-studied ligand-gated receptor. Neuronal genes lag behind in this study. We are fortunate however, that the

primary sequences of these two ion channel types share a high degree of homology, making it possible to extend the findings of one class to the other. Examination of the amino acid sequence reveals the presence of three distinct domains (reviewed in Changeux et al., 1992a; Changeux, Devillers-Thiery, Galzi, and Revah, 1992b; Changeux et al., 1992c): a large extracellular $NH_2$-terminus that comprises nearly half of the mature protein and contains the agonist binding site in the alpha subunit, four highly conserved putative transmembrane segments and an intracellular loop of uncertain function linking the third and fourth transmembrane regions. A large amount of work has been done on the first two domains; because of its difference among subunits, the intracellular loop's function has remained a mystery.

*Extracellular Segment*

There is a large body of evidence implicating the large extracellular segment in ligand-binding (reviewed in Changeux et al., 1992c; Changeux, 1993). In the *Torpedo* alpha subunit, a close cousin of the muscle subunits, at least six residues have consistently been labeled by affinity ligands. Three are Tyr residues, at positions 93 (Galzi, Revah, Black, Goeldner, Hirth, and Changeux, 1990), 190 (Dennis, Giraudat, Kotzyba-Hibert, Goeldner, Hirth, Chang, Lazure, Chretien, and Changeux, 1988; Abramson, Li, Culver, and Taylor, 1989) and 198 (Middleton and Cohen, 1991). A Trp residue at position 149 (Dennis et al., 1988) and two characteristic cysteines at positions 192 and 193 (Kao, Dwork, Kaldany, Silver, Wideman, Stein, and Karlin, 1984; Dennis et al., 1988) are further

typically labeled amino acids. All these residues are conserved in all functional muscle and neuronal subunits. Although similar detailed studies using affinity agents have not been performed with neuronal subunits, it is safe to extrapolate that all above residues serve an analogous function in neuronal alpha subunits.

Recent experiments with *d*-tubocurarine (*d*-TC), a competitive antagonist, have detected labeling of non-alpha subunits, suggesting that the binding site may span beyond the confines of the alpha subunits (Fu and Sine, 1994). It is known that neuronal beta subunits have a significant effect on agonist sensitivities (Luetje et al., 1991). It is unclear whether this effect is mediated allosterically through the alpha subunits or whether the beta subunits contribute *bona fide* residues to the agonist binding site.

*Channel Structure*

The second transmembrane segment M2 is now generally thought to form the ion channel pathway. Non-competitive inhibitors, thought to enter the pore when the channel is open, have labeled several residues of *Torpedo* M2 segments. Some of these agents include chlorpromazine (Giraudat, Dennis, Heidmann, Chang, and Changeux, 1986; Giraudat, Dennis, Heidmann, Haumont, Lederer, and Changeux, 1987; Giraudat, Galzi, Revah, Changeux, Haumont, and Lederer, 1989), trimethylphosphonium (Hucho, Oberthur, and Lottspeich, 1986) and 3-(trifluoromethyl)-3-(m-iodophenyl)diazirine (TID) (White, Howard, Cohen, and Cohen, 1991; White and Cohen, 1992). Mutagenesis of residues in this segment has provided elegant evidence that residues in it are lining the

pore. Imoto *et al.* (1988) changed charged residues flanking M2; they determined that mutations of these amino acids to neutral residues changed the channel conductance proportionally to the reduction in negative charge (Imoto, Busch, Sakmann, Mishina, Konno, Nakai, Bujo, Mori, Fukuda, and Numa 1988). Changes of hydrophobic residues within M2 to larger or more hydrophobic amino acids decreased the conductance of larger cations (Villarroel, Herlitze, Witzemann, Koenen, and Sakmann, 1992) and organic cations (Cohen, Labarca, Czyzyk, Davidson, and Lester, 1992a; Cohen, Labarca, Davidson, and Lester, 1992b). The association rate of the open channel blocker QX-222 was also affected by mutations in M2 (Leonard, Yu, Labarca, Davidson, and Lester, 1987; Leonard, Labarca, Charnet, Davidson, and Lester, 1988). Akabas *et al.* (1992) mutated consecutive residues in M2 to Cys and the accessibility of the cysteines was assayed by applying sulfhydryl-sensitive reagents (Akabas, Stauffer, Xu, and Karlin, 1992). The surprising finding of this work was the accessibility of position 248 to the reagents when the channel was not activated by ACh. This implies that the gate is very close to the cytoplasmic end of the M2 helix. However, this finding was later challenged by three-dimensional electron micrograph reconstructions of tubular *Torpedo* nAChR crystals by Unwin (Unwin, 1993; Unwin, 1995).

The cloning of the homooligomeric $\alpha 7$ subunit (Couturier et al., 1990; Seguela et al., 1993) has renewed the interest in nAChRs. Because of its nature, it was possible to do experiments that could not be performed on muscle subunits. The ability of making a single mutation that is incorporated five times in the pentamer has led to dramatic

advances in at least three areas. Mutating a highly conserved Leu residue in the second transmembrane helix led to startling effects on many channel properties. The desensitization and half-maximal dose of activation levels were altered (Revah, Bertrand, Galzi, Devillers-Thiery, Mulle, Hussy, Bertrand, Ballivet, and Changeux, 1991) and compounds that act as competitive antagonists in the wild-type $\alpha 7$ oligomer started acting as agonists (Bertrand, Devillers-Thiery, Revah, Galzi, Hussy, Mulle, Bertrand, Ballivet, and Changeux, 1992). A few select mutations within M2 led to a change in permeability properties of the channel from cationic to anionic (Galzi, Devillers-Thiery, Hussy, Bertrand, Changeux, and Bertrand, 1992). Furthermore, the modularity of the receptors was shown when the large extracellular $NH_2$-terminal segment of $\alpha 7$ was deleted and replaced with the analogous portion of the serotonergic $5HT_3$ receptor (Eisele, Bertrand, Galzi, Devillers-Thiery, Changeux, and Bertrand, 1993). This chimeric receptor showed distinct ligand-binding and channel specificities.

## *Experimental Background*

Much of the work regarding agonist-receptor interactions has focused on the alpha subunit of nAChRs. From the work of Luetje and Patrick (1991), we were encouraged to find a report highlighting the importance of heretofore largely unstudied beta subunits in determining agonist potencies at neuronal nAChRs. We therefore embarked in a series of experiments designed to further our knowledge of the exact role of the beta subunit in

contributing to the pharmacological profiles of agonists. β2 and β4 are highly similar (~80% amino acid identity) yet show remarkable differences in their ability to open channels with different agonists when expressed along with the α3 subunit in *Xenopus* oocytes. With a series of three sets of experiments of increasing difficulty and resolution we attempted to find regions of the beta subunits that were responsible for agonist potency differences and other effects we later determined were also affected by the type of beta subunit.

The first, and simplest series of experiments entailed the construction of chimeric beta subunits assayed by single doses of four agonists: acetylcholine (ACh), cytisine (CYT), tetramethylammonium (TMA), and nicotine (NIC). It can be gleaned from Fig. 1 that these four agonists represent a varied set of chemical structures, from the "minimal" agonist TMA containing only a quaternary ammonium moiety, to NIC with multiple rings and aromatic structures. It was our belief that because of their different structures we might have been able to dissect in greater detail eventual amino acids that contact various parts of the molecules. Most of these agonists were very sensitive to the type of beta subunit present, with the β2 subunit having generally quite lower efficacies to these compounds compared to β4. The analysis of our findings are found in chapter one.

Encouraged by the results of our first series of experiments, we embarked on a set of more ambitious data acquisition projects designed to focus our attention on the effect of the native agonist (ACh) on the chimeras we constructed. Our aim was to dissect a wider set of parameters under a more stringent set of conditions. In order to accomplish

this we designed an improved data acquisition protocol (a faster perfusion system) and distilled information from many dose-response relations from the many beta-subunit chimeras we had constructed. The results from this project are found in chapter two.

Finally, to improve on our steady-state measurements from dose-response relations, we designed a set of experiments designed to obtain kinetic parameters from voltage-perturbation measurements. The results of these experiments forms the third and last chapter of the thesis.

*Summary*

Throughout our experiments we have constantly identified a region in the beta subunits from amino acids 94 to 120 as having a crucial role in determining all phenotypes we investigated. Although the most recent structural evidence appears to discount a direct participation of the beta subunits in sharing an agonist binding site with alpha subunits (Unwin, 1995), our experiments suggest that the beta subunit can in fact affect the binding process. The most straightforward explanations of this apparent paradox are (*a*) the agonist molecule has to contact beta-subunit residues at the "mouth" of a gorge before reaching the *de facto* binding site, thereby affecting agonist on/off rates and consequently the binding constant; or (*b*) the beta subunit allosterically alters the structure of the binding site. More detailed structural work is necessary to resolve these issues.

# REFERENCES

Abramson, S. N., Y. Li, P. Culver, and P. Taylor. 1989. An analog of lophotoxin reacts covalently with Tyr190 in the alpha subunit of the nicotinic acetylcholine receptor. *The Journal of Biological Chemistry.* 264: 12666-12672.

Akabas, M. H., D. A. Stauffer, M. Xu, and A. Karlin. 1992. Acetylcholine receptor channel structure probed in cysteine-substitution mutants. *Science* 258: 307-310.

Bertrand, D., A. Devillers-Thiery, F. Revah, J.-L. Galzi, N. Hussy, C. Mulle, S. Bertrand, M. Ballivet, and J.-P. Changeux. 1992. Unconventional pharmacology of a neuronal nicotinic receptor mutated in the channel domain. *Proceedings of the National Academy of Sciences, USA.* 89: 1261-1265.

Boulter, J., J. Connolly, E. Deneris, D. Goldman, S. Heinemann, and J. Patrick. 1987. Functional expression of two neuronal nicotinic acetylcholine receptors from cDNA clones identifies a gene family. *Proceedings of the National Academy of Sciences, USA.* 84: 7763-7767.

Boulter, J., K. Evans, D. Goldman, G. Martin, D. Treco, S. Heinemann, and J. Patrick. 1986. Isolation of a cDNA clone coding for a possible neural nicotinic acetylcholine receptor α-subunit. *Nature.* 319: 368-370.

Britto, L. R. G., D. E. Hamassakibritto, E. S. Ferro, K. T. Keyser, H. J. Karten, and J. M. Lindstrom. 1992. Neurons of the chick brain and retina expressing both α-

bungarotoxin sensitive and α-bungarotoxin insensitive nicotinic acetylcholine receptors - an immunohistochemical analysis. *Brain Research.* 590: 193-200.

Changeux, J.-P. 1993. Chemical signaling in the brain. *Scientific American.* 269: 58-79.

Changeux, J.-P., P. Benoit, A. Bessis, J. Cartaud, A. Devillers-Thiery, B. Fontaine, J.-L. Galzi, A. Klarsfled, and R. Laufer. 1990. The acetylcholine receptor: functional architecture and regulation. *Advances in Second Messenger and Phosphoprotein Research.* 24: 15-19.

Changeux, J.-P., A. Devillers-Thiery, J.-L. Galzi, and D. Bertrand. 1992a. New mutants to explore nicotinic receptor functions. *Trends in Pharmacological Sciences.* 13: 299-301.

Changeux, J.-P., A. Devillers-Thiery, J.-L. Galzi, and F. Revah. 1992b. The acetylcholine receptor: a model af an allosteric membrane protein mediating intercellular communication. *CIBA Foundation Symposia.* 164: 66-97.

Changeux, J.-P., J.-L. Galzi, A. Devillers-Thiery, and D. Bertrand. 1992c. The functional architecture of the acetylcholine nicotinic receptor explored by affinity labeling and site-directed mutagenesis. *Quarterly Reviews of Biophysics.* 25: 395-432.

Clarke, P. B. S., R. D. Schwartz, S. M. Paul, C. B. Pert, and A. Pert. 1985. Nicotinic binding in rat brain: autoradiographic comparison of [$^3$H] acetylcholine, [$^3$H] nicotine, and [$^{125}$I] α-bungarotoxin. *The Journal of Neuroscience.* 5: 1307-1315.

Cohen, B. N., C. Labarca, L. Czyzyk, N. Davidson, and H. A. Lester. 1992a. $TRIS^+/Na^+$ permeability ratios of nicotinic acetylcholine receptors are reduced by mutations

near the intracellular end of the M2 region. *Journal of General Physiology.* 450: 545-572.

Cohen, B. N., C. Labarca, N. Davidson, and H. A. Lester. 1992b. Mutations in M2 alter the selectivity of the mouse nicotinic acetylcholine receptor for organic and for alkali metal cations. *Journal of General Physiology.* 100: 373-400.

Conroy, W. G., A. B. Vernallis, and D. K. Berg. 1992. The α5 gene product assembles with multiple acetylcholine receptor subunits to form distinctive receptor subtypes in brain. *Neuron.* 9: 679-691.

Corriveau, R. A., and D. K. Berg. 1993. Coexpression of multiple acetylcholine receptor genes in neurons: quantification of transcripts during development. *The Journal of Neuroscience.* 13: 2662-2671.

Couturier, S., D. Bertrand, J.-M. Matter, M.-C. Hernandez, S. Bertrand, N. Millar, S. Valera, T. Barkas, and M. Ballivet. 1990. A neuronal nicotinic acetylcholine receptor subunit (α7) is developmentally regulated and forms a homo-oligomeric channel blocked by α-BTX. *Neuron.* 5: 847-856.

Deneris, E., J. Boulter, L. W. Swanson, J. Patrick, and S. Heinemann. 1989. β3: A new member of the nicotinic acetylcholine receptor gene family is expressed in the brain. *The Journal of Biological Chemistry.* 264: 6268-6272.

Deneris, E. S., J. Connolly, J. Boulter, E. Wada, K. Wada, L. W. Swanson, J. Patrick, and S. Heinemann. 1988. Primary structure and expression of β2: a novel subunit of neuronal nicotinic acetylcholine receptors. *Neuron.* 1: 45-54.

Deneris, E. S., J. Connolly, S. W. Rogers, and R. Duvoisin. 1991. Pharmacological and functional diversity of neuronal nicotinic acetylcholine receptors. *Trends in Pharmacological Sciences.* 12: 34-40.

Dennis, M., J. Giraudat, F. Kotzyba-Hibert, M. Goeldner, C. Hirth, J.-Y. Chang, C. Lazure, M. Chretien, and J.-P. Changeux. 1988. Amino acids of the *Torpedo marmorata* acetylcholine-receptor α subunit labeled by a photoaffinity ligand for the acetylcholine binding site. *Biochemistry.* 27: 2346-2357.

Devay, P., X. Qu, and L. Role. 1994. Regulation of nAChR subunit gene expression relative to the development of presynaptic and postsynaptic projections of embryonic chick sympathetic neurons. *Developmental Biology.* 162: 56-70.

Dineley-Miller, K., and J. Patrick. 1992. Gene transcripts for the nicotinic acetylcholine receptor subunit, β4, are distributed in multiple areas of the rat central nervous system. *Molecular Brain Research.* 16: 339-344.

Duvoisin, R. M., E. S. Deneris, J. Patrick, and S. Heinemann. 1989. The functional diversity of the neuronal nicotinic acetylcholine receptors is increased by a novel subunit: β4. *Neuron.* 3: 487-496.

Eisele, J.-L., S. Bertrand, J.-L. Galzi, A. Devillers-Thiery, J.-P. Changeux, and D. Bertrand. 1993. Chimeric nicotinic serotonergic receptor combines distinct ligand-binding and channel specificities. *Nature.* 366: 479-483.

Elgoyhen, A. B., D. S. Johnson, J. Boulter, D. E. Vetter, and S. Heinemann. 1994. α9- an acetylcholine receptor with novel pharmacological properties expressed in rat cochlear hair cells. *Cell.* 79: 705-715.

Fu, D. X., and S. M. Sine. 1994. Competitive antagonists bridge the α-γ subunit interface of the acetylcholine receptor through quaternary ammonium-aromatic interactions. *The Journal of Biological Chemistry.* 269: 26152-26157.

Galzi, J.-L., A. Devillers-Thiery, N. Hussy, S. Bertrand, J.-P. Changeux, and D. Bertrand. 1992. Mutations in the channel domain of a neuronal nicotinic receptor convert ion selectivity from cationic to anionic. *Nature.* 359: 500-505.

Galzi, J.-L., F. Revah, D. Black, M. Goeldner, C. Hirth, and J.-P. Changeux. 1990. Identification of a novel amino-acid α-tyrosine-93 within the cholinergic ligands-binding sites of the acetylcholine-receptor by photoaffinity-labeling: additional evidence for a 3-loop model of the cholinergic ligands-binding sites. *The Journal of Biological Chemistry.* 265: 10430-10437.

Giraudat, J., M. Dennis, T. Heidmann, J.-Y. Chang, and J.-P. Changeux. 1986. Structure of the high-affinity binding site for noncompetitive blockers of the acetylcholine receptor: serine-262 of the γ subunit is labeled by [$^3$H]chlorpromazine. *Proceedings of the National Academy of Sciences. USA.* 83: 2719-2723.

Giraudat, J., M. Dennis, T. Heidmann, P. Haumont, F. Lederer, and J.-P. Changeux. 1987. Structure of the high-affinity binding site for noncompetitive blockers of

the acetylcholine receptor: [$^3$H]chlorpromazine labels homologous residues in the β and δ chains. *Biochemistry.* 26: 2410-2418.

Giraudat, J., J.-L. Galzi, F. Revah, J.-P. Changeux, P.-Y. Haumont, and F. Lederer. 1989. The noncompetitive blocker [$^3$H]chlorpromazine labels segment M2 but not segment M1 of the nicotinic acetylcholine receptor α-subunit. *FEBS Letters.* 253: 190-198.

Hucho, F., W. Oberthur, and F. Lottspeich. 1986. The ion channel of the nicotinic acetylcholine receptor is formed by the homologous helices MII of the receptor subunits. *FEBS Letters.* 205: 137-142.

Imoto, K., C. Busch, B. Sakmann, M. Mishina, T. Konno, J. Nakai, H. Bujo, Y. Mori, K. Fukuda, and S. Numa. 1988. Rings of negatively charged amino acids determine the acetylcholine receptor channel conductance. *Nature.* 335: 645-648.

Kao, P. N., A. J. Dwork, R. R. J. Kaldany, M. L. Silver, J. Wideman, S. Stein, and A. Karlin. 1984. Identification of the α subunit half-cystine specifically labeled by an affinity reagent for the acetylcholine receptor binding site. *The Journal of Biological Chemistry.* 259: 11662-11665.

Karlin, A. 1993. Structure of nicotinic acetylcholine receptors. *Current Opinion in Neurobiology.* 3: 299-309.

Lambolez, B., E. Audinat, P. Bochet, F. Crepel, and J. Rossier. 1992. AMPA receptor subunits expressed by single purkinje cells. *Neuron.* 9: 247-258.

Leonard, J. P., L. Yu, C. Labarca, N. Davidson, and H. A. Lester. 1987. Effects of a local anesthetic (QX-222) on gating properties of mouse-*Torpedo* hybrid acetylcholine receptors expressed in *Xenopus* oocytes. *Society for Neuroscience Abstracts.* 13: 97. (Abstr.)

Leonard, R. J., C. Labarca, P. Charnet, N. Davidson, and H. A. Lester. 1988. Evidence that the M2 membrane-spanning region lines the ion channel pore of the nicotinic receptor. *Science.* 242: 1578-1581.

Luetje, C. W., and J. Patrick. 1991. Both α– and β-subunits contribute to the agonist sensitivity of neuronal acetylcholine receptors. *The Journal of Neuroscience.* 11: 837-845.

Luetje, C. W., K. Wada, S. Rogers, S. N. Abramson, K. Tsuji, S. Heinemann, and J. Patrick. 1990. Neurotoxins distinguish between different neuronal nicotinic acetylcholine receptor subunit combinations. *The Journal of Neurochemistry.* 55: 632-640.

Middleton, R. E., and J. B. Cohen. 1991. Mapping of the acetylcholine binding-site of the nicotinic acetylcholine-receptor - [$^3$H]nicotine as an agonist photoaffinity label. *Biochemistry.* 30: 6987-6997.

Revah, F., D. Bertrand, J.-L. Galzi, A. Devillers-Thiery, C. Mulle, N. Hussy, S. Bertrand, M. Ballivet, and J.-P. Changeux. 1991. Mutations in the channel domain alter desensitization of a neuronal nicotinic receptor. *Nature.* 353: 846-849.

Role, L. W. 1992. Diversity in primary structure and function of neuronal nicotinic acetylcholine receptor channels. *Current Opinion in Neurobiology.* 2: 254-262.

Sargent, P. B. 1993. The diversity of neuronal nicotinic acetylcholine receptors. *Annual Review of Neuroscience.* 16: 403-443.

Seguela, P., J. Wadiche, K. Dineley-Miller, J. A. Dani, and J. W. Patrick. 1993. Molecular cloning, functional properties, and distribution of rat brain α7 - a nicotinic cation channel highly permeable to calcium. *The Journal of Neuroscience.* 13: 596-604.

Swanson, L. W., D. M. Simmons, P. J. Whiting, and J. Lindstrom. 1987. Immunohistochemical localization of neuronal nicotinic receptors in the rodent central nervous system. *The Journal of Neuroscience.* 7: 3334-3342.

Unwin, N. 1993. Nicotinic acetylcholine-receptor at 9-Å resolution. *The Journal of Molecular Biology.* 229: 1101-1124.

Unwin, N. 1995. Acetylcholine receptor channel imaged in the open state. *Nature.* 373: 37-43.

Villarroel, A., S. Herlitze, V. Witzemann, M. Koenen, and B. Sakmann. 1992. Asymmetry of the rat acetylcholine receptor subunits in the narrow region of the pore. *Proceedings of the Royal Society of London B.* 249: 317-324.

White, B. H., and J. B. Cohen. 1992. Agonist-induced changes in the structure of the acetylcholine receptor M2 regions revealed by photoincorporation of an

uncharged nicotinic noncompetitive antagonist. *The Journal of Biological Chemistry.* 267: 5770-5783.

White, B. H., S. Howard, S. G. Cohen, and J. B. Cohen. 1991. The hydrophobic photoreagent 3-(trifluoromethyl)-3-m-([$^{125}$I]iodophenyl)diazirine is a novel noncompetitive antagonist of the nicotinic acetylcholine receptor. *The Journal of Biological Chemistry.* 266: 21595-21607.

Figure 1. Structural respresentation of the agonists used in the first series of our experiments.

# AGONISTS

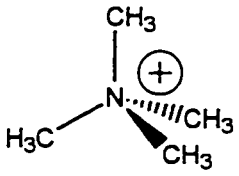


Tetramethylammonium (TMA)

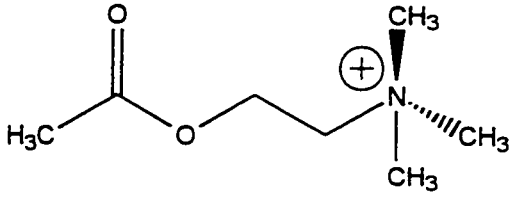


Acetylcholine (ACh)

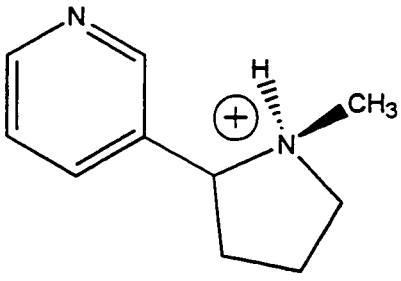


Nicotine (NIC)

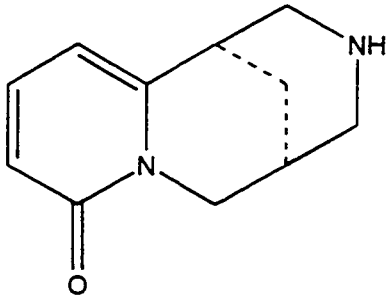


Cytisine (CYT)

# REGIONS OF β4•β2 SUBUNIT CHIMERAS THAT CONTRIBUTE TO THE AGONIST SELECTIVITY OF NEURONAL NICOTINIC RECEPTORS

Antonio Figl,[#] Bruce N. Cohen,[*] Michael W. Quick,[*] Norman Davidson,[*] and Henry A. Lester[*]

From the [#]Division of Chemistry and Chemical Engineering,

[*]Division of Biology 156-29

California Institute of Technology

Pasadena CA 91125, USA

Page A-2 (Abstract) missing.

# INTRODUCTION

The recent cloning of multiple α and β subunits for neuronal nicotinic acetylcholine receptors (nAChRs) has enabled studies of nAChR's formed from a variety of α and β subtypes (reviewed in Deneris, Connolly, Rogers, and Duvoisin, 1991). Expression of all possible combinations of the α and β subtypes in *Xenopus* oocytes shows that both subunits contribute to the relative sensitivity to ganglionic stimulants and neurotoxins (Deneris et al., 1991; Luetje and Patrick, 1991), channel conductance and gating properties (Papke and Heinemann, 1991; Charnet, Labarca, Cohen, Davidson, Lester, and Pilar, 1992; Papke, Boulter, Patrick and Heinemann, 1989) of neuronal nAChRs. Receptors containing the β4 subtype generally give larger responses than receptors containing the β2 subtype to ganglionic stimulants such as cytisine (CYT) and nicotine (NIC) (Leutje et al., 1991). To localize the regions of β4 and β2 that contribute to agonist selectivity, we constructed chimeras of β4 and β2 consisting of $NH_2$-terminal sequences from β4 of varying length and appropriate COOH-terminal counterparts from β2. These were expressed in combination with α3 in *Xenopus* oocytes.

# METHODS

Fifteen β4•β2 chimeras were constructed using a previously described PCR method (Higuchi, 1990) so that they contained an $NH_2$-terminal end from β4 and a COOH-terminal end from β2. For example, the arrow labeled 7 in Fig. 1 denotes the chimera β4(7)•β2 that contains the seven most $NH_2$-terminal residues from β4 and the remaining 470 COOH-terminal residues from β2. mRNA for α3 and the β subunits was transcribed *in vitro* (Guastella, Nelson, Nelson, Czyzyk, Keynan, Miedel, Davidson, Lester, and Kanner, 1990) and 18 ng of each subunit was coinjected into stage V or VI *Xenopus laevis* oocytes. The oocytes were incubated 2-7 d in a modified Barth's solution containing 5% horse serum. We measured the peak current produced by bath application of 30 μM acetylcholine (ACh), 30 μM cytisine (CYT), 30 μM nicotine (NIC), and 100 μM tetramethylammonium (TMA) at a typical holding potential of -80 mV using a two-electrode voltage clamp. Receptors that gave ACh responses too large for accurate recording at -80 mV were measured at more depolarized potentials (-70 to -20 mV). ACh responses of the chimeric and wild-type (WT) receptors were typically in the 100-2,000 nA range. The recording solution contained 96 mM NaCl, 2 mM NaOH, 1 mM $MgCl_2$, and 5 mM HEPES (pH 7.4). External $Ca^{2+}$ was omitted to minimize the activation of the $Ca^{2+}$ activated $Cl^-$ conductance (Vernino, Amador, Luetje, Patrick, and Dani, 1992). All recordings were made at ambient temperature (23-25°C).

# RESULTS

The region of β4 $NH_2$-terminal to the first transmembrane region M1 (residues 1 to 214) was sufficient to confer complete β4-like CYT (Fig. 2) and TMA (Fig. 3), but not NIC (Fig. 4), sensitivity on the receptors containing the chimeric β4•β2 subunits. The relative responses of the α3β2 WT to CYT, TMA, and NIC were 0.03 ± 0.01 (mean ± SD, n = 5), 0.60 ± 0.14 (n = 5), and 0.25 ± 0.11 (n = 5); the relative responses of the α3β4 WT to these same agonists were 2.47 ± 0.59 (n = 7), 1.80 ± 0.47 (n = 3), and 1.36 ± 0.80 (n = 7). The relative responses of the α3β4(214)•β2 chimeric receptor, which contains most of the putative extracellular region of β4, were 2.38 ± 0.26 (n = 2) to CYT, 1.98 ± 0.46 (n = 6) to TMA, and 0.81 ± 0.09 (n = 5) to NIC. Thus, the relative response of α3β4(214)•β2 to CYT and TMA did not differ substantially from the relative response of the α3β4 WT to these agonists.

Chimeras β4(105)•β2 and β4(109)•β2 differ by only one residue (108β4Val↔β2Phe); as do chimeras β4(109)•β2 and β4(111)•β2 (110β4Thr↔β2Ser). These chimeras displayed dramatic differences in relative sensitivity to CYT when expressed with α3 (Fig. 2). Fig. 2 also shows that (*a*) all six chimeras with ≥ 111 $NH_2$-terminal residues from β4 (and the remaining COOH-terminal residues from β2) displayed ≥ 70% of the relative α3β4 WT response to CYT and (*b*) all eight chimeras with ≤ 105 $NH_2$-terminal residues from β4 displayed ≤ 13% of the relative α3β4 WT response to CYT. The relative CYT response of the α3β2 WT was 1% of the relative CYT response of the α3β4 WT receptor. Thus, chimeric receptors containing β4 residues at 108 and 110 displayed a

relative CYT sensitivity near that of the β4 WT while chimeric receptors containing β2 residues at these positions displayed a relative CYT sensitivity much nearer to that of the β2 WT.

Inclusion of two adjacent regions of β4 (112Val, 113Ile and 115Arg, 116Ser) dramatically increased the relative sensitivity of the chimeric receptors to TMA. Fig. 3 shows that (*a*) all four chimeras with ≥ 116 $NH_2$-terminal residues from β4 displayed ≥ 83% of the α3β4 WT relative response to TMA and (*b*) all eight chimeras with ≤ 111 $NH_2$-terminal residues from β4 displayed ≤ 39% of the α3β4 WT relative response to TMA. The relative TMA response of the α3β2 WT was 33% of the relative response of the α3β4 WT to TMA. Thus, chimeric receptors containing β4 residues at 112, 113, 115, and 116 displayed a relative TMA sensitivity near that of the β4 WT while chimeric receptors containing β2 residues at these positions displayed a relative TMA sensitivity much closer to that of the β2 WT.

There also appears to be a transition in the relative CYT responses, but not for the TMA responses from values < 0.06 for α3β4(7)•β2 (n = 5) and α3β4(12)•β2 (n = 7) to values > 0.30 for α3β4(61)•β2 (n = 5) (Fig. 2). However, our data are insufficiently precise to localize the important region.

There was no clearly demarcated zone responsible for the relative NIC sensitivity of β4 (Fig. 4). However, chimeras with transitions from β4 to β2 between 94β2Val/β4Ile and 122β2Phe/β4Gln displayed dramatic variations in the mean nicotine sensitivity when expressed with α3.

# DISCUSSION

Our results are consistent with previous work showing that both the α and β subunits influence the pharmacological selectivity of the neuronal nAChR (Luetje et al., 1991) and that non-α subunits from *Torpedo* nAChRs bind cholinergic ligands (Czajkowski and Karlin, 1991; White and Cohen, 1988). In addition to previously noted differences between the sensitivity of α3β2 and α3β4 to CYT, and NIC relative to ACh (Luetje et al., 1991), we found that α3β4 is more sensitive than α3β2 to the ganglionic stimulant TMA. Two lines of evidence show that the greater relative response of α3β4 to CYT, TMA, and NIC cannot be due solely to a decrease in the ACh response of α3β4. First, normalized to the NIC response, the CYT and TMA response was 0.05 and 0.42 for α3β2 but 1.37 and 0.76 for α3β4. Second, the present data show that distinct regions of β4 contribute to the relative CYT and TMA sensitivity. Nonetheless, differences in the ACh sensitivity of α3β2 and α3β4 may be responsible for part of the difference between the agonist selectivities of the two receptors.

Our data suggest that the region of the β subunit that is most critical for relative CYT and TMA sensitivity lies in the middle of the putative extracellular $NH_2$-terminal sequence. Neuronal nicotinic receptors are thought to be composed of five subunits (Anand, Conroy, Schoepfer, Whiting, and Lindstrom, 1991; Cooper, Couturier, and Ballivet, 1991). Each subunit contains four transmembrane repeats (Claudio, 1989). The portion of each subunit $NH_2$-terminal to M1 forms the bulk of the extracellular portion of the receptor (Claudio, 1989). The M2 transmembrane segment (Claudio, 1989) and

possibly M1 (DiPaola, Kao, and Karlin, 1990) form the channel pore. Confirming an earlier report (Papke, Duvoisin, and Heinemann, 1991), we have shown that the chimeric receptor α3β4(214)•β2, containing all of the putative extracellular region $NH_2$-terminal to M1, has complete β4-like relative sensitivity to CYT and to TMA.

The relative NIC response of α3β4(214)•β2 differed from that of α3β4 and the results did not reveal any single area in the β4•β2 chimeras responsible for relative NIC sensitivity. Thus, there may be (*a*) several regions of the β subunit involved in NIC selectivity; or (*b*) the chimeras may cause novel structural changes in the receptor which interfere with NIC responses.

Previous authors (Luetje et al., 1991) suggested that the small CYT response of receptors containing α3β2 is due to open-channel block by CYT. However, in contrast to previous examples of agonist block of the nAChR (Sine and Steinbach, 1984; Ogden and Colquhoun, 1985), putative block of the ACh response of α3β2 by CYT is not voltage dependent (Luetje et al., 1991). If the channel-block hypothesis is correct, then our results suggest either (*a*) that the open-channel blocking site for CYT is in the extracellular portion of α3β2 or (*b*) that the regions we have identified in β4•β2 chimeras affect the structure of the channel indirectly. A more straightforward interpretation is that CYT, TMA, and NIC may be more effective either (*a*) at binding to α3β4 than to α3β2 or (*b*) at inducing the conformational change that opens the α3β4 channel. In this case, the regions we identified probably influence one of these molecular events at the neuronal nAChR. Dose response data and agonist competition experiments will be necessary to resolve these questions.

# REFERENCES

Anand, R., W. G. Conroy, R. Schoepfer, P. Whiting, and J. Lindstrom. 1991. Nicotinic acetylcholine receptors expressed in *Xenopus* oocytes have a pentameric quaternary structure. *The Journal of Biological Chemistry.* 266: 11192-11198.

Charnet, P., C. Labarca, B. N. Cohen, N. Davidson, H. A. Lester, and G. Pilar. 1992. Pharmacological and kinetic properties of α4β2 neuronal nicotinic acetylcholine receptors expressed in *Xenopus* oocytes. *Journal of Physiology.* 450: 375-394.

Claudio, T. 1989. *In* Frontiers in molecular biology, molecular neurobiology. D. Glover and D. Hames, editors. IRL, London. 9-88.

Cooper, E., S. Couturier, and M. Ballivet. 1991. Pentameric structure and subunit stoichiometry of a neuronal nicotinic acetylcholine receptor. *Nature.* 350: 235-238.

Czajkowski, C. and A. Karlin. 1991. Agonist binding site of *Torpedo* electric tissue nicotinic acetylcholine receptor - a negatively charged region of the delta subunit within 0.9 nm of the alpha subunit binding-site disulfide. *The Journal of Biological Chemistry.* 266: 22603-22612.

Deneris, E. S., J. Connolly, J. Boulter, E. Wada, K. Wada, L. W. Swanson, J. Patrick, and S. Heinemann. 1988. Primary structure and expression of β2 - a novel subunit of neuronal nicotinic acetylcholine receptors. *Neuron.* 1: 45-54.

Deneris, E. S., J. Connolly, S. W. Rogers, and R. Duvoisin. 1991. Pharmacological and functional diversity of neuronal nicotinic acetylcholine receptors. *Trends in*

*Pharmacological Science.* 12: 34-40.

DiPaola, M., P. N. Kao, and A. Karlin. 1990. Mapping the α-subunit site photolabeled by the noncompetitive inhibitor [$^3$H]-quinacrine azide in the active state of the nicotinic acetylcholine receptor. *The Journal of Biological Chemistry.* 75: 11017-11029.

Duvoisin, R. M., E. S. Deneris, J. Patrick, and S. Heinemann. 1989. The functional diversity of the neuronal nicotinic acetylcholine receptors is increased by a novel subunit: β4. *Neuron.* 3: 487-496.

Guastella, J. G., N. Nelson, H. Nelson, L. Czyzyk, S. Keynan, M. C. Miedel, N. Davidson, H. Lester, and B. Kanner. 1990. Cloning and expression of a rat brain GABA transporter. *Science.* 249: 689-706.

Higuchi, R. 1990. Recombinant PCR. *In* PCR Protocols, a Guide to Methods and Applications. M. A. Innis, D. H. Gelfand, J. J. Sninsky, and T. J. White, editors. Academic Press, San Diego, CA. 177-183.

Luetje, C. W. and J. Patrick. 1991. Both α- and β-subunits contribute to the agonist sensitivity of neuronal acetylcholine receptors. *The Journal of Neuroscience.* 11: 837-845.

Ogden, D. C. and D. Colquhoun. 1985. Ion channel block by acetylcholine, carbachol and suberyldicholine at the frog neuromuscular junction. *Proceedings of the Royal Society of London B.* 225: 329-355.

Papke, R. L., J. Boulter, J. Patrick, and S. Heinemann. 1989. Single-channel currents of rat neuronal nicotinic acetylcholine receptors expressed in *Xenopus* oocytes.

*Neuron.* 3: 589-596.

Papke, R. L. and S. F. Heinemann. 1991. The role of the $\beta_4$ subunit in determining the kinetic properties of rat neuronal nicotinic acetylcholine $\alpha_3$ receptors. *Journal of Physiology.* 440: 95-112.

Papke, R. L., R. Duvoisin, and S. F. Heinemann. 1991. *Society for Neuroscience Abstracts.* 17: 1333. (Abstr.)

Sine, S. M. and J. H. Steinbach. 1984. Agonists block currents through acetylcholine-receptor channels. *Biophysical Journal.* 46: 277-283.

Vernino, S., M. Amador, C. W. Luetje, J. Patrick, and J. A. Dani. 1992. Calcium modulation and high calcium permeability of neuronal nicotinic acetylcholine receptors. *Neuron.* 8: 127-134.

White, B. H. and J. B. Cohen. 1988. Photolabeling of membrane-bound *Torpedo* nicotinic acetylcholine receptor with the hydrophobic probe 3-trifluoromethyl-3-(m-[$^{125}$I]iodophenyl)diazirine. *Biochemistry.* 27, 8741-8751.

Figure 1. Aligned sequences of the $NH_2$-terminal regions of β2 (Deneris et al., 1988) and β4 (Duvoisin et al., 1989). Downward arrows indicate the β4 to β2 transition point of each chimera. Numbering is based on the β4 sequence. Outlines denote identical residues. Shading denotes homologous residues.

Figure 1



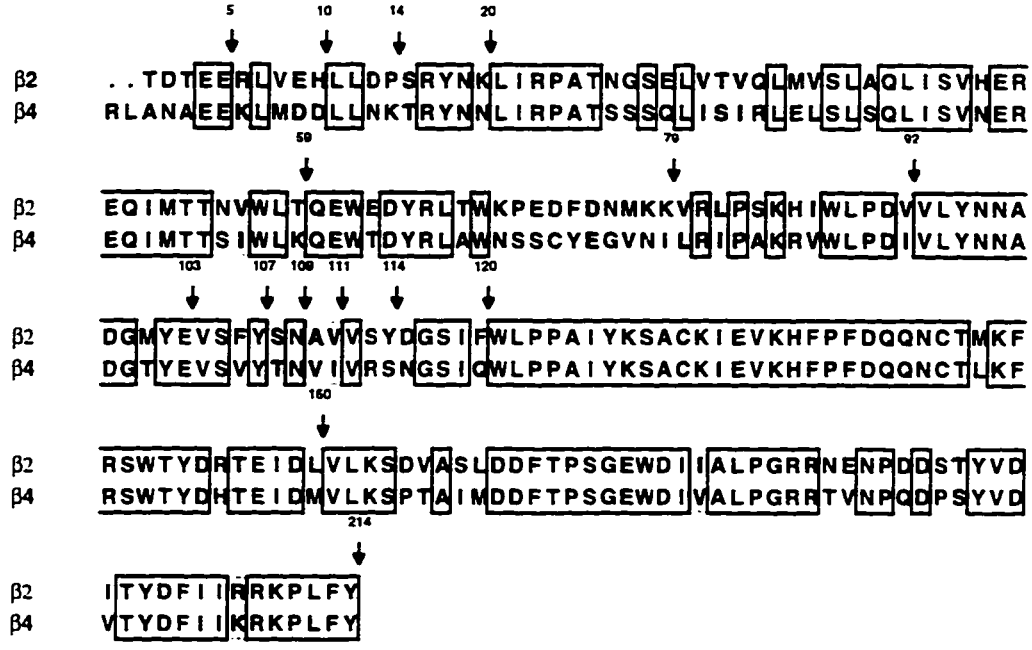
5
10
14
20
β2 . . TDTEERLVEHLLDPSRYNKLIRPATNGSELVTVQLMVSLAQLISVHER
β4 RLANAEEKLMDDLLNKTRYNNLIRPATSSSQLISIRLELSLSQLISVNER
59
70
92
β2 EQIMTTNVWLTQEWEDYRLTWKPEDFDNMKKVRLPSKHIWLPDVVLYNNA
β4 EQIMTTSIWLKQEWTDYRLAWNSSCYEGVNILRIPAKRVWLPDIVLYNNA
103
107
109
111
114
120
β2 DGMYEVSFYSNAVVSYDGSIFWLPPAIYKSACKIEVKHFPFDQQNCTMKF
β4 DGTYEVSVYTNVIVRSNGSICWLPPAIYKSACKIEVKHFPFDQQNCTLKF
160
β2 RSWTYDRTEIDLVLKSDVASLDDFTPSGEWDIIALPGRRNENPDDSTYVD
β4 RSWTYDHTEIDMVLKSPTAIMDDFTPSGEWDIVALPGRRTVNPQDPSYVD
214
β2 ITYDFIIRRKPLFY
β4 VTYDFIIKRKPLFY

Figure 2. Ratio of the CYT-induced current [*I* (30μM CYT)] to the ACh-induced current [*I* (30 μM ACh)] versus the number of $NH_2$-terminal residues from β4 in the β4•β2 chimera. Position zero and 475 (marked with open circles) correspond to the wild-type β2 and β4 subunits, respectively. Dotted lines above and below the circles denote ± one SD. Sample sizes for individual data points were typically 3-8 oocytes. Inset shows the region with the most dramatic changes in relative CYT sensitivity in greater detail. Bars in inset denote ± one SD.

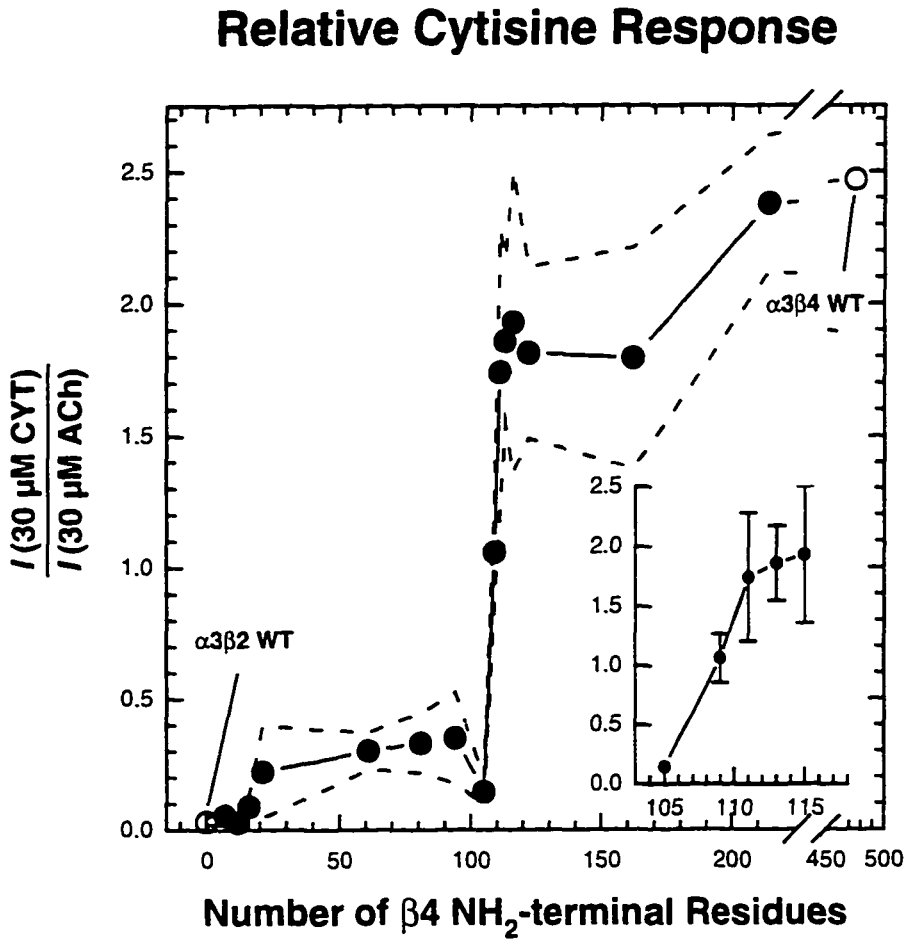
Relative Cytisine Response
I(30 µM CYT) / I(30 µM ACh)
α3β2 WT
α3β4 WT
Number of β4 NH2-terminal Residues

Figure 3. Ratio of the TMA-induced current [*I* (100 μM TMA)] to the ACh-induced current [*I* (30μM ACh)] versus the number of $NH_2$-terminal residues from β4.

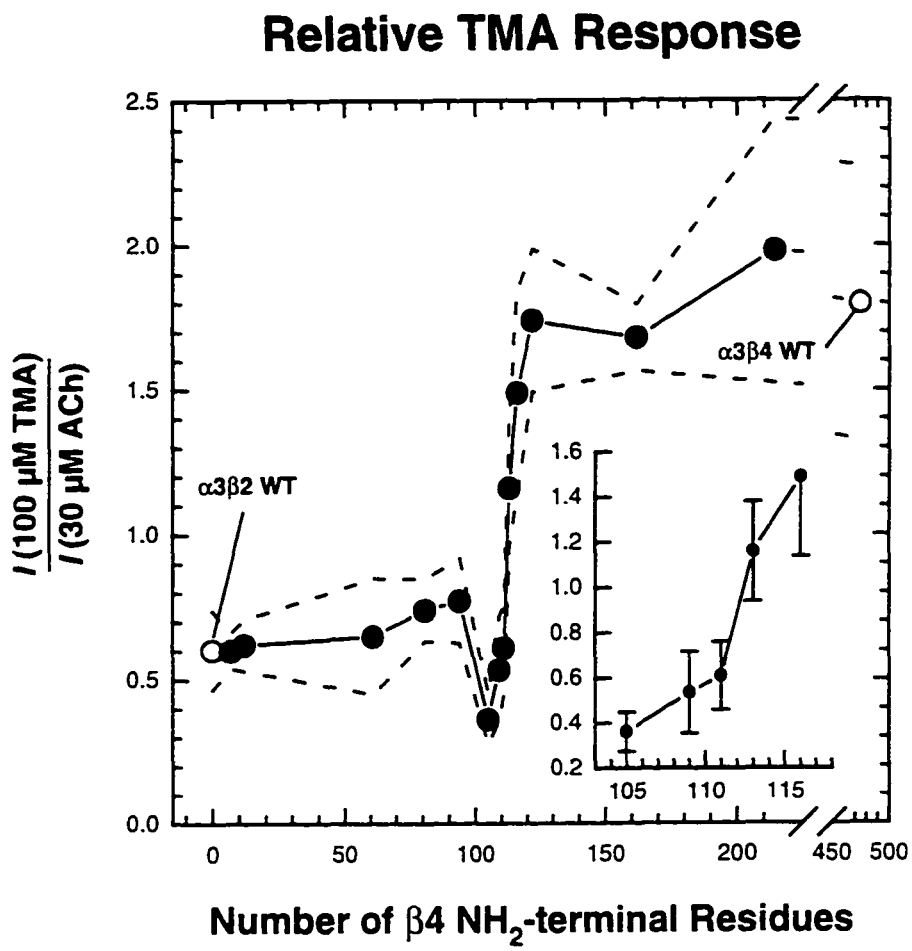
Relative TMA Response
I(100 µM TMA) / I(30 µM ACh)
α3β2 WT
α3β4 WT
Number of β4 NH2-terminal Residues

Figure 4. Ratio of the NIC-induced current [*I* (30 μM NIC)] to the ACh-induced current [*I* (30μM ACh)] versus the number of $NH_2$-terminal residues from β4.

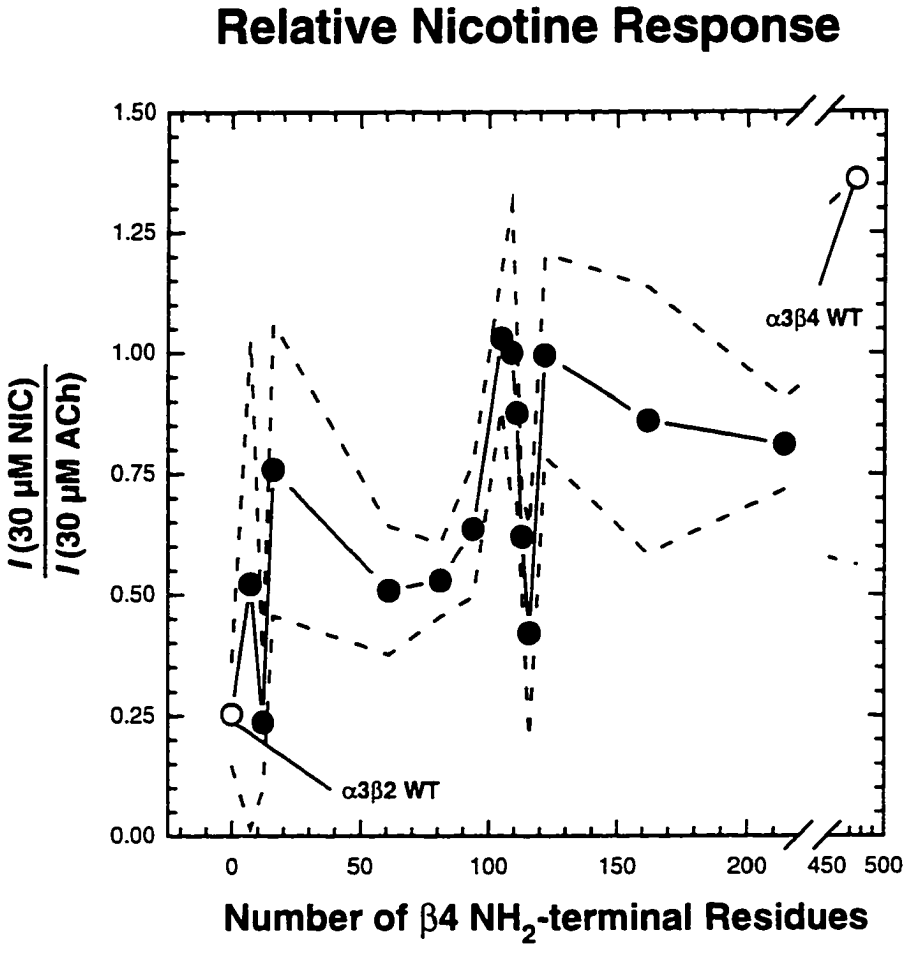
Relative Nicotine Response
I (30 µM NIC) / I (30 µM ACh)
1.50
1.25
1.00
0.75
0.50
0.25
0.00
α3β4 WT
α3β2 WT
0
50
100
150
200
450
500
Number of β4 NH2-terminal Residues

# REGIONS OF β2 AND β4 RESPONSIBLE FOR DIFFERENCES BETWEEN THE STEADY-STATE DOSE-RESPONSE RELATIONSHIPS OF THE α3β2 AND α3β4 NEURONAL NICOTINIC RECEPTORS

Bruce N. Cohen,[•] Antonio Figl,[‡] Michael W. Quick,[§] Cesar Labarca,[§] Norman Davidson,[§] and Henry A. Lester[§]

From the [•]Division of Biomedical Sciences

University of California, Riverside

Riverside, CA 92521-0121

[‡]Division of Chemistry and Chemical Engineering,

[§]Division of Biology, 156-29

California Institute of Technology

Pasadena, California 91125

Reproduced from *The Journal of General Physiology*, 1995, vol. 105, pp. 1-20.

## ABSTRACT

We constructed chimeras of the rat β2 and β4 neuronal nicotinic subunits to locate the regions that contribute to differences between the acetylcholine (ACh) dose-response relationships of the α3β2 and α3β4 receptors. Expressed in *Xenopus* oocytes, the α3β2 receptor displays an $EC_{50}$ for ACh ~twentyfold less than the $EC_{50}$ of the α3β4 receptor. The apparent Hill slope ($n_{app}$) of α3β2 is near one whereas the α3β4 receptor displays an $n_{app}$ near two. Substitutions within the first 120 residues convert the $EC_{50}$ for ACh from one wild-type value to the other. Exchanging just β2:104-120 for the corresponding region of β4 shifts the $EC_{50}$ of ACh dose-response relationship in the expected direction but does not completely convert the $EC_{50}$ of the dose-response relationship from one wild-type value to the other. However, substitutions in the β2:104-120 region do account for the relative sensitivity of the α3β2 receptor to cytisine, tetramethylammonium, and ACh. The expression of β4-like (strong) cooperativity requires an extensive region of β4 (β4:1-301). Relatively short β2 substitutions (β2:104-120) can reduce cooperativity to β2-like values. The results suggest that amino acids within the first 120 residues of β2 and the corresponding region of β4 contribute to an agonist binding site that bridges the α and β subunits in neuronal nicotinic receptors.

# INTRODUCTION

Both the α and non-α subunits of the nicotinic acetylcholine receptor (nAChR) play a role in the activation of the receptor by agonist (reviewed in Deneris, Connolly, Rogers, and Duvoisin, 1991; Karlin, 1993; Papke, 1993). Although many studies show that agonist binds to the α subunit (reviewed in Karlin, 1993), present opinion is divided about the possibility of an agonist binding site at the α/non-α subunit interface (Cockcroft, Osguthorpe, Barnard, and Lunt, 1990; Karlin, 1993; Unwin, 1993). The evidence for an α-only binding site is that 9 Å images of *Torpedo* nAChRs reveal a unique cleft within the α subunit that could act as an agonist binding pocket (Unwin, 1993). However, there is no evidence that agonists actually bind within this cleft and contact only α-subunit residues. On the other hand, previous experiments show that (*a*) the muscle-type α subunit (α1) binds nicotinic agonists with appreciable affinities only if it is complexed with a non-α subunit (Blount and Merlie, 1988) and (*b*) the competitive antagonist *d*-tubocurarine (*d*TC) photolabels residues on the γ and δ subunits of *Torpedo* nAChRs (Pedersen and Cohen, 1990; Chiara and Cohen, 1992), which is strong evidence for a direct participation of the non-α subunits in an agonist binding site. However, *d*TC is a larger molecule than ACh and may not contact exactly the same residues that ACh does. Large quantities of purified neuronal nAChRs are not available for direct biochemical and structural analyses of potential agonist binding sites. We have exploited

the fact that α3β2 and α3β4 neuronal nAChRs expressed in *Xenopus* oocytes display different relative sensitivities to the ganglionic agonists, cytisine (CYT), tetramethylammonium (TMA), acetylcholine (ACh) and nicotine (Leutje and Patrick, 1991; Figl, Cohen, Quick, Davidson, and Lester, 1992), and different dose-response relationships for ACh (Couturier, Erkman, Valera, Rungger, Bertrand, Boulter, Ballivet, and Bertand, 1990; Cachelin and Jaggi, 1991; Leutje, Piattoni, and Patrick, 1993; Wong, Mennerick, Clifford, Zorumski, and Isenberg, 1993), to locate the residues of β2 and β4 involved in agonist activation of the receptor.

In an earlier study on coexpressed α3 and β subunits, we used β4•β2 chimeras. Extending the β4 $NH_2$-terminal region of a chimera from residues β4:1-105 to β4:1-122 (Fig. 1) changed the CYT/ACh and TMA/ACh response ratios from α3β2-like (β2-like) to α3β4-like (β4-like) levels (Figl et al., 1992). These data suggested that β4:106-122, and the corresponding region of β2 (β2:104-120), contributes to an agonist binding site that bridges the α and non-α subunits. To test this hypothesis, we have extended the earlier studies with (*a*) more chimeric and mutated β subunits and (*b*) electrophysiological measurements of the agonist dose-response relationship, which we summarize by the half-maximal agonist concentration ($EC_{50}$) and Hill coefficient ($n_{app}$). The results show that the region of β4 that converts the $EC_{50}$ for ACh from a β2-like to a β4-like value overlaps the previously localized region that converts the CYT/ACh response ratios of β4 $NH_2$-terminal chimeras from β2-like to β4-like values (Figl et al., 1992) and suggest that an important component of the agonist binding site lies within the first 120 residues of β2

and the corresponding region of β4. Some of our results have been reported previously in abstract form (Figl, Cohen, Gollub, Davidson, and Lester, 1993).

# METHODS

## *Construction of the β Chimeras and Mutants*

We created chimeras between the β2 and β4 subunits by taking advantage of shared restriction sites in the two subunits and using the polymerase chain reaction (PCR) to generate overlapping cDNA fragments (Higuchi, 1990) from the two subunits. Fig. 1 shows an alignment of β2 and β4 amino-acid sequences. Most of the chimeras contained the $NH_2$-terminal region from one β subtype joined to the succeeding COOH-terminal residues from the other β subtype ($NH_2$-terminal chimeras). We refer to the $NH_2$-terminal chimeras in the text by transition points between the two types of β subunits. For example, β2(229)•β4 is a chimera containing the first 229 residues of β2 joined to residues 232-475 of β4 (see Fig. 1). Chimeras containing internal substitutions are labelled by the end points of the substitution. For example, β4•β2(104-120)•β4 is a chimera in which we substituted β2:104-120 for residues 106-122 of the β4 subunit (these labels have been shortened to β2(104-120) and β2(106-122) in Fig. 7-8).

To create the β2(229)•β4 and β4(231)•β2 chimeras, we excised the cDNA fragments for residues β2:1-229 and β4:1-231 from the wild-type subunits with EcoRI and BbsI, subcloned the excised fragments into the complementary restricted plasmid from the opposite β subunit, and sequenced the region around the β4/β2 transition to check the final product. The remaining chimeras were constructed in three steps: (*a*) we synthesized

two or more separate PCR fragments; (*b*) we annealed and amplified the PCR fragments; and (*c*) we inserted the annealed fragment into the appropriate restriction sites in the wild-type plasmid. We normally introduced a silent mutation into the chimera during the initial PCR reaction to allow us to check the final product by restriction analysis. In addition, all the chimeras were verified by DNA sequencing. We made point mutations using the Altered Sites Kit (Promega Corp., Madison, WI) and verified the mutations by restriction analysis and DNA sequencing. Point mutations are denoted in the text by subscripts that contain the single letter code for the original residue, followed by its position in the sequence, and the residue to which it was mutated. We synthesized mRNA *in vitro* using the MEGAscript Kit (Ambion, Austin, TX) or a previously published method (Guastella, Nelson, Nelson, Czyzyk, Keynan, Miedel, Davidson, Lester, and Kanner, 1990) and checked the size of the synthesized mRNA by agarose gel electrophoresis.

## *Oocyte Expression*

Stage V-VI *Xenopus* oocytes were isolated as described previously (Quick and Lester, 1994) and injected with mRNA in a stoichiometric ratio for α:β of 2:3. The amount of mRNA injected (≤ 25 ng/subunit) was adjusted to maintain a maximum response ($I_{max}$) of ≤ 10 μA at -50 mV. Prior to recording, the oocytes were incubated for 2-7 d at 18°C in a modified Barth's solution supplemented with 50 mg/ml gentamicin, 2.5 mM pyruvate,

and 5% horse serum (Quick and Lester, 1994).

## *Electrophysiological Recordings*

The oocytes were voltage-clamped at -50 mV with two, 3 M KCl-filled microelectrodes made from thick-walled borosilicate glass (model BF150-86-10, Sutter Instrument Co., Novato, CA) and an AxoClamp 2A voltage clamp (Axon Instruments, Foster City, CA). During the experiments, we perfused the recording chamber (~1.5 ml vol) with 98 mM NaCl, 1 mM $MgCl_2$, and 5 mM HEPES (pH 7.4) at room temperature (20-24°C) at 10-20 ml/min. We omitted $Ca^{2+}$ from the recording solution because the entry of $Ca^{2+}$ through neuronal nAChRs can activate the endogenous $Ca^{2+}$-activated $Cl^-$ current of the oocyte (Vernino, Amador, Leutje, Patrick, and Dani, 1992).

We applied agonists to the oocytes by pinching-off the outflow of a U tube (Bormann, 1992) with a solenoid-activated pinch valve (Cole-Palmer, Niles, IL) under computer control. The time constant of the approach to a steady-state response ($\tau_{on}$) was 0.4-0.5 s at slowly desensitizing agonist doses. To check the effective [agonist] reaching the oocyte from the U tube, we applied a slowly desensitizing dose of ACh (1 mM) to an oocyte expressing $\alpha3\beta2$ using the bath and U tube perfusion systems. Bath and U tube application of 1 mM ACh produced the same steady-state response. Endogenous muscarinic responses were rare and easily identified by their oscillatory nature and delayed onset after agonist application from the U tube. We did not use

oocytes exhibiting muscarinic responses.

## *Collection and Analysis of the Dose-Response Data*

We recorded the responses to 6-11 different agonist doses to measure the dose-response relationships for individual oocytes. The agonist was applied in 6 s pulses separated by a 2-3 min rinse with control saline. The responses were filtered at 20 Hz and digitized at a sampling frequency of 50 Hz using an MS-DOS computer equipped with pCLAMP V5.5 software (Axon Instruments, Foster City, CA).

We fit the dose-response data for individual oocytes to the Hill equation,

$$I_{peak} = \frac{I_{max}}{1 + \left( \frac{EC_{50}}{[A]} \right)^{n_{app}}}$$

where $I_{peak}$ was the peak response at agonist concentration $[A]$, using weighted nonlinear least-squares regression. To reduce the interdependence of the parameters $I_{max}$, $EC_{50}$, and $n_{app}$, we allowed only the $I_{max}$ and the $EC_{50}$ to vary when fitting to the Hill equation. The $n_{app}$ was fixed at the mean slope of the Hill plots for the receptor subtype being fit. The $n_{app}$ was determined ($a$) from the Hill plot by linear regression of $\log[I_{peak}/(I_{max} - I_{peak})]$ against log[agonist] where $I_{max}$ was the maximum observed response and ($b$) from the log-log plot by regression at the foot of the dose-response relationship. The correlation between these two measurements of the $n_{app}$ was 0.89 for the 26 receptor types discussed

in the text. Regression of the log-log slope against the corresponding Hill slope predicted a log-log slope of 1.1 for a Hill slope of 1.0 and a log-log slope of 1.9 for a Hill slope of 2.0. We preferred the estimates of the $n_{app}$ from the Hill plot because (*a*) the slope of the Hill plot was based on more points per oocyte than the initial log-log slope measurements, (*b*) log-log slope measurements tend to underestimate the true $n_{app}$, (*c*) the Hill plot included more data points with a higher signal/noise ratio than the initial log-log plot, and (*d*) the $n_{app}$'s from the Hill plot generally fit the dose-response relationship better than the $n_{app}$'s from the log-log plots. The $n_{app}$'s reported in the text are from Hill slopes rather than from log-log slopes unless stated otherwise. We weighted the residuals by $1/\sqrt{I_{peak}}$ for the fit to the Hill equation because the variance of $I_{peak}$ at the high end of the dose-response relationship was larger than the variance of $I_{peak}$ at the low end. Repeated measurements on a single oocyte showed that long-term desensitization reduced the $I_{max}$ but did not affect the $EC_{50}$ or $n_{app}$.

To compare measurements of the $EC_{50}$ with widely different variances, we transformed the $EC_{50}$'s to log values. Unless otherwise stated, the measurement errors reported in the text are standard deviations (SD's) and the SD's for the $EC_{50}$'s given in the text are for untransformed data. To construct normalized dose-response relationships for the receptors, we normalized the individual dose-response relationships to the fitted $I_{max}$'s and pooled the resulting data. We then refit the Hill equation allowing only the $EC_{50}$ to vary. The error reported for the normalized $EC_{50}$ measurements is the standard error of estimate (SEE).

# *Correction of the Peak Response for Desensitization*

Rapid desensitization reduces the peak response because some receptors desensitize while the [agonist] is still rising around the oocyte. We used the following three-state scheme (SCHEME I) to calculate depression of the peak response by rapid desensitization,

$$C \xrightarrow{k_1} O \xrightarrow{k_2} D,$$

SCHEME I

where $C$, $O$, and $D$ are the closed, open, and desensitized states of the receptor, $k_1$ is the rate constant for the [ACh] to reach a steady state around the oocyte, and $k_2$ represents the rate constant for desensitization. We obtained $k_1$ directly from the rate constant of the rising phase of the response with 1 μM ACh and $k_2$ directly from the rate constant of the decay of the response within the agonist pulse (in the Results section, $1/k_1$ and $1/k_2$ are termed $\tau_{on}$ and $\tau_{desen}$). The relationship between the peak amplitude of the observed response ($I_{peak}$) and the peak amplitude of the calculated response ($I_{calc}$) is,

$$I_{calc} = \frac{I_{peak}}{\frac{k_1}{k_2 - k_1}\left[\left(\frac{k_1}{k_2}\right)^{k_1/(k_2-k_1)} - \left(\frac{k_1}{k_2}\right)^{k_2/(k_2-k_1)}\right]}$$

At high [ACh]'s, the decay of the response consisted of two exponential components. These components were corrected separately using Eq. 1 and then summed to obtain the final calculated peak response.

# RESULTS

## *The β Subunit Affects the Agonist Dose-Response Relationship*

Consistent with previous data (Couturier et al., 1990; Leutje et al., 1993; Wong et al., 1993), we found that the β subunit profoundly affects the sensitivity of neuronal nAChRs to ACh. Expressing α3 with β2, instead of with β4, shifted the ACh dose-response relationship at -50 mV considerably to the left and reduced its slope (Fig. 2). The traces in Fig. 2, *A* and *B* are typical ACh responses of α3β2 (Fig. 2 *A*) and α3β4 (Fig. 2 *B*) from oocytes with similar maximum responses. We fit the ACh dose-response relationships for α3β2 and α3β4 to the Hill equation (Fig. 2 *C*) using the $n_{app}$'s for α3β2 and α3β4 determined from Hill plots of the ACh responses (Fig. 2 *D*). Similar to previous results (Couturier et al., 1990; Leutje et al., 1993; Wong et al., 1993), the $EC_{50}$ for ACh was 11 ± 4 μM (mean ± SD, n = 29 oocytes) for the rat α3β2 receptor and 219 ± 12 μM (n = 3) for the rat α3β4 receptor. The $n_{app}$ for α3β2 was 1.1 ± 0.2 (n = 29) and the $n_{app}$ for α3β4 was 2.2 ± 0.1 (n = 3). Fig. 2 *D* shows Hill plots for the two receptors. Measurements of the $n_{app}$ from the initial slope of a log-log plot of the dose-response relationship (where desensitization and agonist self-block are minimal) gave similar, but slightly smaller, $n_{app}$'s for α3β2 (0.9 ± 0.1 , n = 11) and α3β4 (1.9 ± 0.1, n = 3). Fig. 2 *E*

shows examples of the initial portions of the log(dose)-log(response) relationships for the two wild-type receptors. The agreement of these measurements shows that the difference between the $n_{app}$'s of α3β2 and α3β4 was not due to desensitization or open-channel block by the agonist. Injecting equal amounts of mRNA generally gave much larger maximal ACh responses for α3β4 than for α3β2 (~tenfold) but we did not study these differences further.

The dose-response relationships of α3β2 and α3β4 for TMA displayed differences comparable to, but less pronounced than, those for ACh (Fig. 3). Fig. 3, *A* and *B* show sample responses of α3β2 (Fig. 3 *A*) and α3β4 (Fig. 3 *B*) to TMA. Rapid desensitization is less pronounced for both wild-type receptors with TMA as the agonist. The $EC_{50}$ of α3β2 for TMA (76 ± 11 μM, n = 7) was fivefold smaller than that of α3β4 (424 ± 94 μM, n = 6) and the $n_{app}$ of α3β2 for TMA (1.4 ± 0.1, n = 7) determined from Hill plots of the dose-response data was significantly smaller than the $n_{app}$ of α3β4 (2.0 ± 0.2, n = 6). As with ACh, the β2 subunit shifts the TMA dose-response considerably to the left (Fig. 3 *C*). Thus, the β subunit affects the activation of neuronal nAChRs by an agonist that contains only the quaternary ammonium portion of the ACh molecule; and the effects of the β subunit on the agonist dose-response relationship persist even with an agonist that desensitizes the receptor more slowly than ACh.

## *Rapid Desensitization Fails to Account for Differences in the $EC_{50}$'s of α3β2 and α3β4*

The response of α3β2 to ACh (Fig. 2 *A*) desensitized more quickly than the response of α3β4 to ACh (Fig. 2 *B*). The time constant $\tau_{on}$ for activation of the α3β2 response to 1 μM ACh to reach a steady-state was 0.4-0.5 s. The time constant $\tau_{desen}$ for the desensitization of the α3β2 response decreased from 5-7 s at 3 μM ACh to 0.6-0.8 s at 300 μM ACh. Desensitization of the α3β2 response to 300 μM ACh was biphasic with an additional slow time constant of 5-6 s. The α3β4 receptor displayed little desensitization during the 6 s agonist pulse. The $\tau_{desen}$ for α3β4 was 5-6 s at 1-2 mM ACh and was too slow to measure at 20-500 mM ACh.

We corrected the peak ACh response of the wild-type receptors for apparent desensitization (see Methods) and fit the corrected data to the Hill equation to determine how much of the difference in the $EC_{50}$'s could be due to a difference in the rate of desensitization. Correcting the peak response of α3β2 for apparent desensitization left $n_{app}$ unchanged but increased the $EC_{50}$ of α3β2 for ACh twofold. Desensitization of α3β4 did not significantly affect the ACh dose-response relationship. Thus, allowing for the potential effects of desensitization, the $EC_{50}$ of α3β4 for ACh was still tenfold larger than the $EC_{50}$ of α3β2. The differences in desensitization accounted for such a small fraction of the differences between the $EC_{50}$'s of the wild-type receptors that we decided not to

attempt to correct the amplitudes of the peak responses. We were unable to resolve desensitization occurring on a time scale faster than 1 s (Maconochie and Knight, 1992) using our drug application system (see Methods). Such desensitization would produce an apparent decrease in the $EC_{50}$ of the dose-response relationship in our experiments.

## *$NH_2$-terminal Substitutions of 105 or More Residues Increase the $EC_{50}$ for ACh*

Substitutions of 94 or fewer β4 residues had only small effects on the $EC_{50}$ for ACh (Fig. 4 *A*); the $EC_{50}$'s of the α3β4(16)•β2, α3β4(81)•β2, and α3β4(94)•β2 chimeras for ACh (13-18 μM) were within a factor of two of the $EC_{50}$ of α3β2 for ACh. However, if the β4 $NH_2$-terminal region of the chimeras was extended from 94 to 109 residues, the $EC_{50}$ for ACh increased dramatically to a β4-like value. Fig. 4 *B* presents data for the interesting region between residues β4:94 and β4:109 and shows the rightward shift of the normalized ACh dose-response relationships as more β4 residues are included. All the β4 $NH_2$-terminal chimeras with 113 or more β4 $NH_2$-terminal residues displayed β4-like $EC_{50}$'s for ACh (more than tenfold larger than that of α3β2). Thus, the β4/β2 residue substitutions necessary for β4-like ACh sensitivity in the β4•β2 chimeras lie in the first 113 residues of β4.

There are only two β4/β2 residue substitutions in β4:95-109 (see Fig. 1). The addition of these two substitutions increased the $EC_{50}$ of the β4 $NH_2$-terminal chimeras

from β2-like to β4-like levels. Therefore, we made the site-directed mutations $\beta2_{M101T,F106V}$ to change just these residues in the β2 subunit. The $EC_{50}$ of the mutated receptor for ACh ($19 \pm 4$ μM, n = 5) was within a factor of two of the value for α3β2 ($11 \pm 4$ μM). Thus, the increase in the $EC_{50}$ of α3β4(109)•β2 over the $EC_{50}$ of α3β4(94)•β2 depended on residue substitutions within the first 94 residues of β4 in addition to the two substitutions β2:Met101↔β4:Thr103 and β2:Phe106↔β4:Val108. Previous experiments (Chiara et al., 1992; O'Leary, Filatov, and White, 1994) also suggest that a tryptophan (γ:Trp55, δ:Trp57) in the first 60 residues of the non-α subunits contributes to the agonist binding sites of the *Torpedo* nAChR.

We also made the mutation $\alpha3\beta4(61)_{S28N}$•β2 to determine if the loss of a potential glycosylation site at β2:Asn26 was responsible for the slight decrease in the $EC_{50}$ of α3β4(61)•β2 below that of α3β2. The $EC_{50}$ ($6 \pm 3$ μM, n = 4) and $n_{app}$ ($0.8 \pm 0.1$, n = 4) of $\alpha3\beta4(61)_{S28N}$•β2 for ACh were not significantly different from the $EC_{50}$ ($5 \pm 1$ μM, n = 6) and the $n_{app}$ ($1.0 \pm 0.1$, n = 6) of α3β4(61)•β2. Thus, the removal of a potential glycosylation site at β2:Asn26 was not responsible for the effect of α3β4(61)•β2 on the $EC_{50}$ for ACh.

## *Increasing the $n_{app}$ to β4-like Values Requires an Extensive Region of β4*

The $n_{app}$ of the β4•β2 chimeras showed a more gradual dependence on the β4/β2 transition point than the $EC_{50}$. The $n_{app}$'s of these chimeras fell into three categories, β2-like ($n_{app}$ = 1.0-1.2), intermediate ($n_{app}$ = 1.6), and β4-like ($n_{app}$ = 2.0-2.2). The chimeras containing 109 or less β4 $NH_2$-terminal residues exhibited β2-like $n_{app}$'s; the chimeras containing 109-231 β4 $NH_2$-terminal residues exhibited intermediate $n_{app}$'s except for α3β4(122)•β2 ($n_{app}$ = 1.2 ± 0.2, n = 2); and the chimeras containing 301 or more β4 $NH_2$-terminal residues exhibited β4-like $n_{app}$'s. The $\beta2_{M101T,F106V}$ mutation did not affect the $n_{app}$ for ACh.

We are not surprised by the differences between the regions of β4 that affect the $EC_{50}$ and those that affect the $n_{app}$. Areas of contact between the subunits outside the agonist binding site may affect the cooperativity of a multisubunit receptor (Koshland, Neméthy, and Filmer, 1966). Nevertheless, the overlap between the β4 residues that increase the $EC_{50}$'s of the β4•β2 chimeras and the residues that increases the $n_{app}$ from β2-like to intermediate values suggests that β4:106-122 and β2:104-120 may be areas where the α and β subunits contact each other. The results for the β4 $NH_2$-terminal chimeras also suggest that these subunits contact each other somewhere between the end of the first putative transmembrane domain M1 and the initial portion of the M3-M4 intracellular loop. However, our data do not allow us to exclude the alternative

hypothesis that these residue substitutions produce a conformational change in the receptor that affects cooperativity indirectly.

## *Substituting β2:1-120 for the Corresponding Region of β4 Reduces the $EC_{50}$ to a β2-like Value*

We constructed a number of β2•β4 chimeras to determine the region of the β2 subunit required to reduce the $EC_{50}$ of the chimeras to β2-like values (Fig. 5 *A*). Similar to results for the β4•β2 chimeras, substituting the first 120 residues of β2 for the corresponding region of β4 reduced the $EC_{50}$ for ACh to 16 ± 8 μM (n = 3) which resembles the $EC_{50}$ of α3β2 (11 ± 4 μM). Fig. 5 *B* shows the effect of this substitution on the ACh dose-response relationship. Substituting the first 92 residues of β2 also reduced the $EC_{50}$ for ACh (Fig. 5 *A*). Thus, residue substitutions in the first 92 regions of β2 do affect the sensitivity of the receptor to agonist but this effect is masked in the β4 $NH_2$-terminal chimeras.

There is an anomalous member of the β2•β4 series; the $EC_{50}$ of α3β2(229)•β4 for ACh was close to that of α3β4 (Fig. 5 *A*). This anomalous $EC_{50}$ does not seem to be due to a disruption of the agonist binding site. Previous data shows that this chimera displays a β2-like affinity for the irreversible competitive inhibitor, neuronal bungarotoxin (Papke, Duvoisin, and Heinemann, 1993), and we found that α3β2(229)•β4 exhibits a clear β2-like

insensitivity to CYT relative to ACh (Fig. 6).

Thus, the results for the β4 and β2 $NH_2$-terminal chimeras show that β2/β4 substitutions in the first 120 residues of β2 and the first 113 residues of β4 are sufficient to convert the $EC_{50}$ for ACh from one wild-type value to another.

## *Short β2 $NH_2$-terminal Substitutions Disrupt the Cooperativity of the Receptor*

β2 $NH_2$-terminal sequences of 92 or more residues reduced the $n_{app}$ for ACh to a value near that of α3β2 for ACh (1.1 ± 0.2) (Fig. 5 *C*). Morever, a single measurement of the $n_{app}$ (1.1) for α3β2(59)•β4 from the initial portion of the log-log dose response relationship suggests that even substituting the first 59 residues of β2 for the corresponding region of β4 may suffice to reduce the $n_{app}$ of the chimera to a β2-like value. Thus, as for the β4 $NH_2$-terminal chimeras, changes in the $EC_{50}$'s of the β2 $NH_2$-terminal chimeras were not synchronous with changes in the $n_{app}$. If the $n_{app}$ is determined by areas of contact between the subunits, then these results suggest that an extensive region of subunit/subunit contacts, particularly at the $NH_2$-terminals of the α3 and β4 subunits, are required for the receptor to display the strong cooperativity observed for the α3β4 receptor. The small $n_{app}$ of the α3β2(120)•β4 raises the possibility that there may also be heterogeneity in the assembly of this receptor. The α3β2(92)•β4 and α3β2(229)•β4 chimeras also display Hill coefficients that are slightly less than one.

## *Exchanging Just β2:104-120 and β4:106-122 Shifts the $EC_{50}$ in the Expected Direction*

Mutations show that the two β4/β2 substitutions β2:Met101↔β4:Thr103 and β2:Phe106↔β4:Val108 are not sufficient to change the $EC_{50}$ of the ACh dose-response relationship. We therefore constructed the reciprocal chimeras α3β4•β2(104-120)•β4 and α3β2•β4(106-122)•β2 to test whether more extensive substitutions in this area could affect the $EC_{50}$ for ACh. Exchanging β2:104-120 and β4:106-122 shifted the $EC_{50}$ for ACh towards the opposing wild-type value (Fig. 7, *A* and *B*). Substituting β2:104-120 for the corresponding region of β4 reduced the $EC_{50}$ for ACh to 90 ± 20 μM (n = 4), a value less than half that of α3β4 (219 ± 12 μM). The reciprocal substitution (β4:106-122 for the corresponding region of β2) increased the $EC_{50}$ about threefold over the $EC_{50}$ for α3β2, to 28 ± 6 μM (n = 8). Consistent with the results for the β2 and β4 $NH_2$-terminal chimeras, substituting β2:104-120 reduced the cooperativity of the chimera to 1.3 ± 0.1 (n = 4) while the reciprocal substitution did not significantly increase the $n_{app}$ for ACh (1.3 ± 0.2, n = 8). Thus, eight residue substitutions in β2:104-120 and β4:106-122 (see Fig. 1) had an effect on the $EC_{50}$ and $n_{app}$ for ACh that was independent of substitutions elsewhere in the β subunits.

## *Substituting β2:104-120 Also Affects Agonist Selectivity*

Previous data (Figl et al., 1992) show that extending the β4 region of a β4 $NH_2$-terminal chimera from β4:1-105 to β4:1-122 increases the 30 μM CYT/30 μM ACh (CYT/ACh) and 100 μM TMA/30 μM ACh (TMA/ACh) response ratios from β2-like to β4-like levels. We tested the effects of exchanging β2:104-120 and β4:106-122 to determine whether these regions accounted for the effects of the β4 $NH_2$-terminal chimeras on agonist selectivity.

Substituting β2:104-120 for β4:106-122 reduced the CYT/ACh and TMA/ACh response ratios to β2-like values (Fig. 8, *A* and *B*), but the reciprocal substitution β4:106-122 for β2:104-120 produced only a small increase in the CYT/ACh or TMA/ACh response ratios toward β4-like values. Thus, similar to the effects of β2 substitutions on cooperativity, short internal substitutions reduce, but do not restore, the relative sensitivity of the α3β4 receptor to ganglionic agonists such as CYT and TMA. The structural basis for this correspondence between the effects of internal substitutions on agonist selectivity and cooperativity is unclear. Nonetheless, the effects of exchanging β4:106-122 and β2:104-120 on several measurements associated with agonist activation of the receptor suggest that these areas are places where the α and β subunits contact to form an agonist binding site.

## *The Sole M2 Substitution Does Not Affect the ACh Dose-Response Relationship*

Dose-response relationships for nAChRs are affected by mutations at several residues in the M2 transmembrane domain (reviewed in Karlin, 1993). There is a single β2/β4 substitution in the M2 region (β2:Val253↔β4:Phe255). We made the reciprocal point mutations $\beta4_{F255V}$ and $\beta2_{V253F}$ to test whether this substitution could shift the agonist dose-response relationship. Neither mutation significantly affected the $EC_{50}$ or $n_{app}$. The $n_{app}$ of $\alpha3\beta4_{F255V}$ was 2.0 ± 0.1 (n = 3); the $n_{app}$ of $\alpha3\beta2_{V253F}$ was 1.2 ± 0.1 (n = 3); the $EC_{50}$ of $\alpha3\beta4_{F255V}$ was 231 ± 18 μM (n = 3); and, the $EC_{50}$ of $\alpha3\beta2_{V253F}$ was 9 ± 1 μM (n = 3).

# DISCUSSION

The data reported in this paper describe the steady-state dose-response relations of chimeric and mutated β2 and β4 subunits expressed with the α3 subunit in oocytes. The data show that the first 120 residues of β2 and a comparable, but slightly shorter, region of β4 largely account for the different $EC_{50}$'s of the wild-type dose-response relationships. In the sharpest region of transition, chimeras that differ at only two residues have more than a tenfold difference in the $EC_{50}$. However, when we examined the corresponding mutant $\beta2_{M101T,F106V}$ it retained the $EC_{50}$ of the wild-type β2 subunit. This important result shows that the two critical residues are interacting with other upstream residues during activation of the receptor. Longer substitutions in this region (β2:104-120′β4:106-122) do affect (*a*) the ACh dose-response relationship and (*b*) the relative responses to several ganglionic agonists. The domains we have identified that affect the $EC_{50}$ probably affect agonist binding and may contribute to an agonist binding site that bridges the α and β subunits.

Our experiments also bear on the regions responsible for the cooperativity of the receptor ($n_{app}$). Regions of the β subunits responsible for differences in the $n_{app}$ overlap with, but are not identical to, those responsible for differences in the $EC_{50}$. The β2:104-120 and β4:106-122 regions affect both measures. However, for the β4 $NH_2$-terminal chimeras, the transition from β2-like to β4-like cooperativity occurs more

gradually than the transition from a β2-like to a β4-like $EC_{50}$ and requires an extensive $NH_2$-terminal region of the β4 subunit. The high level of cooperativity of α3β4 is disrupted by short β2 substitutions. If receptor cooperativity is determined by areas of contact between the subunits (Koshland et al., 1966), then one of these contact regions appears to lie in β2:104-120 and β4:106-122.

The differences we observed between the ACh dose-response relationships of the α3β2 and α3β4 receptors are similar to those reported previously by Couturier et al. (1990), Leutje et al. (1993), and Wong et al. (1993) but differ substantially from those reported by Cachelin et al. (1991). Cachelin et al. (1991) report a much smaller value for the $EC_{50}$ of α3β4 for ACh (30 μM) and a much larger value for the $EC_{50}$ of α3β2 for ACh (354 μM). They report similar, but less diverse, $n_{app}$'s for the two receptor subtypes ($n_{app}$ = 1.4 for α3β2; $n_{app}$ = 1.8 for α3β4). The reason for this discrepancy is unclear but most of the previous measurements, including data from a mammalian expression system (Wong et al., 1993), are consistent with our data.

The α3β2(229)•β4 chimera is anomalous because it displays a large, β4-like $EC_{50}$ for ACh even though it includes regions of sequence that confer a β2-like $EC_{50}$ in another chimera tested. Nonetheless, the α3β2(229)•β4 chimera exhibits a β2-like CYT/ACh response ratio and a β2-like irreversible block by neuronal bungarotoxin (Papke et al., 1993). Based on its agonist selectivity and affinity for neuronal bungarotoxin, we suggest that the large $EC_{50}$ of this chimera arises from a change in the conformational states of the receptor that enhances the relative stability of the closed singly-liganded receptor state

(Koshland et al., 1966) rather than from a change in the agonist binding site.

## *Channel Block by the Agonist Fails to Account for Differences in the $n_{app}$*

Measurements of the Hill coefficient at the foot of the dose-response relationship show that the differences between the $n_{app}$'s of the wild-type receptors are not due to channel block by the agonist because open-channel block is minimal in this region. However, open-channel block by the agonist could reduce the apparent $EC_{50}$ of the agonist dose-response relationship. To assess the importance of this effect, we calculated the dissociation constant $K_i$ of agonist for an open-channel blocking site that would yield a β2-like $EC_{50}$, assuming that (*a*) the agonist can open all the channels (a worst-case analysis), (*b*) α3β2 and α3β4 display a β4-like $EC_{50}$ for ACh (219 μM) in the absence of channel block, and (*c*) the $n_{app}$ for α3β2 is ~1. The fractional response of the receptor ($I_{peak}/I_{max}$) under these conditions is,

$$\frac{I_{peak}}{I_{max}} = \frac{1}{1 + \frac{219mM}{[ACh]} + \frac{[ACh]}{K_i}}$$

A $K_i$ of 10 mM would be required to bring the $EC_{50}$ to 24 μM. Concentration- and voltage-jump experiments on neuronal nAChRs in bovine chromaffin cells suggest that the

actual dissociation constant of ACh for the channel blocking site of neuronal nAChRs is closer to 700-1400 μM (Maconochie et al., 1992), or 70- to 140-fold greater than the value required to bring the $EC_{50}$ for α3β2 to 24 μM. Moreover, with a $K_i$ of 10 mM, the maximum response would occur at ~50 μM ACh. Higher agonist concentrations would reduce the amplitude of the response, contrary to our data for α3β2 (Fig. 2 *A*). Additionally, the sole substitution in M2, which is thought to contain the binding site for open-channel blockers, has no effect. These results strongly suggest that agonist self-block does not account for the differences in the $EC_{50}$'s that we observed.

## *Residues in a Homologous Region of γ and δ Determine Curare Binding*

Three residue substitutions in the mouse γ and δ subunits (γ:Ile116↔δ:Val118, γ:Tyr117↔δ:Thr119, γ:Ser161↔δ:Lys163) account for a tenfold increase in the affinity of the αβγ receptor over the abd receptor for the competitive antagonist (+)-dimethyltubocurarine (Sine, 1993). Residues β2:Ile118 and β2:Phe119 in the rat neuronal nicotinic receptor are homologous to γ:Ile116 and γ:Tyr117 in the mouse receptor and they are in the β2:104-120 domain of the rat neuronal nicotinic receptor. More recent evidence (Xie, Chiara, and Cohen, 1994) shows that the competitive antagonist *d*TC also photolabels residues γ:Tyr111 and γ:Tyr117 in the *Torpedo* nAChR (homologous to β2:Ser113 and β2:Phe119 in the rat neuronal nicotinic receptor). Thus, in

a domain homologous to β2:104-120 in the rat neuronal nicotinic receptor, we find (*a*) residues in the *Torpedo* γ subunit that are photolabelled by *d*TC and (*b*) residues in the mouse γ and δ subunits that affect competitive antagonist binding. Residues in β2:104-120 affect the $n_{app}$, the $EC_{50}$, and agonist selectivity of neuronal nicotinic receptors. The proximity of residues in the muscle-type nicotinic receptors that affect binding and photolabelling by a competitive antagonist with those in the neuronal nicotinic receptor that affect the $n_{app}$, the $EC_{50}$, and agonist selectivity supports the hypothesis that residues β2:104-120 contribute to an α/β ligand binding site in neuronal nAChRs.

## *Differences in Channel Gating Do Not Account for Differences in the Wild-type $EC_{50}$*

We consider a simple sequential model to suggest that differences in agonist binding, rather than in the rates of conformational change, are primarily responsible for the difference between the $EC_{50}$'s of α3β2 and α3β4 for ACh. This kinetic scheme (SCHEME II) can be summarized as follows,

$$nA + R \xrightarrow{K_1^n} C \xrightarrow{K_2} O \xrightarrow{K_3} I \qquad \text{SCHEME II}$$

where $n$ is the Hill coefficient, $A$ is the agonist, $R$ is the free receptor, $C$ is the closed

agonist-bound receptor, $O$ is the conducting state of the receptor, $I$ is an agonist-bound inactivated state of the receptor, and $K_1$-$K_3$ are dissociation constants. At equilibrium, the fraction of open receptors $P_o$ is,

$$P_o = \frac{1}{1 + \frac{1}{K_3} + K_2 + \frac{K_2 K_1^n}{[A]^n}}$$

The $EC_{50}$ is,

$$EC_{50} = K_1 \sqrt[n]{\frac{K_2 K_3}{1 + K_3 + K_3 K_2}}$$

According to the data of Papke and Heinemann (1991), $K_2$ = 1.1 and 0.45, and $K_3$ = 10 and 20 for α3β2 and α3β4, respectively. The point here is not the absolute values of these numbers, but the fact that they differ by relatively small amounts for the two receptors. A similar conclusion is reached from our own kinetic data on voltage-jump relaxations, to be published separately. These differences would change the $EC_{50}$ by less than twofold. Thus, differences in the cooperativity of binding and conformational transitions of α3β2 and α3β4 cannot account for the twentyfold difference we observed between the $EC_{50}$'s of the wild-type receptors for ACh. This model suggests that the wild-type dissociation constants for agonist binding ($K_1$'s) differ by more than tenfold.

Regardless of the particular kinetic model used, the differences between the mean open times of the α3β2 and α3β4 channels do not account for the differences in the $EC_{50}$'s

of α3β2 and α3β4 for ACh. The open channel lifetime is usually interpreted as the rate constant for leaving the open state of the channel. The long open channel lifetime of the primary α3β4 channel is 75% greater than the long open channel lifetime of the primary α3β2 channel (Papke et al., 1991). All else being equal, this difference in open channel lifetime would be associated with a smaller $EC_{50}$ for α3β4 than for α3β2, contrary to the data.

*Conclusions*

Our study is the first attempt to determine the regions of sequence that account for the differences in the complete agonist dose-response relationship produced by two naturally occurring subunits of a channel. Past experiments on binding of antagonists or open-channel blockers have pinpointed just a few residues; however, channel activation in response to agonists is certainly a more complex phenomenon, involving binding, conformational changes, and interactions between the subunits. It is therefore encouraging that clear trends emerge from the data. Our results emphasize the involvement of one region, β2:104-120, in the binding event and suggest that a broader region of sequence is involved in the subunit contacts and/or conformational changes that open the channel.

# REFERENCES

Blount, P., and J. P. Merlie. 1988. Native folding of an acetylcholine receptor α subunit expressed in the absence of other receptor subunits. *The Journal of Biological Chemistry.* 263: 1072-1080.

Bormann, J. 1992. U-tube drug application. *In* Practical electrophysiological methods, a guide for in vitro studies in vertebrate neurobiology, H. Kettenmann and R. Grantyn, editors. Wiley-Liss, New York, NY. 136-140.

Cachelin, A. B., and R. Jaggi. 1991. β subunits determine the time course of desensitization in rat α3 neuronal nicotinic receptors. *Pflügers Archiv.* 419: 579-582.

Chiara, D. C., and J. B. Cohen. 1992. Identification of amino acids contributing to high and low affinity *d*-tubocurarine sites on the *Torpedo* nicotinic acetylcholine receptor subunits. *The FASEB Journal.* 6: A106. (Abstr.)

Cockcroft, V. B., D. J. Osguthorpe, E. A. Barnard, and G. G. Lunt. 1990. Modeling of agonist binding to the ligand-gated ion channel superfamily of receptors. *Proteins: Structure, Function, and Genetics.* 8: 386-397.

Couturier, S., L. Erkman, S. Valera, D. Rungger, S. Bertrand, J. Boulter, M. Ballivet, and D. Bertrand. 1990. α5, α3, and non-α3: three clustered avian genes encoding neuronal nicotinic acetylcholine receptor-related subunits. *The*

*Journal of Biological Chemistry.* 265: 17560-17567.

Deneris, E. S., J. Connolly, S. W. Rogers, and R. Duvoisin. 1991. Pharmacological and functional diversity of neuronal nicotinic acetylcholine receptors. *Trends in Pharmacological Science.* 12: 34-40.

Figl, A., B. N. Cohen, J. Gollub, N. Davidson, and H. A. Lester. 1993. Novel functional domains of the rat neuronal nicotinic β subunit. *Society for Neuroscience Abstracts.* 19: 8 (Abstr.)

Figl, A., B. N. Cohen, M. W. Quick, N. Davidson, and H. A. Lester. 1992. Regions of β4•β2 subunit chimeras that contribute to the agonist selectivity of neuronal nicotinic receptors. *FEBS Letters.* 308: 245-248.

Guastella, J. G., N. Nelson, H. Nelson, L. Czyzyk, S. Keynan, M. C. Miedel, N. Davidson, H. A. Lester, and B. I. Kanner. 1990. Cloning and expression of a rat brain GABA transporter. *Science.* 249: 1303-1306.

Higuchi, R. 1990. Recombinant PCR. *In* PCR protocols, a guide to methods and applications, M. A. Innis, D. H. Gelfand, J. J. Sninsky, and T. J. White, Editors. Academic Press, Inc. San Diego, CA. 177-184.

Karlin, A. 1993. Structure of nicotinic acetylcholine receptors. *Current Opinion in Neurobiology.* 3: 299-309.

Koshland, D. E., G. Neméthy, and D. Filmer. 1966. Comparison of experimental binding data and theoretical models in proteins containing subunits. *Biochemistry.* 5: 365-385.

Leutje, C. W., and J. Patrick. 1991. Both α- and β-subunits contribute to the agonist sensitivity of neuronal nicotinic acetylcholine receptors. *The Journal of Neuroscience.* 11: 837-845.

Leutje, C. W., M. Piattoni, and J. Patrick. 1993. Mapping of ligand binding sites of neuronal nicotinic acetylcholine receptors using chimeric α subunits. *Molecular Pharmacology.* 44: 657-666.

Maconochie, D. J., and D. E. Knight. 1992. A study of the bovine adrenal chromaffin nicotinic receptor using patch clamp and concentration-jump techniques. *Journal of Physiology.* 454: 129-153.

O'Leary, M. E., G. N. Filatov, and M. M. White. 1994. Characterization of the *d*-tubocurarine binding site of the *Torpedo* acetylcholine receptor. *The American Journal of Physiology.* In press.

Papke, R. L. 1993. The kinetic properties of neuronal nicotinic receptors: genetic basis of functional diversity. *Progress in Neurobiology.* 41: 509-551.

Papke, R. L., R. M. Duvoisin, and S. F. Heinemann. 1993. The amino terminal half of the nicotinic β-subunit extracellular domain regulates the kinetics of inhibition by neuronal bungarotoxin. *Proceedings of the Royal Society of London B.* 252: 141-148.

Papke, R. L., and S. F. Heinemann. 1991. The role of the β4 subunit in determining the kinetic properties of rat neuronal nicotinic acetylcholine α3-receptors. *Journal of Physiology.* 440: 95-112.

Pedersen, S. E., and J. B. Cohen. 1990. *d*-Tubocurarine binding sites are located at the α–γ and α–δ subunit interfaces of the nicotinic acetylcholine receptor. *Proceedings of the National Academy of Sciences, USA.* 87: 2785-2789.

Quick, M. W., and H. A. Lester. 1994. Methods for expression of excitability proteins in *Xenopus* oocytes. *In* Methods in Neurosciences. P.M. Conn. editor. Academic Press, San Diego, CA. 261-279.

Sine, S. M. 1993. Molecular dissection of subunit interfaces in the acetylcholine receptor: identification of residues that determine curare selectivity. *Proceedings of the National Academy of Sciences, USA.* 90: 9436-9440.

Unwin, N. 1993. Neurotransmitter action: opening of ligand-gated ion channels. *Neuron.* 10: 31-41.

Vernino, S., M. Amador, C. W. Leutje, J. Patrick, and J. A. Dani. 1992. Calcium modulation and high calcium permeability of neuronal nicotinic acetylcholine receptors. *Neuron.* 8: 127-134.

Wong, E. T., S. Mennerick, D. B. Clifford, C. F. Zorumski, and K. E. Isenberg. 1993. Expression of a recombinant neuronal nicotinic acetylcholine receptor in transfected HEK-293 cells. *Society for Neuroscience Abstracts.* 19: 291. (Abstr.)

Xie, Y., D. C. Chiara, and J. B. Cohen. 1994. Mutational analysis of novel residues identified within the binding site of *d*-tubocurarine of *Torpedo* acetylcholine receptor. *International Symposium on Nicotine.* P16. (Abstr.)

Figure 1. The aligned amino acid sequences of the rat β2 and β4 neuronal nAChR subunits. The boxes outline identical residues and the shading denotes homologous residues. Residue 1 begins after the termination of the leader sequences (not shown). The arrows above the β4 sequence point to the transitions in the β4 $NH_2$-terminal chimeras between the β4 and β2 sequence. The arrows beneath the β2 sequence point to the transitions in the β2 $NH_2$-terminal chimeras between the β2 and β4 sequence. The numbers above (below) the arrows are the last residues in the β4 (β2) $NH_2$-terminal regions of the chimeras. The lines beneath the β2 sequence denote the transmembrane regions M1-M4.

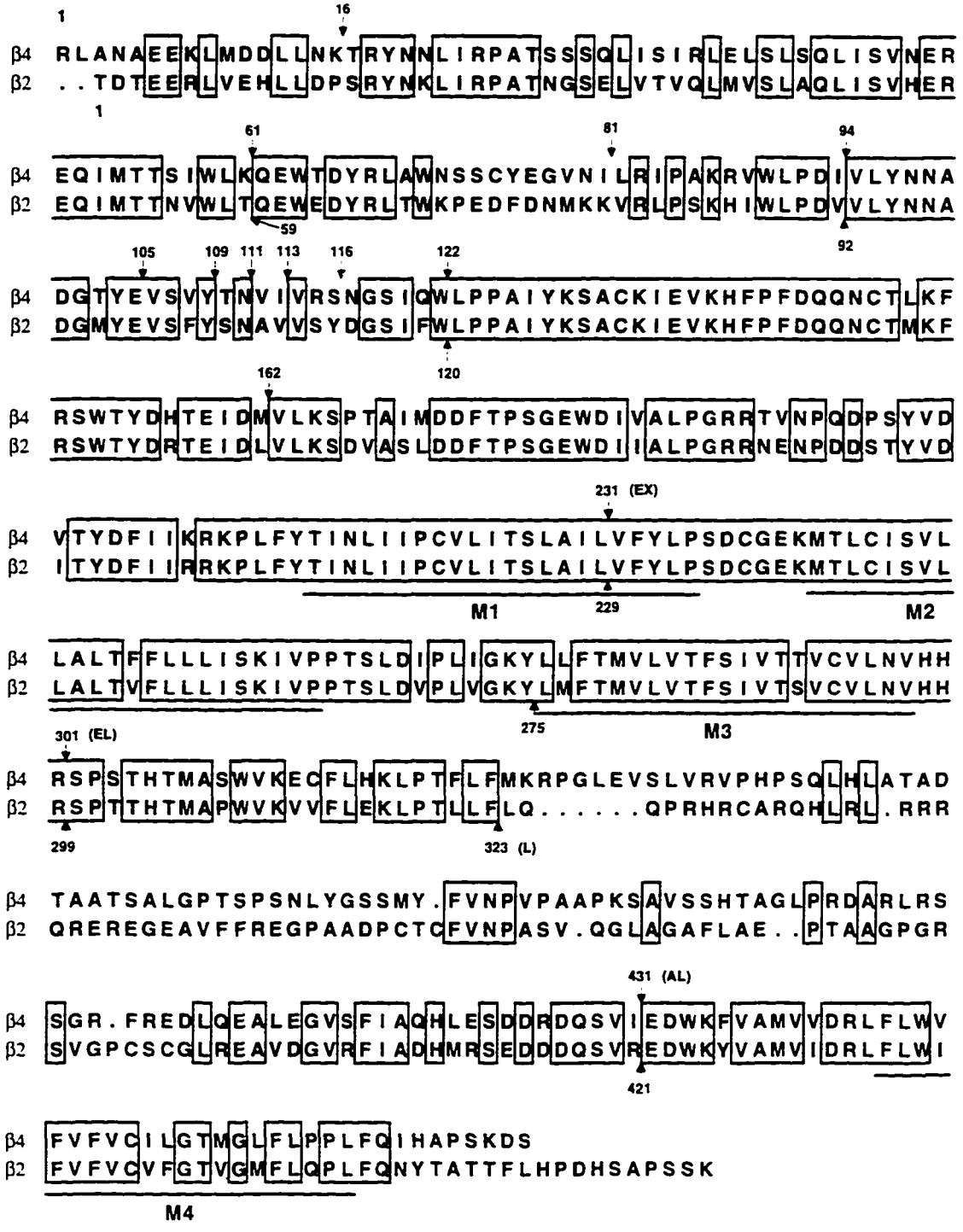
β4 RLANAEEKLMDDLLNKTRYNNLIRPATSSSQLISIRLELSLSQLISVNER
β2 ..TDTEERLVEHLLDPSRYNKLIRPATNGSELVTVQLMVSLAQLISVHER
β4 EQIMTTSIWLKQEWTDYRLAWNSSCYEGVNILRIPAKRVWLPDIVLYNNA
β2 EQIMTTNVWLTQEWEDYRLTWKPEDFDNMKKVRLPSKHIWLPDVVLYNNA
β4 DGTYEVSVYTNVIVRSNGSIQWLPPAIYKSACKIEVKHFPFDQQNCTLKF
β2 DGMYEVSFYSNAVVSYDGSIFWLPPAIYKSACKIEVKHFPFDQQNCTMKF
β4 RSWTYDHTEIDMVLKSPTAIMDDFTPSGEWDIVALPGRRTVNPQDPSYVD
β2 RSWTYDRTEIDLVLKSDVASLDDFTPSGEWDIIALPGRRNENPDDSTYVD
β4 VTYDFIIKRKPLFYTINLIIPCVLITSLAILVFYLPSDCGEKMTLCISVL
β2 ITYDFIIRRKPLFYTINLIIPCVLITSLAILVFYLPSDCGEKMTLCISVL
M1
M2
β4 LALTFFLLLISKIVPPTSLDIPLIGKYLLFTMVLVTFSIVTTVCVLNVHH
β2 LALTVFLLLISKIVPPTSLDVPLVGKYLMFTMVLVTFSIVTSVCVLNVHH
M3
β4 RSPSTHTMASWVKECFLHKLPTFLFMKRPGLEVSLVRVPHPSQLHLATAD
β2 RSPTTHTMAPWVKVVFLEKLPTLLFLQ.....QPRHRCARQHLRL.RRR
β4 TAATSALGPTSPSNLYGSSMY.FVNPVPAAPKSAVSSHTAGLPRDARLRS
β2 QREREGEAVFFREGPAADPCTCFVNPASV.QGLAGAFLAE..PTAAGPGR
β4 SGR.FREDLQEALEGVSFIAQHLESDDRDQSVIEDWKFVAMVVDRLFLWV
β2 SVGPCSCGLREAVDGVRFIADHMRSEDDDQSVREDWKYVAMVIDRLFLWI
β4 FVFVCILGTMGLFLPPLFQIHAPSKDS
β2 FVFVCVFGTVGMFLQPLFQNYTATTFLHPDHSAPSSK
M4

Figure 2. Expressing α3 with β2, rather than with β4, reduces the $EC_{50}$ and apparent Hill coefficient ($n_{app}$) of the ACh dose-response relationship. (*A*) Responses of α3β2 to 1-300 μM ACh. The numbers are the [ACh] in μM. The square pulse above the traces is the duration of the application of ACh from the U tube. (*B*) Responses of α3β4 to 20-1000 μM ACh. (*C*) Dose-response plots for α3β2 and α3β4. The symbols denote different oocytes expressing α3β2 (filled circles, open circles, filled inverted triangle, open inverted triangles, filled squares) or α3β4 (open squares, filled upright triangles, open upright triangles). The lines are fits to the Hill equation (see Methods). The $EC_{50}$'s and the $I_{max}$'s are 17 μM and 1863 nA (filled circles), 13 mM and 1757 nA (open circles), 15 mM and 2056 nA (filled inverted triangles), 9 mM and 1461 nA (hollow inverted triangles), 13 mM and 1498 nA (filled squares), 216 mM and 1944 nA (open squares), 232 mM and 2061 nA (filled upright triangles), and 209 mM and 2100 nA (open upright triangles). Voltage = -50 mV. (*D*) Hill plots for the peak ACh responses ($I_{peak}$) of α3β2 and α3β4. $I_{max}$ is the maximum observed $I_{peak}$. The symbols denote different oocytes: α3β2 (filled circles, hollow circles), α3β4 (filled inverted triangles, hollow inverted triangles, filled squares). Overlap obscures some of the data. The $n_{app}$'s are 0.9 (filled circles), 1.0 (open circles), 2.2 (filled inverted triangles), 2.3 (inverted triangles), and 2.2 (filled squares). (*E*) Log-log plots of the foot of the ACh dose-response relationship show that the slope of the α3β4 log dose-log response relationship is ~twice that of α3β2. The symbols represent data from six oocytes (each oocyte is represented by a different symbol). The lines are regression lines fit to the log-log data. The slopes for α3β4 were 2.0 (filled circles), 2.0

(open circles), and 1.8 (filled inverted triangle); the slopes for $\alpha 3\beta 2$ were 1.1 (hollow inverted triangles), 1.0 (filled squares), and 1.0 (hollow squares).

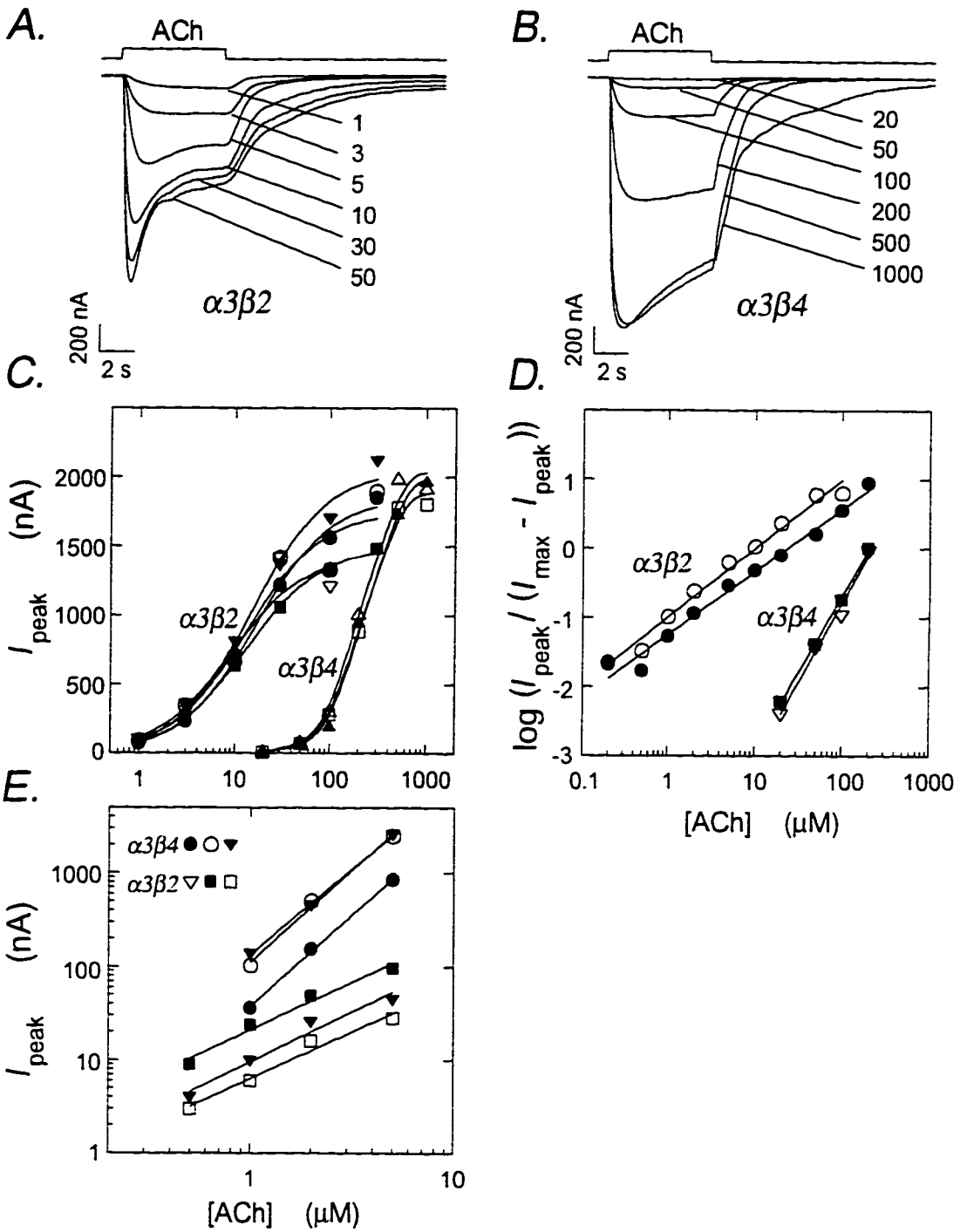
A.
ACh
1
3
5
10
30
50
α3β2
200 nA
2 s
B.
ACh
20
50
100
200
500
1000
α3β4
200 nA
2 s
C.
I peak (nA)
2000
1500
1000
500
0
α3β2
α3β4
1
10
100
1000
D.
log (I peak / (I max - I peak))
1
0
-1
-2
-3
α3β2
α3β4
0.1
1
10
100
1000
[ACh] (μM)
E.
α3β4 ● ○ ▼
α3β2 ▽ ■ □
I peak (nA)
1000
100
10
1
1
10
[ACh] (μM)

Figure 3. Expressing α3 with β4, rather than with β2, increases the $EC_{50}$ and the $n_{app}$ of the TMA dose-response relationship. (*A*) Responses of α3β2 to 5-200 μM TMA. The responses are labelled with the [TMA] in μM. The square pulse above the traces shows the timing of the TMA application. (*B*) Responses of α3β4 to 50-2000 μM TMA. (*C*) Expression with β4 shifts the TMA dose-response relationship to the right and increases its slope. The symbols are mean normalized responses ± SD. The $EC_{50}$'s of the TMA dose-response relationships for α3β2 and α3β4 are 75 ± 3 μM (n = 7) and 416 ± 12 μM (n = 6) (± standard error of estimate, ± SEE).

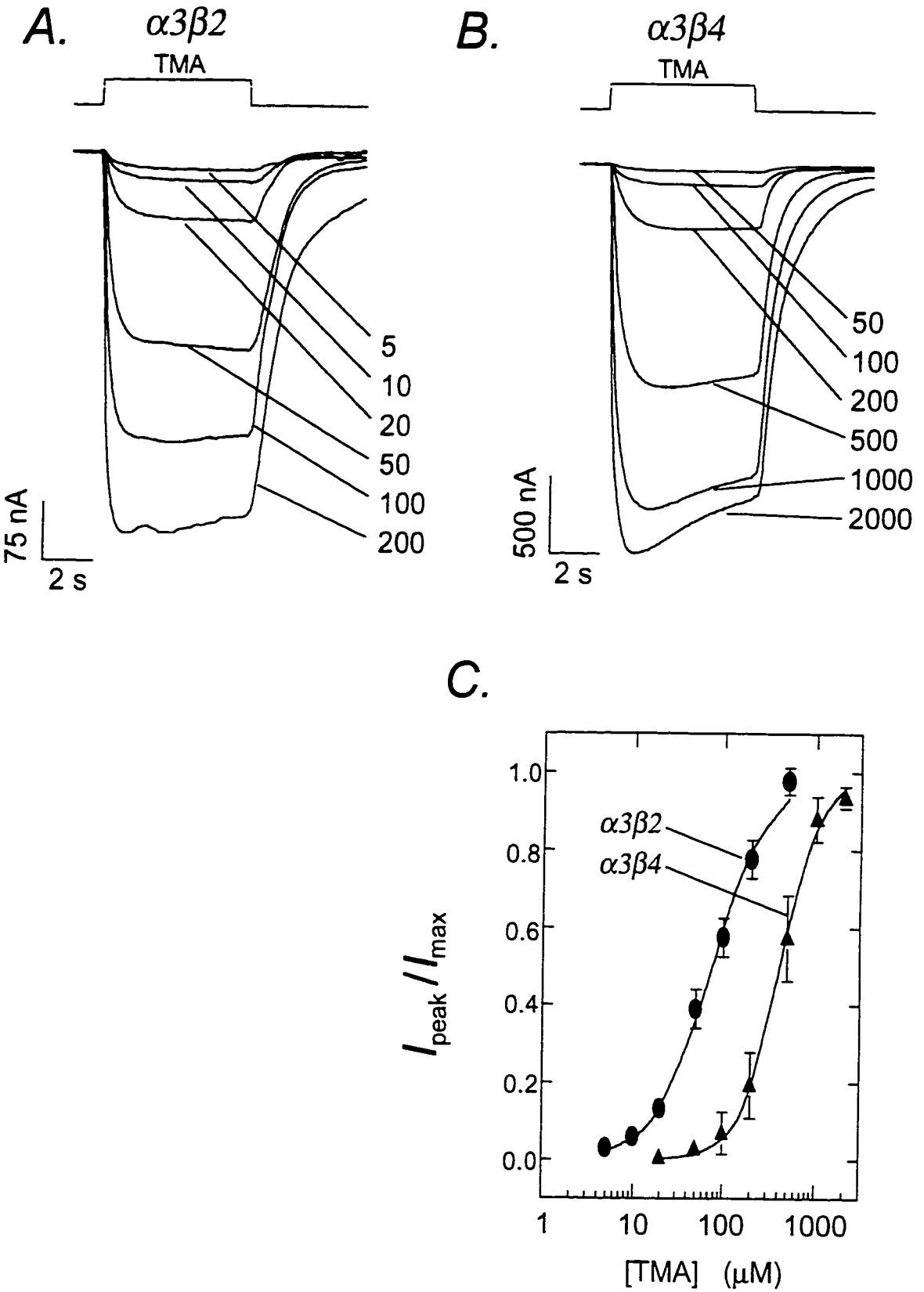
A.
α3β2
TMA
5
10
20
50
100
200
75 nA
2 s
B.
α3β4
TMA
50
100
200
500
1000
2000
500 nA
2 s
C.
α3β2
α3β4
$I_{peak}/I_{max}$
1.0
0.8
0.6
0.4
0.2
0.0
1
10
100
1000
[TMA] (μM)

Figure 4. (*A*) Substituting 105 or more β4 $NH_2$-terminal residues for the corresponding region of β2 increases the $EC_{50}$ for ACh. The horizontal axis is the number of β4 $NH_2$-terminal residues in the chimera: zero for α3β2 and 475 for α3β4. The symbols are the mean values for the two wild types and 14 β4•β2 chimeras (n = 2-29 oocytes). Overlap obscures some of the data. The dashed lines are ± 1 SD. The means and SD's for the $EC_{50}$'s were computed from log transformed data. The vertical line denotes the beginning of M1. (*B*) The addition of two residue substitutions in the β4:95-109 sequence (see Fig. 1) shifts the ACh dose-response relationship dramatically to the right. The symbols are the mean normalized responses ± SD (see Methods) for α3β4(94)•β2, α3β4(105)•β2, and α3β4(109)•β2. The lines are fits to the Hill equation (see Methods). The $EC_{50}$'s for ACh are 16 ± 1 μM (n = 9), 60 ± 4 μM (n = 4), and 338 ± 23 μM (n = 6), respectively (± SEE). (*C*) Substituting ≥ 301 β4 $NH_2$-terminal residues increases the $n_{app}$ for ACh to ≥ 2.0.

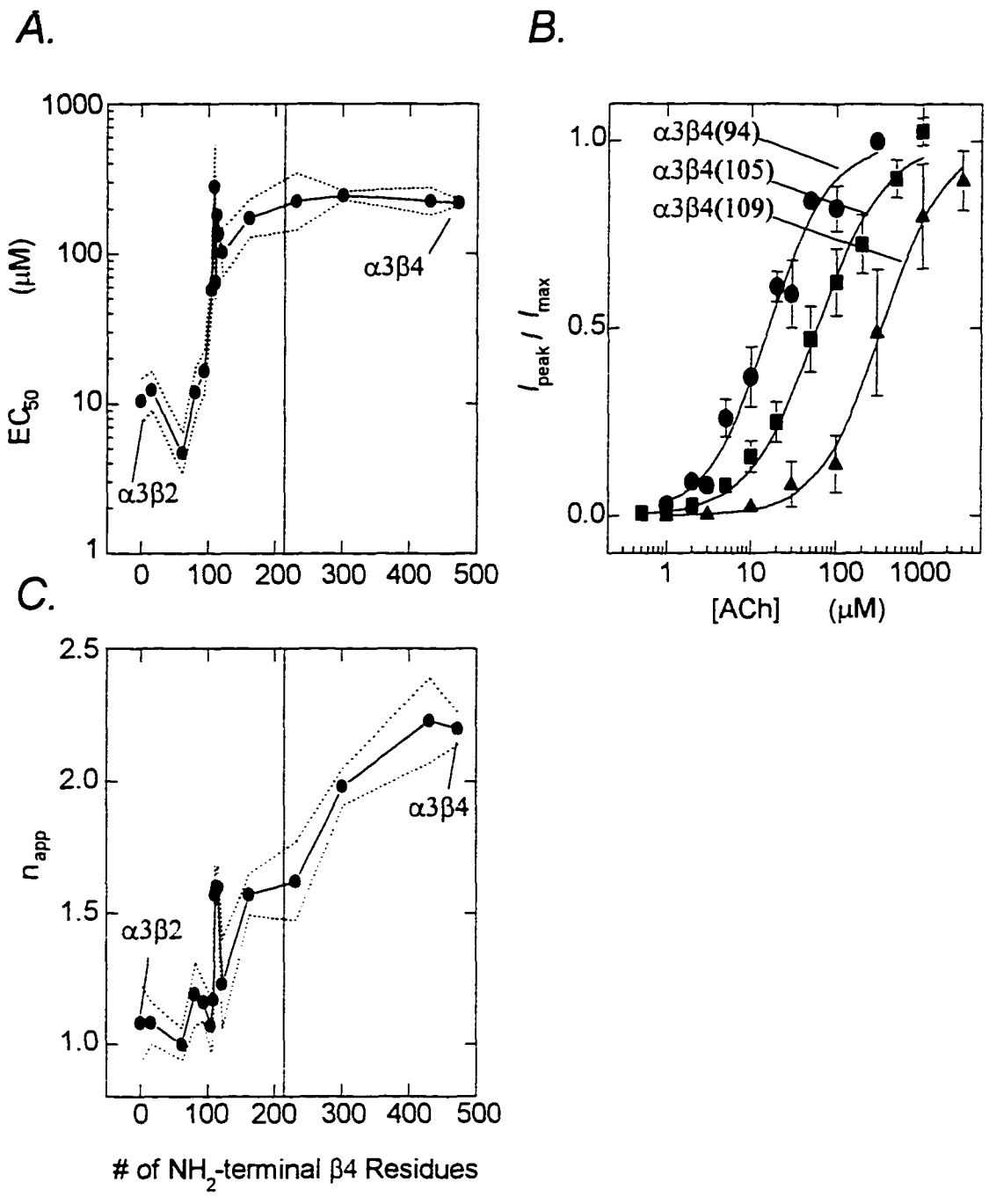
A.
B.
C.
1000
100
10
1
EC50 (μM)
α3β4
α3β2
0
100
200
300
400
500
1.0
0.5
0.0
Ipeak / Imax
α3β4(94)
α3β4(105)
α3β4(109)
1
10
100
1000
[ACh] (μM)
2.5
2.0
1.5
1.0
napp
α3β4
α3β2
# of NH2-terminal β4 Residues

Figure 5. (*A*) β2 $NH_2$-terminal substitutions have a more complex effect on the $EC_{50}$ for ACh than β4 $NH_2$-terminal substitutions. The symbols are mean values for the two wild-types and five β2 $NH_2$-terminal chimeras (n = 3-29). The dashed lines are ± SD. The vertical line denotes the beginning of M1. (*B*) Substituting β2:1-120 for the corresponding region of β4 reduces the $EC_{50}$ to a β2-like value. The symbols are the normalized responses ± SD. The lines are fits to the Hill equation. The $EC_{50}$'s for α3β2(120)•β4 and α3β4 are 15 ± 3 μM (n = 3) and 215 ± 8 μM (n = 3) (± SEE). (*C*) Substituting 93 or more β2 $NH_2$-terminal residues for the corresponding regions of β4 reduces the $n_{app}$ for ACh to β2-like values.

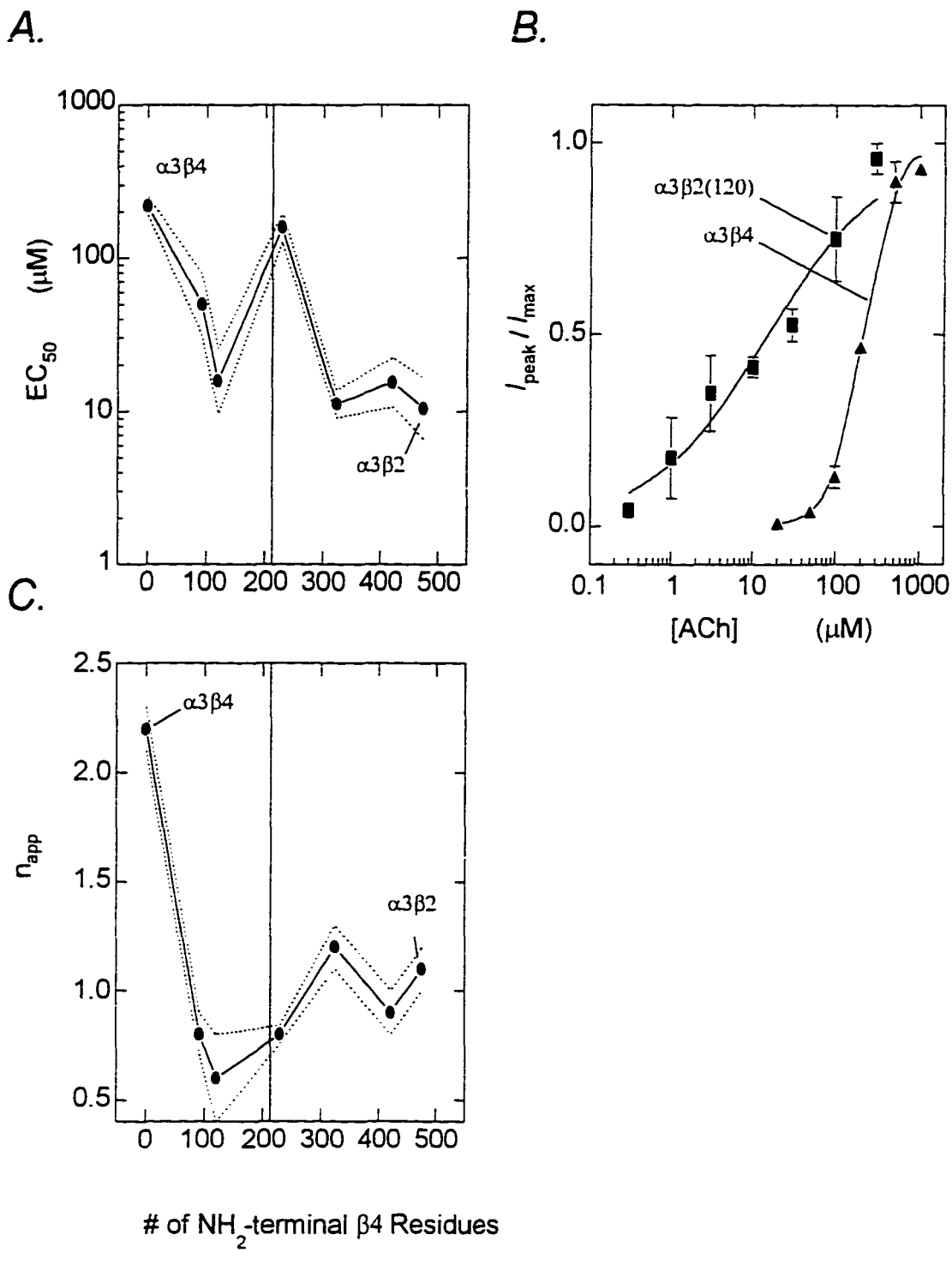
A.
B.
C.
1000
100
10
1
EC50 (μM)
α3β4
α3β2
0
100
200
300
400
500
1.0
0.5
0.0
Ipeak / Imax
α3β2(120)
α3β4
0.1
1
10
100
1000
[ACh] (μM)
2.5
2.0
1.5
1.0
0.5
napp
α3β4
α3β2
# of NH2-terminal β4 Residues

Figure 6. The α3β2(229)•β4 chimera displays a β2-like insensitivity to 30 μM CYT relative to ACh. (*A-D*) Responses to 30 μM CYT and 30 μM ACh at -50 mV. The square pulses above the traces denotes the release of agonist from the U tube.

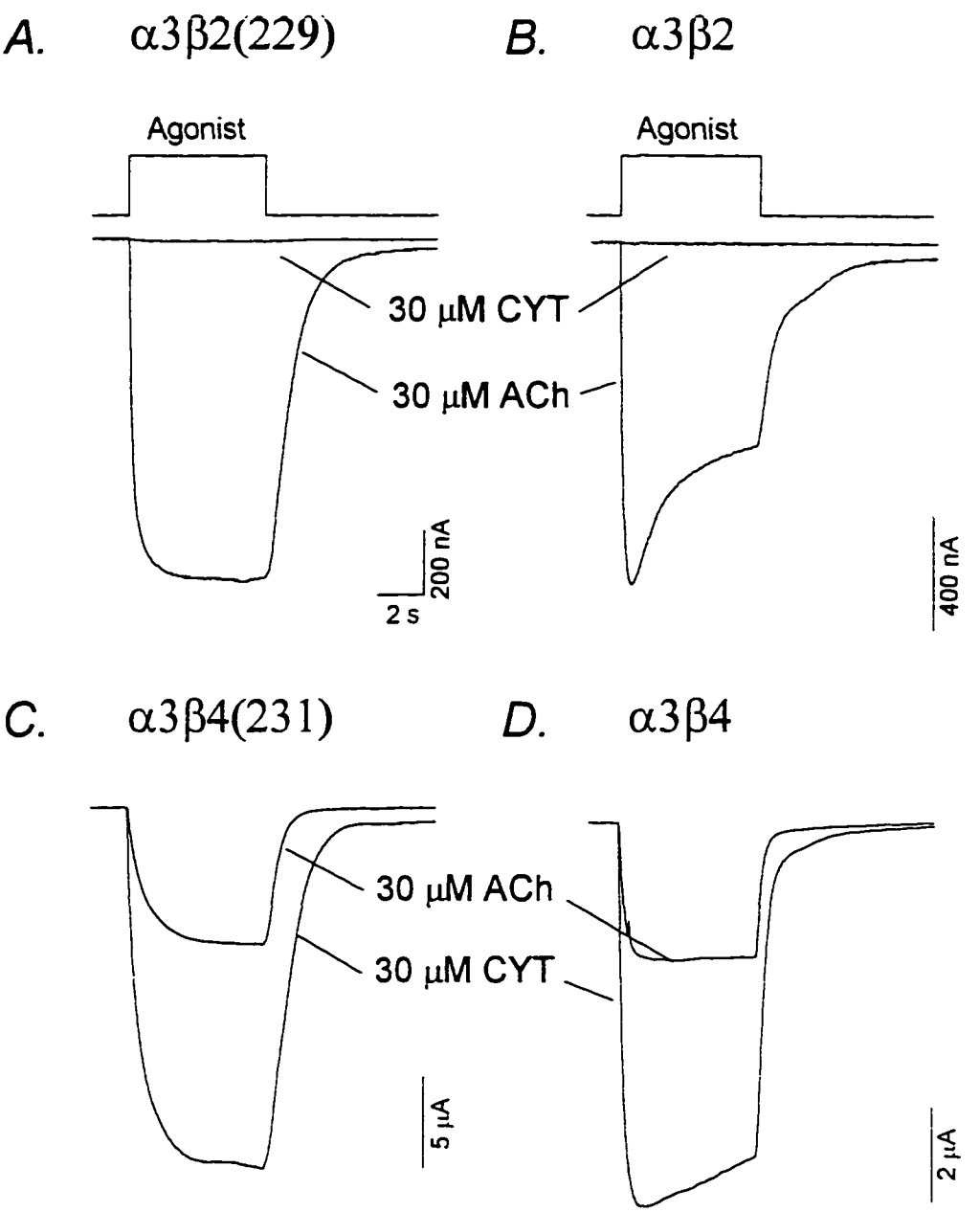
A.
α3β2(229)
B.
α3β2
Agonist
Agonist
30 μM CYT
30 μM ACh
200 nA
2 s
400 nA
C.
α3β4(231)
D.
α3β4
30 μM ACh
30 μM CYT
5 μA
2 μA

Figure 7. Exchanging β2:104-120 and β4:106-122 shifts the $EC_{50}$ of the ACh dose-response relationship in the appropriate direction. (*A*) Substituting β2:104-120 for β4:106-122 shifts the ACh dose-response relationship to right of the α3β4 dose-response relationship. (*B*) Substituting β4:106-122 for β2:104-120 shifts the dose-response relationship to the left of the α3β2 dose-response relationship.

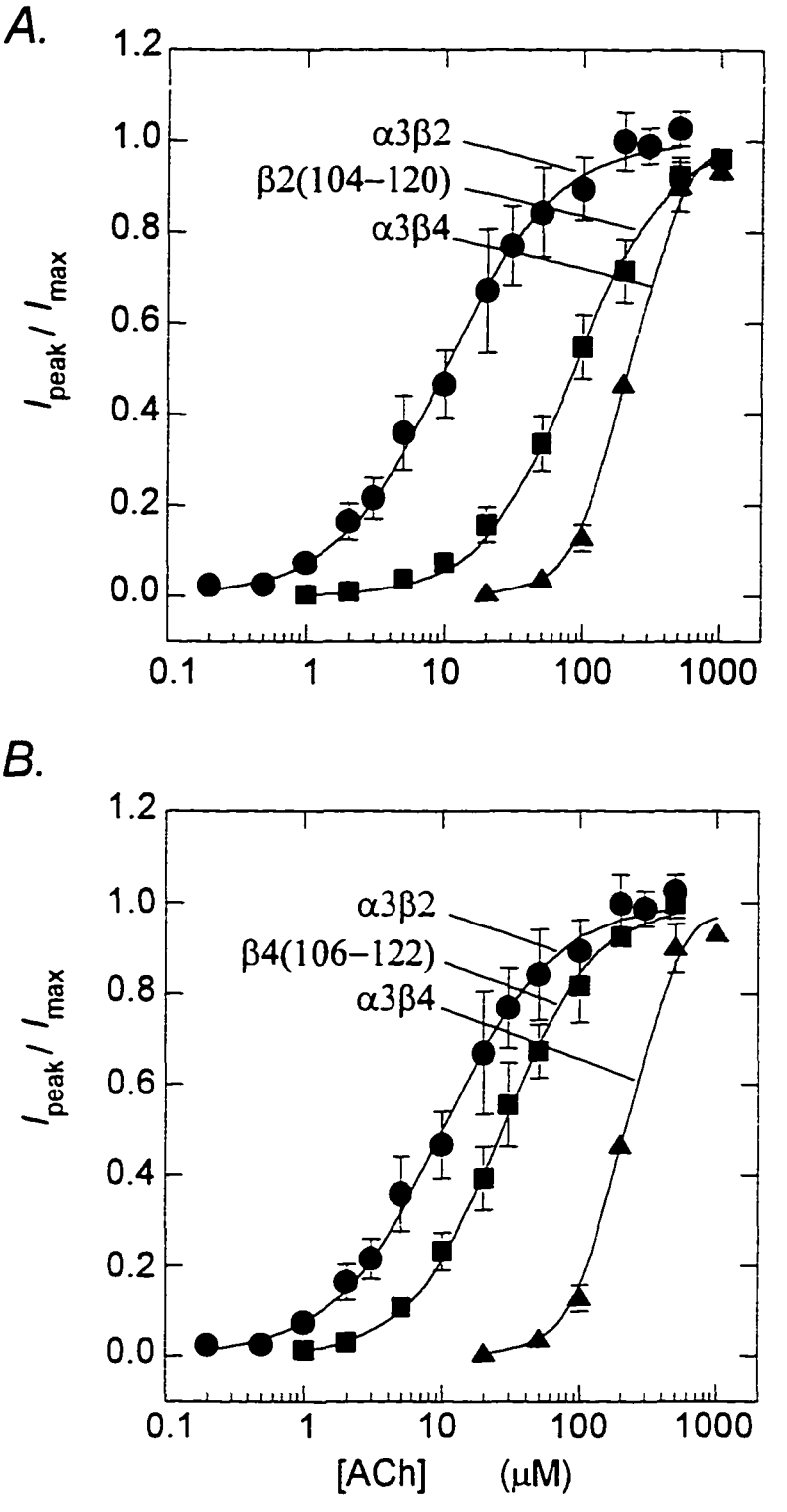
A.
1.2
1.0
0.8
0.6
0.4
0.2
0.0
$I_{peak}$ / $I_{max}$
α3β2
β2(104–120)
α3β4
0.1
1
10
100
1000
B.
1.2
1.0
0.8
0.6
0.4
0.2
0.0
$I_{peak}$ / $I_{max}$
α3β2
β4(106–122)
α3β4
0.1
1
10
100
1000
[ACh] (μM)

Figure 8. Exchanging β2:104-120 and β4:106-122 changes the ratio of the 30 μM cytisine (CYT) and 30 μM ACh responses and the ratio of the 100 μM tetramethylammonium (TMA) and 30 μM ACh responses. (*A*) Substituting β2:104-120 for β4:106-122 reduces the CYT/ACh response ratio to a β2-like value but substituting β4:106-122 for β2:104-120 only marginally increases the CYT/ACh response ratio. The solid bars are means ± SD. (*B*) Substituting β2:104-120 for β4:106-122 reduces the TMA/ACh response ratio to a β2-like value. Substituting β4:106-122 for β2:104-120 increases the TMA/ACh response ratio to an intermediate value.

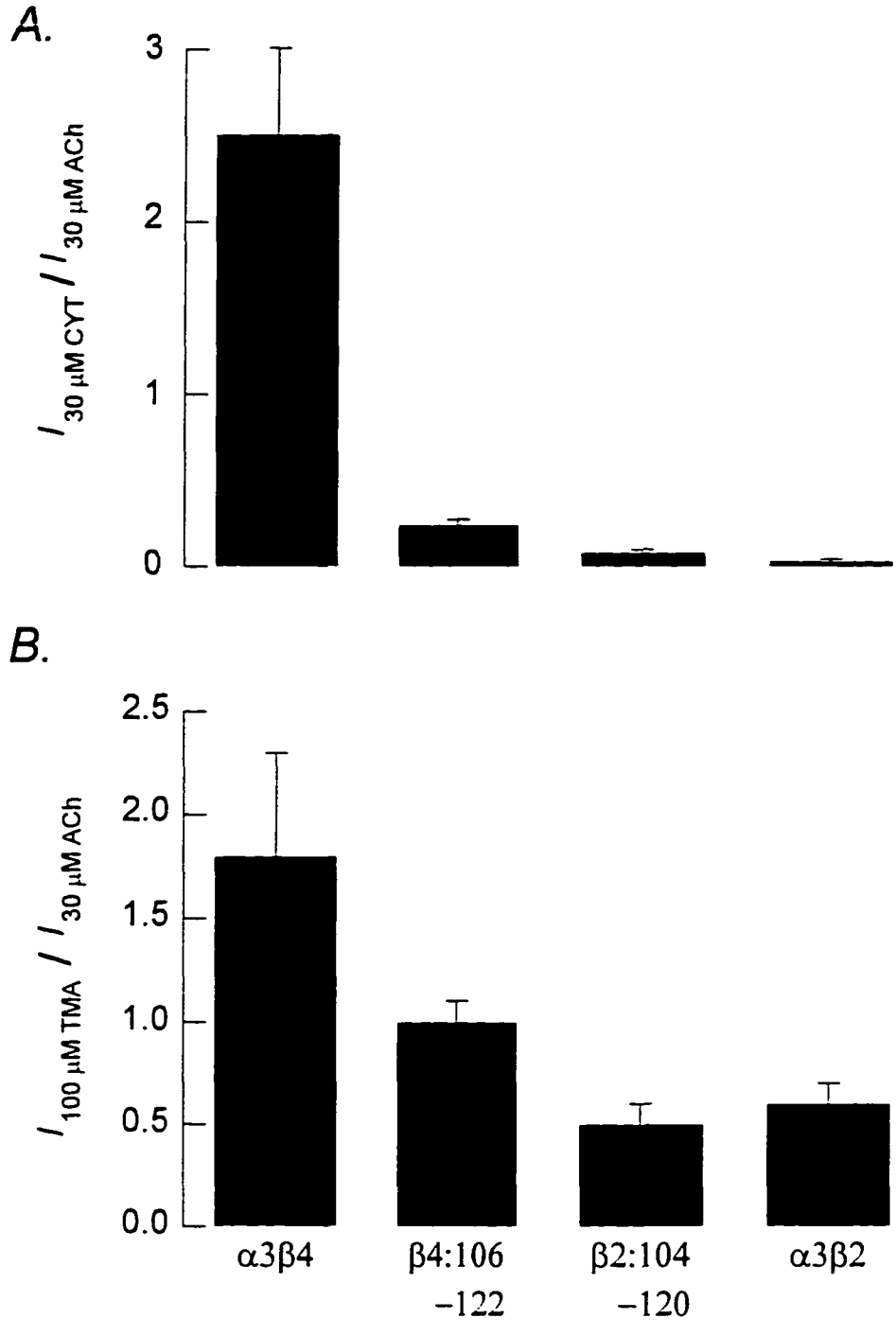
A.
$I_{30\ \mu M\ CYT}$ / $I_{30\ \mu M\ ACh}$
3
2
1
0
B.
$I_{100\ \mu M\ TMA}$ / $I_{30\ \mu M\ ACh}$
2.5
2.0
1.5
1.0
0.5
0.0
α3β4
β4:106
−122
β2:104
−120
α3β2

# VOLTAGE-JUMP RELAXATION KINETICS FOR WILD TYPE AND CHIMERIC β SUBUNITS OF NEURONAL NICOTINIC RECEPTORS

Antonio Figl,* Cesar Labarca,# Norman Davidson,# Henry A. Lester,# and Bruce N. Cohen~

From the *Division of Chemistry and Chemical Engineering; #Division of Biology, California Institute of Technology, Pasadena, California 91125; ~ Division of Biomedical Sciences, University of California at Riverside, Riverside, California, 92521-0121

## ABSTRACT

We have studied voltage-jump relaxations for a series of neuronal nicotinic acetylcholine receptors constructed by coexpression of wild type and chimeric β4/β2 subunits with α3 subunits in *Xenopus* oocytes. With acetylcholine or nicotine as agonists, wild type α3β4 receptors displayed five- to eightfold slower and larger voltage-jump relaxations than did wild type α3β2 receptors. In both cases, the relaxations could best be described by a two exponential-component fit, each component contributing approximately equal amplitudes over a wide range of [ACh]. Relaxation rate constants increased with [ACh] and saturated at 20- to 30-fold lower concentrations for the α3β2 receptor than for the α3β4 receptor, as observed previously for steady-state conductances. Furthermore, the chimeric β4/β2 subunits showed a transition in the concentration dependence of the rate constants in the region between residues 94 and 109, analogous to our previous observation with steady-state conductances. However, our experiments with a series of β-subunit chimeras did not localize residues that govern the absolute value of the kinetic parameters nor identified regions responsible for the voltage sensitivity. Hill coefficients for the relaxations also differed from those previously measured for steady state responses. Relaxation kinetics were virtually unchanged when the α3 subunit was replaced by the α4 subunit. The data reinforce previous conclusions that the region between residues 94 and 109 on the β subunit plays a role in binding agonist but also

show that other regions of the receptor control gating kinetics subsequent to the binding step.

# INTRODUCTION

It is now generally accepted that both α and β subunits of nicotinic acetylcholine receptors (nAChRs) contribute to the pharmacological profiles for agonists and antagonists (Luetje, Wada, Rogers, Abramson, Tsuji, Heinemann, and Patrick, 1990; Luetje and Patrick, 1991; Figl, Cohen, Quick, Davidson, and Lester, 1992; Papke, Duvoisin, and Heinemann, 1993; Wong, Mennerick, Clifford, Zorumski, and Isenberg, 1993; reviewed in Role, 1992; Sargent, 1993). Combinations containing the β4 subunit seem to be generally more sensitive to agonists, irrespective of the α subunit in the heteromultimeric receptor (Luetje et al., 1991). However, there is no direct evidence that non-α subunits actually form an agonist binding pocket (Unwin, 1995).

At the single-channel level, parameters such as open times, burst behavior, and conductances also depend on the type of α/β subunit combination (Papke, Boulter, Patrick, and Heinemann, 1989; Papke and Heinemann, 1991; reviewed in Papke, 1993). Specifically, α2, α3, and α4 produce channels with varied open times and single channel conductances when coexpressed with β2 in *Xenopus* oocytes (Papke et al., 1989). The β subunits appear to be involved in the regulation of the acetylcholine (ACh) dissociation rate from the channel, as well as agonist-bound opening rates (Papke et al., 1991).

Our previous work focused on macroscopic steady-state parameters. We showed that extending a chimeric β subunit from 94 to 109 β4 $NH_2$-terminal residues and

coexpressing it with the α3 subunit in *Xenopus* oocytes was sufficient (*a*) to restore the relative sensitivity to cytisine and tetramethylammonium (TMA) (Figl et al., 1992; Figl, Cohen, Gollub, Davidson, and Lester, 1993) and (*b*) to shift the half-maximal concentration for channel activation ($EC_{50}$) from an α3β2 to an α3β4 value (Cohen, Figl, Quick, Labarca, Davidson, and Lester, 1995).

To test the role of the β subunit in kinetic behavior, we have turned our attention to voltage-jump relaxation analysis of α3β2, α3β4 and receptors containing a series of chimeric β subunits. We show that (*a*) the two wild-type receptors exhibit markedly different relaxation kinetics across a wide ACh concentration range, (*b*) nicotine and ACh produce remarkably similar relaxation profiles, (*c*) exchanging α4 for α3 and coexpressing it with β4 has little effect on the time constants and (*d*) concentration dependence of the relaxation rate constants implicates once again the region between residues 94 and 109 in β4 as crucial in the response to agonists.

# METHODS

## *Construction of Chimeric β Subunits*

We used a previously published method to construct our chimeras (Cohen et al., 1995). In brief, the procedure incorporates a two-step PCR protocol (Higuchi, 1990). The first step generated two partially overlapping DNA fragments. In the second step, the two pieces were combined to generate a cassette incorporating the entire $NH_2$-terminal portion of β4 followed by the shortest possible segment of β2 containing a convenient restriction site. This cassette was cut by the appropriate restriction enzymes and ligated to an equivalently restricted native β2 cDNA to produce the complete chimeric cDNA. We checked the transition regions of the chimeras with a fluorescent dideoxy-terminator sequencing protocol from Applied Biosystems, Inc. (Foster City, CA).

Finally, we synthesized mRNA *in vitro* using the Ambion MEGAscript kit (Ambion Corp., Austin, TX) or a previously published method (Guastella, Nelson, Nelson, Czyzyk, Keynan, Miedel, Davidson, Lester, and Kanner, 1990).

## *Oocyte Expression*

We prepared *Xenopus* stage V-VI oocytes as described previously (Quick and Lester, 1994). α and β subunit cRNAs were injected in a stoichiometric ratio of 2:3. After injection we incubated the oocytes for 2-7 d at 20 °C in a modified Barth's solution supplemented with 5% horse serum, 50 μg/ml gentamicin and 2.5 mM Na-pyruvate.

## *Electrophysiological Recordings*

A detailed description of our U tube recording procedure is described elsewhere (Cohen et al., 1995). The recording solution consisted of 98 mM NaCl, 1 mM $MgCl_2$ and 5 mM HEPES (pH 7.4); we omitted $Ca^{2+}$ to prevent activation of the $Ca^{2+}$-activated $Cl^-$ channels (Vernino, Amador, Luetje, Patrick, and Dani, 1992).

Oocytes expressing endogenous muscarinic currents were not used in our experiments.

## *Data Collection and Analysis*

The holding potential between voltage-clamp episodes was -50 mV. The responses were filtered at 500 or 1000 Hz and analyzed using pCLAMP V. 6.0 software (Axon Instruments; Foster City, CA).

All our relaxations were fit with two exponential components. Relaxation values are expressed as time constants (in ms) or as the reciprocal of this value, rate constants (in $s^{-1}$). The $1/\tau$ values above 100 μM ACh for the α3β2 and 1000 μM ACh for the α3β4 for the fast components, and responses above 50 μM ACh for the α3β2 and 200 μM ACh for the α3β4 receptors for the slow components were not included in our dose-response analysis because they progressively decreased in value. Although we are unsure about the cause of this phenomenon, we suspect that contribution by desensitized or blocked states may be responsible. All data points were averaged across voltage to simplify comparisons. To determine $EC_{50}$'s and $n_{app}$'s for the dose-response relations, we fit the data, by weighted nonlinear least-squares regression, to a modified Hill equation:

$$1/\tau = \frac{1/\tau_{max}}{1+\left(EC_{50}/[ACh]\right)^{n_{app}}} + 1/\tau_0 \qquad (1)$$

where $1/\tau$ was the measured rate constant at agonist concentration [ACh], $1/\tau_0$ was the rate constant at the low-concentration limit and was determined by extrapolation of the

dose-response relationships to [ACh] = 0. We also fixed $n_{app}$ at the value that best approximated the shape of the curve. Thus, only $1/\tau_{max}$ and $EC_{50}$ were left to vary. For the normalization procedure in Fig. 6, we subtracted $1/\tau_0$ from $1/\tau$ and divided the result by $1/\tau_{max}$.

# RESULTS

## *The Voltage-Jump Relaxation Procedure*

This article describes in detail the voltage dependence of α3β2 and α3β4 receptors. We first describe the framework of our analyses.

Fig. 1 shows sample traces illustrating the voltage-clamp protocol used for most experiments in this study. The ACh concentration was 1 μM ACh. The membrane potential was held at -50 mV, stepped to a prepulse value of +50 mV, then jumped again to various test potentials between -150 and -50 mV in 20 mV increments. In general, we found that (*a*) the currents relaxed to more negative steady-state values with time (Fig. 1, *A* and *B*), implying (*a*) that further channels opened upon hyperpolarization; and (*b*) the relaxations were progressively larger at more negative test potentials (Fig. 1 *D*). Fig. 1 also illustrates the marked difference in relaxation phenotype for the two receptors, with α3β2 showing relaxations that are briefer in duration (see also Fig. 4) and smaller in amplitude (Fig. 1 *D*) than their α3β4 counterparts at equivalent ACh concentrations.

These kinetic data can be quantified in several ways. For instance, Fig. 1 *B* shows one- and two-exponential fits to the -150 mV traces in panel *A*. Whereas the single-exponential fit clearly deviates from the data, the two-exponential curves superimpose on the traces. We noticed this behavior at all other voltages and concentrations studied.

The total relaxation amplitude ($I_{ss}$) is the sum of two components: an instantaneous component, $I_{inst}$, and a relaxation component $I_{relax}$. $I_{inst}$ is proportional to the number of channels that are "available" at the prepulse potential (in our case, +50 mV); $I_{relax}$ describes the voltage-dependent opening recruitment of new channels at the test voltage (the preceding paragraph shows that $I_{relax}$ itself consists of two distinct exponential components). Steady-state current-voltage (*I-V*) relations of neuronal nAChRs typically show steep inward rectification (Ifune and Steinbach, 1990b, Ifune and Steinbach, 1992; Sands and Barish, 1992). In order to determine which component of the relaxation, $I_{inst}$ or $I_{relax}$, is responsible for the steady-state rectification, we plotted the voltage dependence of $I_{inst}$ (Fig. 1 *C*). These relations, obtained by extrapolating the currents to the time of the test jump , showed only small nonlinearities; the major rectification in the steady-state current-voltage relations therefore arises from the kinetically resolvable component $I_{relax}$ .

We investigated the relative sizes of the two relaxation components, $I_{inst}$ and $I_{relax}$ to compare the relative voltage dependence of the two receptor types. The contribution of the relaxations can be quantified by plotting the ratio between the instantaneous and steady-state values, $I_{ss}/I_{inst}$ (Fig. 1 *D*). In general, $\alpha3\beta4$ relaxations are much larger than $\alpha3\beta2$ relaxations, underscoring a larger voltage dependence (described below) of $\alpha3\beta4$ receptors. Average values for this parameter, from many experiments, are plotted in Fig. 7 below.

The different voltage sensitivities of the steady-state currents were also reflected by different voltage dependences of the rate constants (Fig. 2). In general, there were no clear voltage dependences of the rate constants for the α3β2 receptor, but the α3β4 receptor displayed a roughly twofold change in both the fast and slow rate constants over the range from -70 mV to -150 mV at the exemplar ACh concentration of 1 μM.

*Availability*

Because neuronal receptors show macroscopic inward rectification partially due to channel blockade by intracellular $Mg^{2+}$, (Ifune and Steinbach, 1990a; Ifune and Steinbach, 1991; Sands et al., 1992) it was not possible to measure currents at positive potentials. We therefore devised a protocol to study voltage-dependent availability by measuring instantaneous currents just after hyperpolarizing voltage jumps from various prepulse potentials (Fig. 3). The data show, as expected, that the fraction of instantaneous current ($I_{inst}/I_{ss}$) decreases at less negative potentials for both α3β2 and α3β4 receptors; the straightforward explanation of this effect is that fewer channels are open at steady state as the membrane is depolarized (Sheridan and Lester, 1977). Availability was quantified by fitting the data by nonlinear least-squares regression with a Boltzmann function:

$$I_{inst}(V)/I_{ss} = \frac{1 - p_{min}}{1 + \exp\left[(V - V_n)/k_n\right]} + p_{min} \qquad (2)$$

where $V_n$ represents the half-maximal activation potential, $k_n$ is the slope factor and expresses the steepness of the voltage dependence and $p_{min}$ is the plateau of availability at depolarized voltages. The data presented in Fig. 3 *C* are a composite of two separate experiments. These data show, again, that the α3β2 receptor is less voltage sensitive than the α3β4 receptor: the slope factors, $k_n$, were 27 mV and 16 mV, respectively.

Surprisingly, there is a plateau of availability for both receptors, at ~ 0.56 for the α3β2 receptor and ~ 0.17 for the α3β4 receptor, implying that in the case of α3β2 receptors, more than half remain "available" for opening at our most positive test potentials. This point is treated in the Discussion.

A final point is that the availability did not depend noticeably on the duration of the prepulse. For the α3β2 receptors, the prepulse was varied between 50 and 400 ms; for the α3β4 receptors, the prepulse was varied between 200 ms and 2 s. In both cases, we saw no significant changes in the relaxation parameters. This indicates that channel availability reached steady state on a time scale more rapid than the briefest prepulses tested.

*Nicotine as Agonist*

Voltage-jump relaxations were also performed with nicotine as agonist (2, 10 and 50 μM). In general, relaxations waveforms closely resembled those for ACh; both receptors showed voltage-dependent steady-state currents, and α3β4 currents were more voltage dependent than α3β2 currents. There were two exponential components, with rate constants ~225 $s^{-1}$ and 40 $s^{-1}$ for the α3β2 receptor and ~ 50 $s^{-1}$ and 5 $s^{-1}$ for the α3β4 receptor. These values are similar to those we observed for ACh as agonist at similar concentrations.

*Initial Theoretical Treatment*

Because the voltage-jump relaxations will be employed throughout this study, we wish to provide a sketch of the theoretical background at this point. The most straightforward interpretations of these relaxations are that (*a*) channels open more frequently at more negative potentials, and/or (*b*) the channels remain open for a longer period of time. Although we cannot yet specify the molecular nature of the voltage-dependent rate-limiting gating step that gives rise to the relaxations, it is generally observed for nicotinic receptors that the number of channels open at more depolarized potentials decreases (Lester, 1992). In particular, for muscle receptors it is usually thought that a change in the dipole moment between the open and closed states gives rise to the voltage dependence (Magleby and Stevens, 1972).

The fact that voltage-dependent availability shows a plateau at positive potentials has been attributed to a change in the dipole moment at these potentials (Dionne and Stevens 1975). However, an equally plausible hypothesis for the plateau derives from the well-known blockade of various neuronal nAChRs by intracellular $Mg^{2+}$ at positive potentials (Lester, 1992). In this alternative hypothesis, $Mg^{2+}$ would trap the channel in a "blocked but open" state, prolonging the lifetime of the open state at positive potentials. This hypothesis gains plausibility from the fact that inwardly rectifying $K^+$ channels display steady-state current relations and plateau values for availability in symmetrical $K^+$ solutions that strongly resemble the present data for ACh receptors (Silver and DeCoursey, 1990; Doupnik, Lim, Kofuji, Davidson, and Lester, 1995). Although it is thought that $Mg^{2+}$ blockade equilibrates within a fraction of 1 ms, it is conceivable that the voltage-jump relaxations also partially reflect voltage-dependent blockade by $Mg^{2+}$ or other intracellular polycations.

Despite these uncertainties about the precise molecular nature of the voltage-jump relaxations, they comprise a readily quantifiable kinetic phenomenon that we can use for studying kinetic properties of chimeric subunits. Furthermore, the two wild-type receptors clearly differ in these voltage-dependent gating properties. In general, gating of the $\alpha3\beta2$ receptor seems less voltage-dependent than that of the $\alpha3\beta4$ receptor and $\alpha3\beta2$ relaxations are much faster than their $\alpha3\beta4$ counterparts.

## *Concentration Dependence of Voltage-Jump Kinetics*

This paper deals with the differing kinetic characteristics of the α3β2 and α3β4 receptors. To help study the underlying mechanism of the relaxations, we measured voltage-jump relaxations over a range of ACh concentrations for the α3β2 and α3β4 receptors (Fig. 4). There was a clear trend toward more rapid relaxations at higher [ACh], for both exponential components and for both receptors. We abstracted these data into the following parameters: zero-concentration limit $1/\tau_0$, high-concentration limit $1/\tau_{max}$, $EC_{50}$, and Hill coefficient $n_{app}$ (Eq. 1). The two receptors showed clearly different concentration dependences. For the α3β2 receptor, both the fast phase and the slow phase showed a plateau at [ACh] > ~ 10 μM; the average $EC_{50}$ values for the fast and slow phases were 2.3 and 3.1 μM, respectively. For the α3β4 receptor, on the other hand, the average $EC_{50}$ values were 67 and 58 μM. The more rapid kinetics of the α3β2 receptor were reflected in the facts that (*a*) at equal concentrations, α3β2 relaxation profiles were faster than α3β4 relaxations (Fig. 4, *A* and *B*); (*b*) the $1/\tau_0$ values for α3β2 (10 $s^{-1}$ and 50 $s^{-1}$) were somewhat higher than the corresponding values for α3β4 (4 $s^{-1}$ and 15 $s^{-1}$); and (*c*) the $1/\tau_{max}$ values for α3β2 (50 $s^{-1}$ and 316 $s^{-1}$) were somewhat higher than the corresponding values for α3β4 (36 $s^{-1}$ and 168 $s^{-1}$).

The Hill coefficients of the α3β2 receptor were 1.7 for both fast and slow components and 0.8 for both components of the α3β4 receptor. Interestingly, the Hill coefficients for the relaxation dose-response data are roughly the opposite of the values we determined for the steady-state dose response relationships ($n_H$ = 1.1 for the α3β2 and $n_H$ = 2.0 for the α3β4 receptors (Cohen et al., 1995)).

There are admittedly some imprecise points in these analyses. First, we pooled the data across all voltages; for α3β4, in particular, the clear voltage dependences of the relaxation time constants (Fig. 2) resulted in voltage-dependent dose-response relations. For instance, for the fast components, we found that $EC_{50}$ was about twofold greater at -70 mV than at -150 mV and $n_{app}$= 1.0 and 1.3, respectively. All estimates for α3β4 $EC_{50}$ exceed the corresponding α3β2 values by ~ tenfold, however; and we felt that pooling the data across all voltages was desirable to provide a simple picture of the results. Second, the relaxation rate constants tended to decrease somewhat at concentrations higher than those presented in Fig. 4. These declines reached a factor of two for the α3β2 receptor at 1 mM ACh; we suspect that they arose from either desensitization or channel block and we did not investigate this phenomenon further.

Each relaxation had two exponential components; and our analysis provided the relative amplitudes of these components. Surprisingly, the amplitudes were roughly equal, independent of both (*a*) [ACh] and (*b*) the subunit composition of the receptor

(Fig. 4, *C* and *D*). Thus, the global average $I_{fast}/I_{tot}$ was 0.55 ± 0.06 for α3β2 and 0.51 ± 0.10 for α3β4 (mean ± SD, n > 30).

Another surprising result of our analysis is that the $EC_{50}$ values for $1/\tau$ do not equal the $EC_{50}$ values for steady-state responses reported in a previous study (Cohen et al., 1995). In general, the $1/\tau$ $EC_{50}$ values for both receptors are lower than those for the steady-state currents by three- to fourfold. In most straightforward relaxation theories that attempt to obtain equilibrium parameters by kinetics, the $EC_{50}$ for $1/\tau$ equals or exceeds that for equilibrium activation (Adams, 1981). Thus, there remain interesting questions about the molecular and mechanistic details of ACh responses in our experiments. Nonetheless, the concentration dependences of the kinetic parameters provide a convenient set of metrics for studying the properties of chimeric subunits.

## *Kinetic Properties of Chimeric β Subunits*

We conducted kinetic experiments on the series of β4/β2 subunit chimeras reported in a previous study (Cohen et al., 1995). For convenience, the transition points of these chimeras are presented again here as Fig. 5. Previous results showed important effects of residues in the region between positions 94 and 109 when various β4/β2 subunit chimeras were coexpressed with the α3 subunit. We therefore concentrated our efforts on chimeras in this crucial region.

Fig. 6, *A* and *B* present the concentration dependences for the voltage-jump rate constants with three of the chimeras that span the width of the region we recently found important in determining $EC_{50}$ phenotypes (Cohen et al., 1995). The rate constants all fall within the same general range observed for the wild-type receptors: 100 to 350 $s^{-1}$ for the fast rate constants (Fig. 6 *A*) and 20 to 80 $s^{-1}$ for the slow rate constants (Fig. 6 *B*). Inspection of Fig. 6, *A* and *B* shows, however, that the rate constants for α3β4(94) tend to saturate at [ACh] > 10 μM, whereas the rate constants for α3β4(109) and for α3β4(122) continue to increase for the highest [ACh] used in these studies, 50 μM.

We have clarified this picture by normalizing the concentration dependences as follows. For each receptor, the dose-response data were fit to the modified Hill equation, Eq. (1) above. The zero-concentration intercepts, $1/\tau_0$, were subtracted, leaving only the concentration-dependent parts of the dose-response relation. Next, the data were normalized by dividing by $1/\tau_{max}$. These subtracted and normalized dose-response relations are plotted in Fig. 6 *C* and 6 *D* (fast and slow rate constants, respectively). The plots emphasize that the three chimeras segregate into two groups: rate constants for α3β4(94) saturate within the range of concentrations tested, while rate constants for α3β4(109) and for α3β4(122) do not saturate within the range studied and appear shifted toward higher concentrations.

The fitted values for $EC_{50}$ quantify these impressions: For the fast components, α3β4(94) had an $EC_{50}$ of 1.9 μM, α3β4(109) an $EC_{50}$ of 98 μM and α3β4(122) an $EC_{50}$ of 190 μM. The $EC_{50}$ values for the slow rate constants were 1.0 μM for the α3β4(94), 250 μM for the α3β4(109) and 340 μM for the α3β4(122) receptors. Thus, the $EC_{50}$ values for the α3β4(94) receptor resemble those for the wild-type α3β2 receptor (2.3 and 3.1 μM for fast and slow relaxations, respectively); whereas the values for α3β4(109) and α3β4(122) chimeras are much greater. It must be appreciated that uncertainties attend the estimate of $EC_{50}$ for data that show little signs of saturation, so that the $EC_{50}$ for the α3β4(109) and α3β4(122) should be considered as roughly comparable to that for the wild-type α3β4 receptor.

Despite the normalizations and other data manipulations involved, our data clearly show the following. When we extended the β4 $NH_2$-terminal portions from residue 94 to residue 109, the dose-response relation shifted rightward (Fig. 6, *A* and *B* for the fast and slow relaxations, respectively). However, this rightward shift was not accompanied by a pronounced drop in the rate constants to α3β4 values (cf. Fig. 4). These results are very similar to our observations, with steady-state measurements, that the dose-response relation shifts rightward by several fold for the same chimeras within the region 94 to 109 (Cohen et al., 1995).

Thus, both our steady-state and kinetic data show that a region of β4, spanning residues 94 to 109, is sufficient to shift the $EC_{50}$ from an α3β2 to an α3β4 value. Nonetheless, the absolute values of the kinetic constants themselves do not vary appreciably within this series of chimeras.

## *Neither Chimeras nor Point Mutations Localize Voltage Dependence or Kinetics*

We comment briefly on the extensive kinetic measurements we have made with 20 other chimeras in the series of Fig. 5. In all cases, these chimeras displayed (*a*) voltage-dependent steady-state responses to ACh, (*b*) voltage-jump relaxations with two exponential components, and (*c*) rate constants for these relaxations in the range of 10 to 400 $s^{-1}$. Thus, the kinetic phenomenology for the chimeric β subunits falls within the range observed for the two wild-type subunits. However, none of the chimeras we tested approached the unique kinetic and steady-state signature of the wild-type α3β4 receptor: slow relaxation rate constants (~ 3 $s^{-1}$) leading to several-fold increases in the conductance.

Examples of the data are shown in Fig. 7, which analyzes steady-state voltage dependence by plotting $I_{ss}/I_{inst}$ versus voltage for several chimeras with progressively longer β4 $NH_2$-termini. Importantly, there are no major changes in voltage sensitivity

within the series that span the range including positions 94 and 109. Therefore, the voltage dependence is not controlled by the same residues that control the $EC_{50}$ for the kinetics. A partial transition to the β4 wild-type phenotype occurs for the α3β4(301) chimera, but its voltage dependence is still much more similar to that of the α3β2 receptor than to that of the α3β4 receptor.

Given the importance of the M2 region for gating of neuronal (Revah, Bertrand, Galzi, Devillers-Thiery, Mulle, Hussy, Bertrand, Ballivet, and Changeux, 1991) and muscle (Labarca, Nowak, Zhang, Tang, Deshpande, and Lester, 1995) nAChRs, we were interested in examining the differences between the β2 and β4 subunits within the M2 region. There is only one amino acid substitution (Fig. 5): β2 has a valine and β4 has a phenylalanine residue at position 13' (Charnet, Labarca, Leonard, Vogelaar, Czyzyk, Gouin, Davidson, and Lester, 1990). We constructed and tested the two appropriate point mutants ($\beta2_{V13'F}$ and $\beta4_{F13'V}$) and found that the voltage-jump relaxation phenotypes for these mutants were unchanged from those of the respective wild-type subunits (data not shown).

## *The Relaxation Profiles of α3β4 and α4β4 Are Virtually Indistinguishable*

Luetje and Patrick (Luetje et al., 1991) showed that sensitivity to agonists such as ACh, nicotine, cytisine and 1,1-dimethyl-4-phenylpiperazinium (DMPP) was controlled by both the α and β subunits. Voltage-jump relaxation experiments have previously been reported for α4β2 receptors expressed in oocytes (Charnet, Labarca, Cohen, Davidson, Lester, and Pilar, 1991); and properties are similar to those reported here for α3β2 receptors: weak voltage dependence and relaxations on a time scale of tens of ms.

In order to determine in greater detail whether relaxation behavior depends strongly on the identity of the α subunit, we substituted α4 for α3 and coexpressed it with β4 in oocytes. We tested this combination for [ACh] in the range from 0.2 to 5 μM. Voltage-jump relaxation waveforms for this combination were virtually indistinguishable from those for the α3β4 combination at the concentrations tested (Fig. 8 *A*); both the fast and slow rate constants for α3β4 and α4β4 are nearly identical (Fig. 8 *B*), at least for the beginning of the dose-response relation. Clearly the β subunit plays a major role in controlling the kinetic behavior of neuronal nicotinic receptors.

# DISCUSSION

## *General Remarks: Role of the β Subunit*

The present article describes for the first time a thorough analysis of the voltage-jump relaxation behavior of α3β2 and α3β4 neuronal nAChRs. We describe in detail both the voltage dependence of steady-state responses, the kinetics of voltage-jump relaxations, and the concentration dependence of these rate constants. In addition, the study continues our analysis of functional domains of neuronal nAChR β subunits. The present data complement our earlier steady-state data (Cohen et al., 1995).

We observe clear differences between the wild-type β2 and β4 subunits when coexpressed with the α3 subunit (Fig. 1 and Fig. 4). The α3β2 receptors display less voltage sensitivity, more rapid kinetics, greater sensitivity to ACh, and a greater Hill coefficient than the α3β4 receptors. The difference in agonist sensitivity was expected from the steady-state data; the difference in Hill coefficient is more surprising.

Furthermore, we are again intrigued by the central role that β subunits appear to play in determining the characteristics of the functional pentamer since replacing the α3 subunit, used for most of our studies, by the α4 subunit had a marginal effect on the relaxation phenotypes at low agonist concentrations (Fig. 8). Because voltage-jump

relaxations at low agonist concentrations reflect primarily the burst duration, we conclude that the burst duration is similar for α3β4 and α4β4 receptors. We do not know whether the kinetics would differ at higher [ACh]; if so, this would reflect a difference in the frequency of bursts at a given concentration.

The M2 region of neuronal nicotinic receptors is known to be important in affecting gating properties (Revah et al., 1991; Bertrand, Devillers-Thiery, Revah, Galzi, Hussy, Mulle, Bertrand, Ballivet, and Changeux, 1992). The two β subunits in this work differed by only one amino acid in M2 ($\beta2_{13'V}$; $\beta4_{13'F}$), yet this mutation was unable to affect any parameter of the relaxation behavior. We must therefore conclude that the regions that determine the voltage sensitivity of the relaxations as contributed by the two β subunits are outside M2.

Strikingly, the present data complement the steady-state data in showing that the region between positions 94 and 109 is crucial in determining how the agonist affects gating. The time scale of gating is not affected by varying the transition point of chimeras in this region; but the transition does affect the relationship between agonist concentration and the time scale of gating. This is a subtle combination of concepts; it can best be understood by referring to Fig. 4 and Fig. 7. Our molecular interpretation of these data follows: channels open more frequently as [ACh] increases. The relationship between [ACh] and the opening frequency depends on residues in the region discussed; but the time scale of the opening events is determined elsewhere in the receptor, as

discussed in the following section. Our experiments do not localize the region that determines the time scale of channel opening: nor do they localize the region that determines the voltage dependence of channel gating.

## *Molecular Basis of the Relaxations*

To analyze the concentration dependence of the kinetics, we use a simple model similar to those employed for extensive voltage-jump studies of muscle nAChRs (Adams, 1975; Neher and Sakmann, 1975; Sheridan and Lester, 1975; Adams et al., 1980). The model involves a fast binding step followed by a slower conformational transition that leads to channel opening:

$$R \underset{k_{-1}}{\overset{k_1[A]^n}{\Leftrightarrow}} A_nR \underset{\alpha}{\overset{\beta}{\Leftrightarrow}} A_nR^*$$

*fast* *slow*

SCHEME I

where $k_1$ and $k_{-1}$ represent the forward and backward rate constants of binding, respectively; $\beta$ and $\alpha$ are the forward and backward rate constants for the channel-opening transition; $n$ is the Hill coefficient; A is the ligand and R the receptor. This

scheme, consisting of two transitions, predicts two relaxation rate constants. With our assumption that the $\beta/\alpha$ transition is slower and rate-limiting, the slower relaxation rate constant becomes:

$$1/\tau = \alpha + \frac{\beta}{1+(K_d/[A])^n} \qquad (3)$$

where $K_d = k_{-1}/k_1$.

According to this scheme, the zero-[ACh] limit is $\alpha$; the high-[ACh] limit is $\alpha + \beta$; and our estimated $EC_{50}$ values equal the dissociation constants ($K_d$) of SCHEME I. A more exact model would explicitly deal with each of the $n$ binding reactions; but for $n \leq 2$, the half-maximal concentration differs by less than fourfold from $K_d$ if $k_{-1}/k_1$ is equal for the two reactions.

It is thought that the opening rate is relatively independent of voltage; on the other hand, the closing rate is dependent on voltage. Single-channel recordings, however, reveal many types of opening and closing transitions, on times scales ranging from tens of μs to tens of s. The observed relaxations, on time scales of ms to hundreds of ms, are generally thought to arise from voltage-dependent "burst durations." A burst is thought to arise from binding of a single pair of agonist molecules and to comprise a series of single-channel openings separated by intervals whose time scale is roughly equal to, or

shorter than, the duration of the openings. We suggest that the present relaxations measure the frequency ($\alpha$) and duration ($1/\beta$) of such bursts. $\alpha3\beta2$ bursts are several fold briefer than $\alpha3\beta4$ bursts, in agreement with this interpretation (Papke et al., 1991). The relaxations are too slow to arise directly from single-channel openings (Charnet et al., 1991; Papke et al., 1991).

Voltage-jump relaxations cannot be caused by a voltage-dependent step that is *slower* than the time scale of the relaxations; but the voltage-dependent step could be much *faster* than the time scale of the relaxations. In the Results section, we point out that a rapidly equilibrating, voltage-dependent open-channel blockade by $Mg^{2+}$ could be influencing our relaxations at positive potentials.

## *Two Components to the Voltage-Jump Relaxations*

We certainly did not begin this study attempting to find complexities in our relaxations. Indeed, muscle nAChR relaxations have been fit with single exponentials for decades; and in an earlier study of $\alpha4\beta2$ receptors from this laboratory, we found that a single exponential component fit the data fairly well under some conditions (Charnet et al., 1991). However, the more extensive data analyzed for the present study showed (*a*) that two components fit each of several thousand relaxations better than did a single component; and (*b*) a third component added little improvement.

What is the physical significance of the two phases? Given our uncertainty about the molecular events that underlie the relaxations. we cannot be certain. Nonetheless, we are struck by the near equality in the amplitudes of the two components over a wide range of [ACh] (Fig. 4, *C* and *D*). We therefore doubt that the two components describe interconvertible states of a single molecule. We suggest instead that the two components reflect distinct, non-interconvertible populations of receptors. The most straightforward, but admittedly daring explanation, is that (*a*) two neuronal nAChR pentamers reside next to each other in the membrane (Zingsheim, Neugebauer, Frank, Hanicke, and Barrantes, 1982), (*b*) the two pentamers are slightly asymmetric, and (*c*) the asymmetry reveals itself in our kinetic experiments as a difference in gating behavior. Structural studies are necessary to resolve this issue.

## *Unresolved Issues*

Several aspects of our data are unexpected on the basis of steady-state measurements. First. the $EC_{50}$ for the relaxation rate constants are several fold smaller than for the steady-state currents. Many theories of gating allow for opening rate constants that continue to increase past saturation of the steady-state response; but no simple theory predicts that opening rates saturate at concentrations lower than steady-state responses. Likewise, we can offer no simple explanation for the fact that the Hill coefficients for the

rates constants differ from those for steady-state responses: $n_{app}$ is near one for α3β2 steady-state currents and for α3β4 rate constants, but near two for α3β4 steady-state currents and for α3β2 rate constants.

Acetylcholine receptor gating remains a complex but fascinating problem. For each region identified as important, such as the 94 to 109 region that influences concentration dependence, other phenomena, such as the kinetics and voltage dependence of the process, remain mysterious.

# REFERENCES

Adams, D. J., T. M. Dwyer, and B. Hille. 1980. The permeability of endplate channels to monovalent and divalent metal cations. *Journal of General Physiology.* 75: 493-510.

Adams, P. R. 1975. A model for the procaine end-plate current. *Journal of Physiology.* 246: 61p-63p.

Adams, P. R. 1981. Acetylcholine receptor kinetics. *Journal of Membrane Biology.* 58: 161-174.

Bertrand, D., A. Devillers-Thiery, F. Revah, J.-L. Galzi, N. Hussy, C. Mulle, S. Bertrand, M. Ballivet, and J.-P. Changeux. 1992. Unconventional pharmacology of a neuronal nicotinic receptor mutated in the channel domain. *Proceedings of the National Academy of Sciences, USA.* 89: 1261-1265.

Charnet, P., C. Labarca, R. J. Leonard, N. J. Vogelaar, L. Czyzyk, A. Gouin, N. Davidson, and H. A. Lester. 1990. An open-channel blocker interacts with adjacent turns of α-helices in the nicotinic acetylcholine receptor. *Neuron.* 2: 87-95.

Charnet, P., C. Labarca, B. N. Cohen, N. Davidson, H. A. Lester, and G. Pilar. 1991. Pharmacological and kinetic properties of α4β2 neuronal nicotinic acetylcholine receptors expressed in *Xenopus* oocytes. *Journal of Physiology.* 450: 375-394.

Cohen, B. N., A. Figl, M. W. Quick, C. Labarca, N. Davidson, and H. A. Lester. 1995. Regions of β2 and β4 responsible for differences between the equilibrium dose-response relationships of the α3β2 and α3β4 neuronal nicotinic receptors. *Journal of General Physiology.* In press.

Doupnik, C. A., N. F. Lim, P. Kofuji, N. Davidson, and H. A. Lester. 1995. Intrinsic gating properties of a cloned G protein-activated inward rectifier $K^+$ channel. *Journal of General Physiology.* In press.

Figl, A., B. N. Cohen, M. W. Quick, N. Davidson, and H. A. Lester. 1992. Regions of β4•β2 subunit chimeras that contribute to the agonist selectivity of neuronal nicotinic receptors. *FEBS Letters.* 308: 245-248.

Figl, A., B. N. Cohen, J. Gollub, N. Davidson, and H. A. Lester. 1993. Novel functional domains of the rat neuronal nicotinic subunit. *Society for Neuroscience Abstracts.* 19: 8. (Abstr.)

Guastella, J. G., N. Nelson, H. Nelson, L. Czyzyk, S. Keynan, M. C. Miedel, N. Davidson, H. A. Lester, and B. Kanner. 1990. Cloning and expression of a rat brain GABA transporter. *Science.* 249: 1303-1306.

Higuchi, R. 1990. Recombinant PCR. *In* PCR protocols, a guide to methods and applications. M. A. Innis, D. H. Gelfand, J. J. Sninsky and T. J. White, editors. Academic Press, Inc., San Diego, CA. 177-184.

Ifune, C. K., and J. H. Steinbach. 1990a. Intracellular magnesium blocks outward current through neuronal nicotinic ACh receptor channels. *Biophysical Journal.* 57: 122a. (Abstr.)

Ifune, C. K., and J. H. Steinbach. 1990b. Rectification of acetylcholine-elicited currents in PC12 pheochromocytoma cells. *Proceedings of the National Academy of Sciences, USA.* 87: 4794-4798.

Ifune, C. K., and J. H. Steinbach. 1991. Voltage-dependent block by magnesium of neuronal nicotinic acetylcholine receptor channels in rat phaeochromocytoma cells. *Journal of Physiology.* 443: 683-701.

Ifune, C. K., and J. H. Steinbach. 1992. Inward rectification of acetylcholine-elicited currents in rat phaeochromocytoma cells. *Journal of Physiology.* 457: 143-165.

Labarca, C., M. W. Nowak, H. Zhang, L. Tang, P. Deshpande, and H. A. Lester. 1995. Conserved leucine residues in the M2 domain of nicotinic receptors govern gating independently and symmetrically. *Nature.* In Press.

Lester, H. A. 1992. The permeation pathway of neurotransmitter-gated ion channels. *Annual Review of Biophysics and Biomolecular Structure.* 21: 267-292.

Luetje, C. W., K. Wada, S. Rogers, S. N. Abramson, K. Tsuji, S. Heinemann, and J. Patrick. 1990. Neurotoxins distinguish between different neuronal nicotinic

acetylcholine receptor subunit combinations. *Journal of Neurochemistry.* 55: 632-640.

Luetje, C. W., and J. Patrick. 1991. Both α- and β-subunits contribute to the agonist sensitivity of neuronal acetylcholine receptors. *The Journal of Neuroscience.* 11: 837-845.

Magleby, K. L., and C. F. Stevens. 1972. The effect of voltage on the time course of end-plate currents. *Journal of Physiology.* 223: 151-171.

Neher, E., and B. Sakmann. 1975. Voltage-dependence of drug-induced conductance in frog neuromuscular junction. *Proceedings of the National Academy of Sciences, USA.* 72: 2140-2144.

Papke, R. L., J. Boulter, J. Patrick, and S. Heinemann. 1989. Single-channel currents of rat neuronal nicotinic acetylcholine receptors expressed in *Xenopus* oocytes. *Neuron.* 3: 589-596.

Papke, R. L., and S. F. Heinemann. 1991. The role of the $\beta_4$ subunit in determining the kinetic properties of rat neuronal nicotinic acetylcholine $\alpha_3$ receptors. *Journal of Physiology.* 440: 95-112.

Papke, R. L., R. M. Duvoisin, and S. F. Heinemann. 1993. The amino terminal half of the nicotinic-subunit extracellular domain regulates the kinetics of inhibition by neuronal bungarotoxin. *Proceedings of the Royal Society of London B.* 252: 141-148.

Papke, R. L. 1993. The kinetic properties of neuronal nicotinic receptors: genetic basis of functional diversity. *Progress in Neurobiology.* 41: 509-551.

Quick, M. W., and H. A. Lester. 1994. Methods for expression of excitability proteins in *Xenopus* oocytes. *In* Ion Channels of Excitable Cells. P. M. Conn, editor. Academic Press, San Diego, CA. 261-279.

Revah, F., D. Bertrand, J.-L. Galzi, A. Devillers-Thiery, C. Mulle, N. Hussy, S. Bertrand, M. Ballivet, and J.-P. Changeux. 1991. Mutations in the channel domain alter desensitization of a neuronal nicotinic receptor. *Nature.* 353: 846-849.

Role, L. W. 1992. Diversity in primary structure and function of neuronal nicotinic acetylcholine receptor channels. *Current Opinion in Neurobiology.* 2: 254-262.

Sands, S. B., and M. E. Barish. 1992. Neuronal nicotinic acetylcholine receptor currents in phaeochromocytoma (PC12) cells: Dual mechanisms of rectification. *Journal of Physiology.* 447: 467-487.

Sargent, P. B. 1993. The diversity of neuronal nicotinic acetylcholine receptors. *Annual Review of Neuroscience.* 16: 403:443.

Sheridan, R. E., and H. A. Lester. 1975. Relaxation measurements on the acetylcholine receptor. *Proceedings of the National Academy of Sciences, USA.* 72: 3496-3500.

Sheridan, R. E., and H. A. Lester. 1977. Rates and equilibria at the acetylcholine receptor of *Electrophorus* electroplaques. A study of neurally evoked postsynaptic currents and of voltage-jump relaxations. *Journal of General Physiology.* 70: 187-219.

Silver, M. R., and T. E. DeCoursey. 1990. Intrinsic gating of inward rectifier in bovine pulmonary artery endothelial cells in the presence or absence of internal $Mg^{2+}$. *Journal of General Physiology.* 103: 109-133.

Unwin, N. 1995. Acetylcholine receptor channel imaged in the open state. *Nature.* 373: 37-43.

Vernino, S., M. Amador, C. W. Luetje, J. Patrick, and J. A. Dani. 1992. Calcium modulation and high calcium permeability of neuronal nicotinic acetylcholine receptors. *Neuron.* 8: 127-134.

Wong, E. T., S. Mennerick, D. B. Clifford, C. F. Zorumski, and K. E. Isenberg. 1993. Expression of a recombinant neuronal nicotinic acetylcholine receptor in transfected HEK-293 cells. *Society for Neuroscience Abstracts.* 19: 291. (Abstr.)

Zingsheim, H. P., D. C. Neugebauer, J. Frank, W. Hanicke, and F. J. Barrantes. 1982. Dimeric arrangement and structure of the membrane-bound acetylcholine receptor studied by electron microscopy. *EMBO Journal.* 1: 541-547.

Figure 1. Voltage-jump relaxations for the α3β2 (left column) and α3β4 (right column) receptors expressed in oocytes at [ACh] = 1 μM. (*A*) Voltage-clamp currents. The membrane potential was held at -50 mV, jumped to a prepulse value of +50 mV for 30 ms or 80 ms (α3β2 or α3β4, respectively), then jumped to various test potentials in the range between -150 and -50 mV in 20 mV increments for 200 ms or 800 ms (α3β2 or α3β4, respectively). Agonist-induced currents have been isolated by subtracting episodes in the absence of ACh. (*B*) Single and double exponential fits to the traces at -150 mV. The fit to a single exponential clearly deviates from the data; the fit to two exponentials superimposes on the data. For α3β2, $\tau_f$ = 16 ms; $\tau_s$ = 75 ms. For α3β4, $\tau_f$ = 108 ms; $\tau_s$ = 340 ms. (*C*) Instantaneous current-voltage relations for the traces in panel (*A*), obtained by extrapolating the double-exponential fits to the time of the jump to yield $I_{inst}$. (*D*) Voltage dependence of the steady-state values, expressed as $I_{ss}/I_{inst}$.

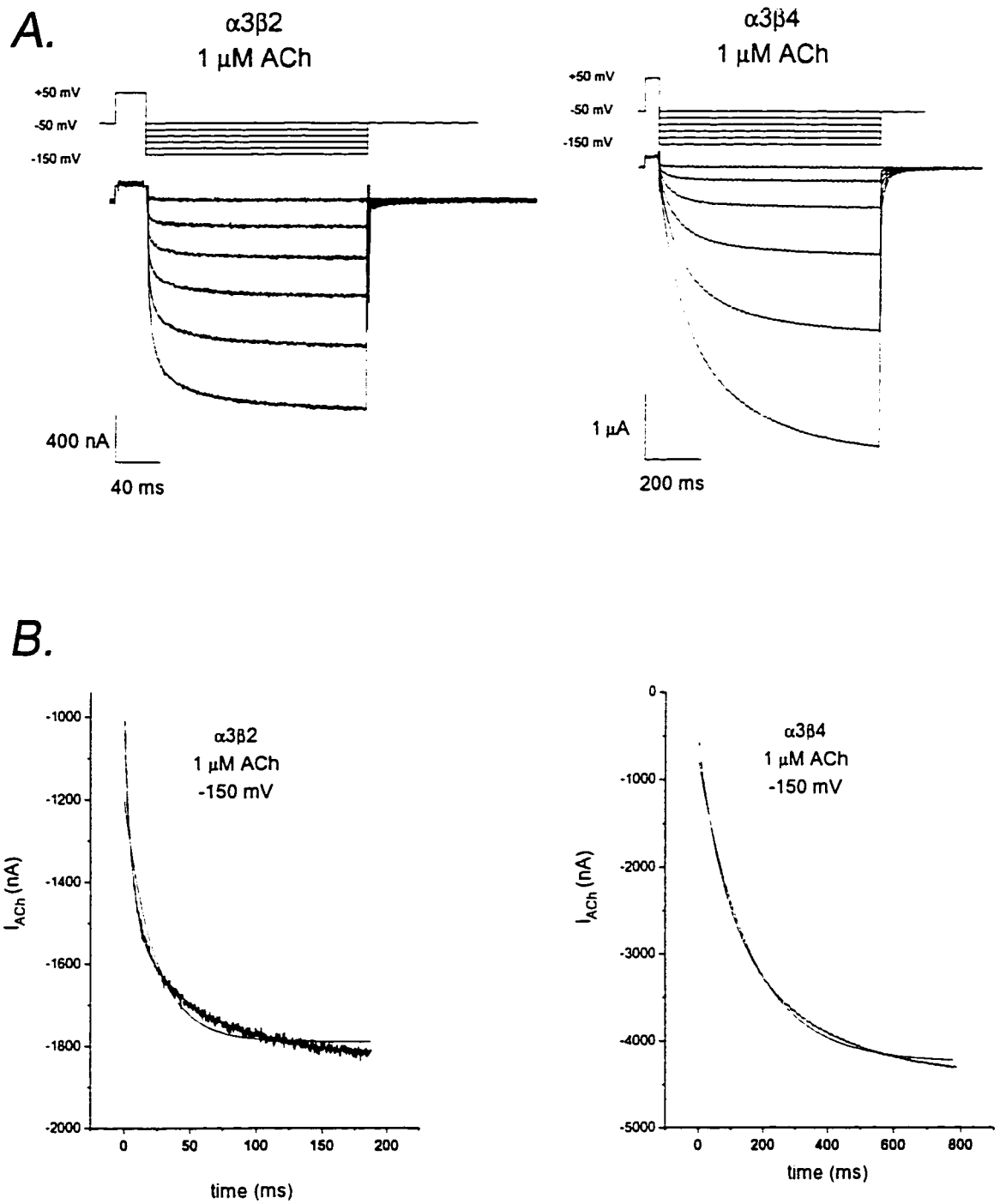
A.
α3β2
1 μM ACh
+50 mV
-50 mV
-150 mV
400 nA
40 ms
α3β4
1 μM ACh
+50 mV
-50 mV
-150 mV
1 μA
200 ms
B.
α3β2
1 μM ACh
-150 mV
I_ACh (nA)
-1000
-1200
-1400
-1600
-1800
-2000
0
50
100
150
200
time (ms)
α3β4
1 μM ACh
-150 mV
I_ACh (nA)
0
-1000
-2000
-3000
-4000
-5000
0
200
400
600
800
time (ms)

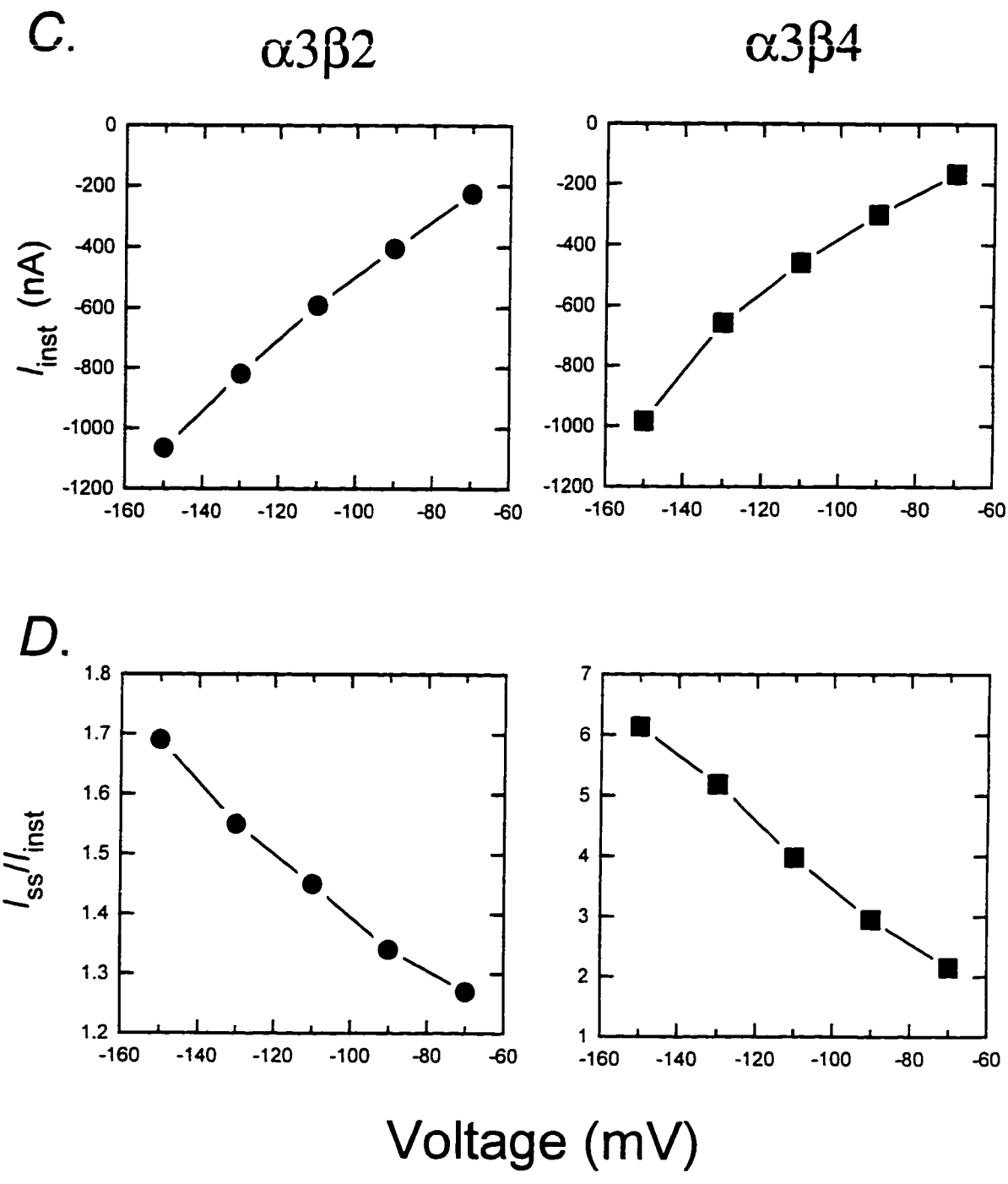
C.
α3β2
α3β4
$I_{inst}$ (nA)
0
-200
-400
-600
-800
-1000
-1200
-160
-140
-120
-100
-80
-60
D.
$I_{ss}/I_{inst}$
1.8
1.7
1.6
1.5
1.4
1.3
1.2
7
6
5
4
3
2
1
Voltage (mV)

Figure 2. Voltage dependence of the relaxation rate constants at [ACh] = 1 μM. Left column, α3β2 receptor; right column, α3β4 receptor. (*A*) Fast rate constants. (*B*) Slow rate constants. Data are mean ± SD, n = 1 to 10 oocytes. Lines represent linear regression fits through the data points.

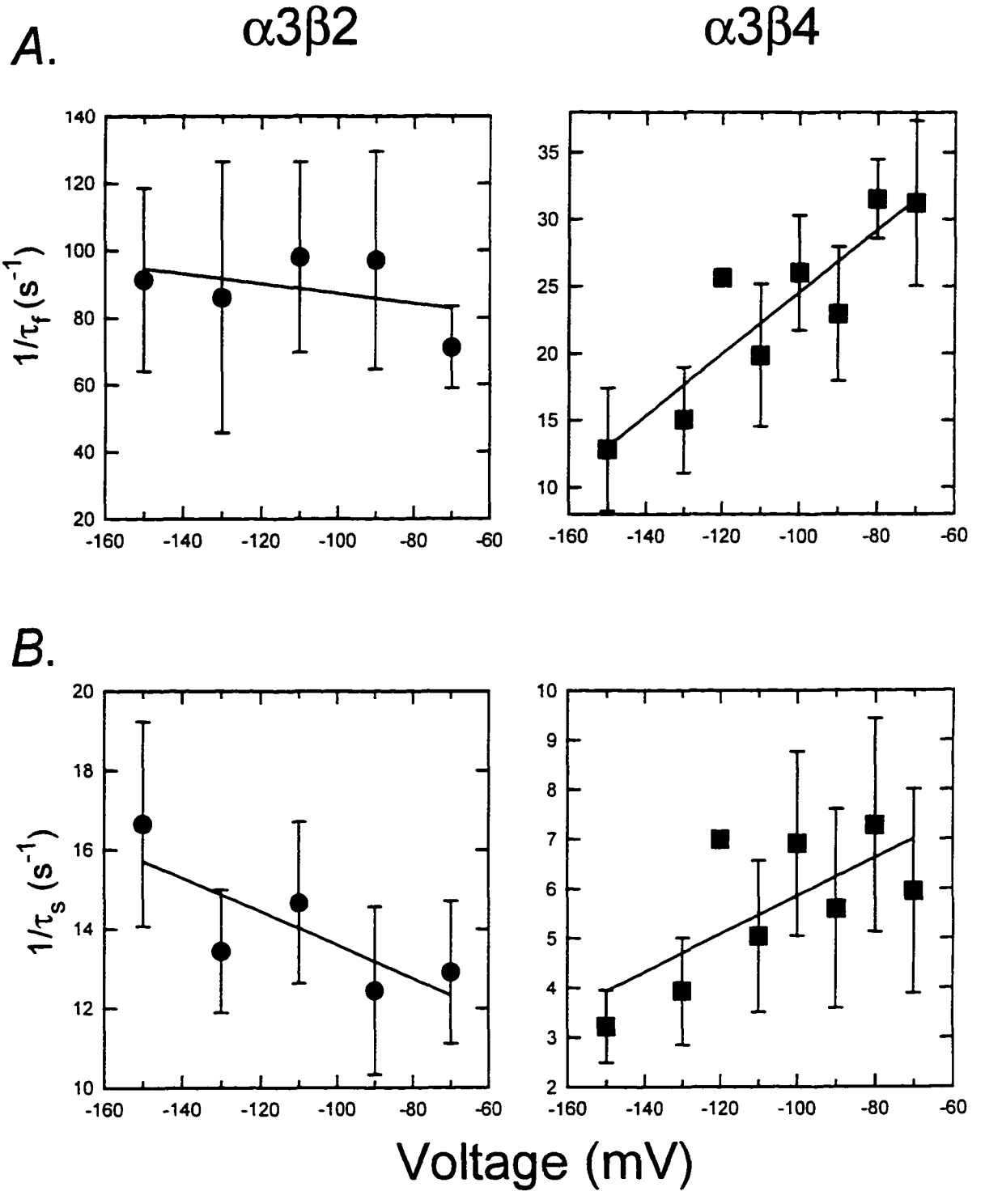
A.
α3β2
α3β4
1/τf (s-1)
B.
1/τs (s-1)
Voltage (mV)

Figure 3. Availability of receptors during depolarizing prepulses. (*A*) α3β2 receptors. Membrane potential was held at -50 mV and stepped to various values between +10 and -120 mV for 400 ms, then to the test potential of -130 mV for 400 ms. Data have been multiplied by scaling factors of 1.0 to 1.12 to correct for desensitization during the trial. The line preceding the prepulses denotes the zero current level. (*B*) α3β4 receptors. The prepulse and test potential durations were both 2 s. (*C*) Average data with this protocol. The waveforms were fit to two exponentials, then extrapolated to the time of the jump to measure the instantaneous current. This instantaneous value, normalized to the steady-state value to account for desensitization and varying expression levels, is plotted versus prepulse potential. Points show mean ± SD, n = 10-14. Boltzmann relations (Eq. 2) are superimposed on the data.

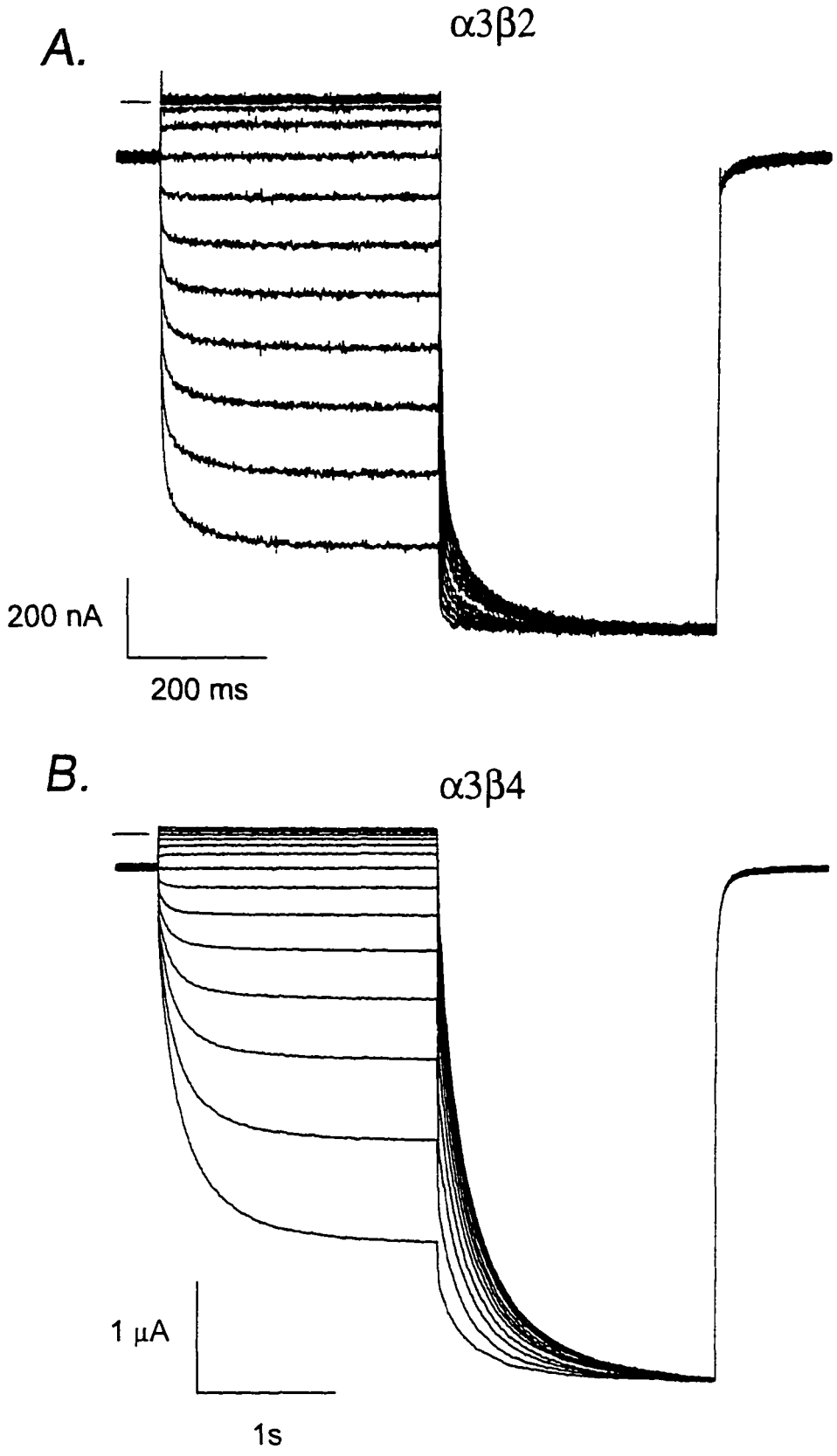
A.
α3β2
200 nA
200 ms
B.
α3β4
1 μA
1s

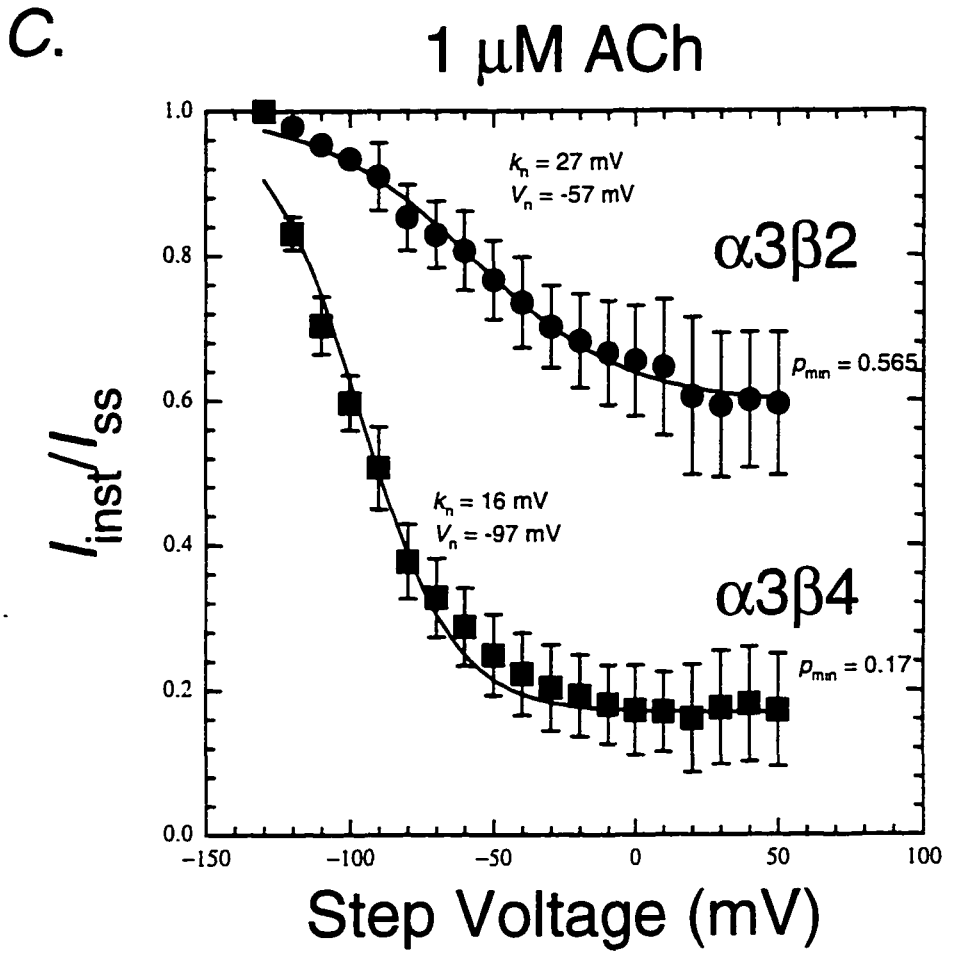
C.
1 μM ACh
$k_n$ = 27 mV
$V_n$ = -57 mV
α3β2
$p_{min}$ = 0.565
$k_n$ = 16 mV
$V_n$ = -97 mV
α3β4
$p_{min}$ = 0.17
$I_{inst}/I_{ss}$
1.0
0.8
0.6
0.4
0.2
0.0
−150
−100
−50
0
50
100
Step Voltage (mV)

Figure 4. Concentration dependence of the voltage-jump kinetics. Data were acquired and analyzed as in Fig. 1 and pooled across all potentials between -50 and -150 mV. The solid lines show $EC_{50}$ values of 2.3 μM and 3.1 μM for the fast and slow components of the α3β2 receptor; 67 μM and 58 μM for the fast and slow components of the α3β4 receptor; and $n_{app}$ values of 1.7 for both components of the α3β2 relaxations and 0.8 for both components of the α3β4 relaxations. (*A*) Fast phase of the relaxations, $1/\tau_f$. (*B*) Slow phase, $1/\tau_s$. (*C*) and (*D*) Fractional contribution of the fast phase expressed as $I_{fast}/I_{tot}$. Points show mean ± SD. n = 2 to 10 oocytes for each point.

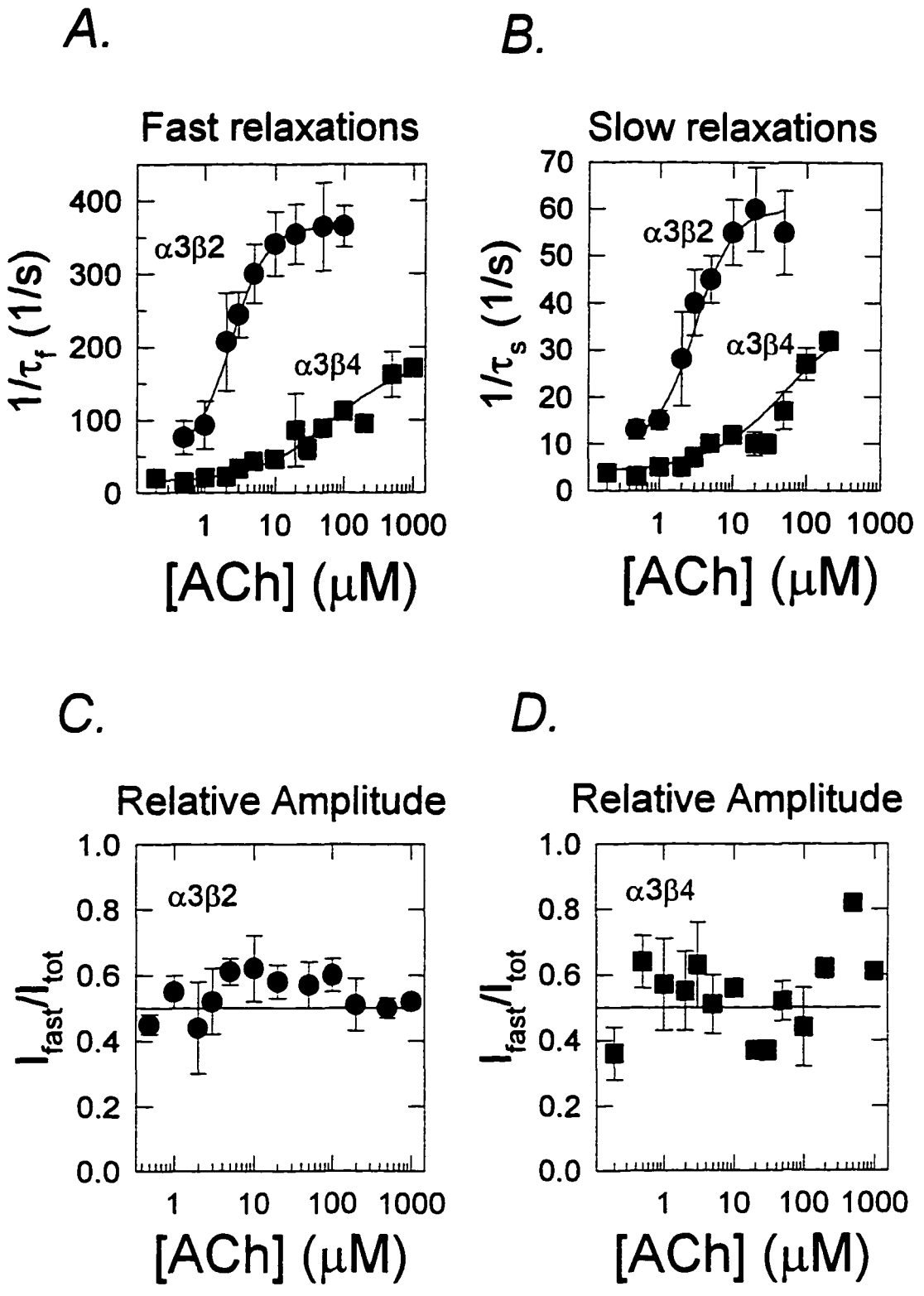
A.
Fast relaxations
1/τf (1/s)
400
300
200
100
0
α3β2
α3β4
1
10
100
1000
[ACh] (μM)
B.
Slow relaxations
1/τs (1/s)
70
60
50
40
30
20
10
0
α3β2
α3β4
1
10
100
1000
[ACh] (μM)
C.
Relative Amplitude
Ifast/Itot
1.0
0.8
0.6
0.4
0.2
0.0
α3β2
1
10
100
1000
[ACh] (μM)
D.
Relative Amplitude
Ifast/Itot
1.0
0.8
0.6
0.4
0.2
0.0
α3β4
1
10
100
1000
[ACh] (μM)

Figure 5. Sequence alignment of neuronal nicotinic β2 and β4 subunits. The putative transmembrane regions M1-M4 are underlined. The arrows indicate the transition point of the β4 $NH_2$-terminal chimeras. The residue preceding the arrow is the last amino acid included from β4. Note the single difference in the M2 transmembrane segments.

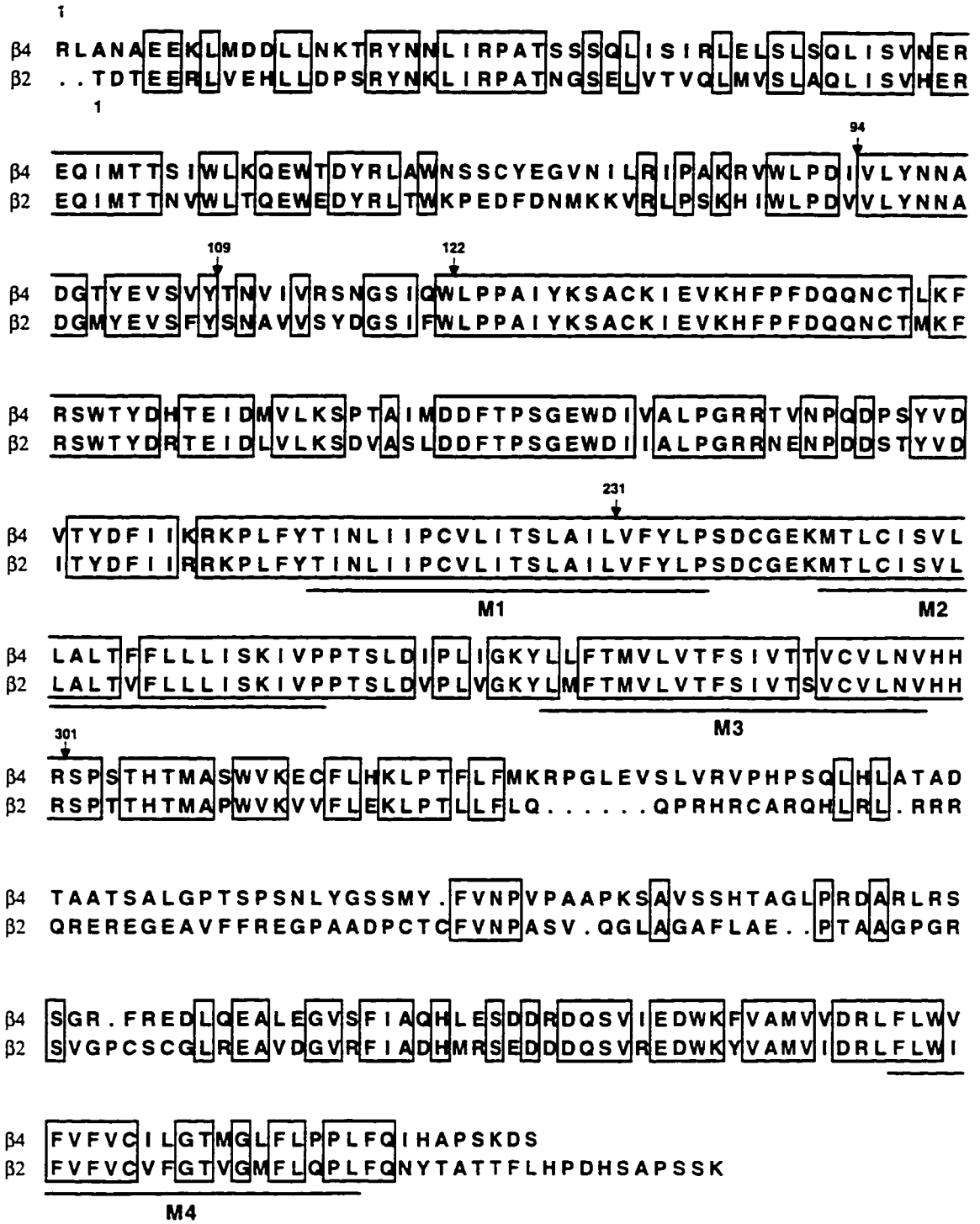
1
β4 RLANAEEKLMDDLLNKTRYNNLIRPATSSSQLISIRLELSLSQLISVNER
β2 ..TDTEERLVEHLLDPSRYNKLIRPATNGSELVTVQLMVSLAQLISVHER
1
94
β4 EQIMTTSIWLKQEWTDYRLAWNSSCYEGVNILRIPAKRVWLPDIVLYNNA
β2 EQIMTTNVWLTQEWEDYRLTWKPEDFDNMKKVRLPSKHIWLPDVVLYNNA
109
122
β4 DGTYEVSVYTNVIVRSNGSIQWLPPAIYKSACKIEVKHFPFDQQNCTLKF
β2 DGMYEVSFYSNAVVSYDGSIFWLPPAIYKSACKIEVKHFPFDQQNCTMKF
β4 RSWTYDHTEIDMVLKSPTAIMDDFTPSGEWDIVALPGRRTVNPQDPSYVD
β2 RSWTYDRTEIDLVLKSDVASLDDFTPSGEWDIIALPGRRNENPDDSTYVD
231
β4 VTYDFIIKRKPLFYTINLIIPCVLITSLAILVFYLPSDCGEKMTLCISVL
β2 ITYDFIIRRKPLFYTINLIIPCVLITSLAILVFYLPSDCGEKMTLCISVL
M1
M2
β4 LALTFFLLLISKIVPPTSLDIPLIGKYLLFTMVLVTFSIVTTVCVLNVHH
β2 LALTVFLLLISKIVPPTSLDVPLVGKYLMFTMVLVTFSIVTSVCVLNVHH
M3
301
β4 RSPSTHTMASWVKECFLHKLPTFLFMKRPGLEVSLVRVPHPSQLHLATAD
β2 RSPTTHTMAPWVKVVFLEKLPTLLFLQ.....QPRHRCARQHLRL.RRR
β4 TAATSALGPTSPSNLYGSSMY.FVNPVPAAPKSAVSSHTAGLPRDARLRS
β2 QREREGEAVFFREGPAADPCTCFVNPASV.QGLAGAFLAE..PTAAGPGR
β4 SGR.FREDLQEALEGVSFIAQHLESDDRDQSVIEDWKFVAMVVDRLFLWV
β2 SVGPCSCGLREAVDGVRFIADHMRSEDDDQSVREDWKYVAMVIDRLFLWI
β4 FVFVCILGTMGLFLPPLFQIHAPSKDS
β2 FVFVCVFGTVGMFLQPLFQNYTATTFLHPDHSAPSSK
M4

Figure 6. Kinetic data for a series of chimeric β subunits. (*A*) Fast and (*B*) Slow voltage-jump relaxations, analyzed and presented as for the wild-type receptors (Fig. 4). The dose-response relations for the wild type α3β2 receptor are superimposed on the data as solid lines (mean) and dashed lines (± SD) n = 2 to 10 oocytes per point for the chimeras. (*C*) and (*D*) Subtracted and normalized data, as described in the text. Solid lines are fitted dose-response relations for the individual receptors; dashed lines are fitted data for α3β2 and α3β4 wild-type receptors. Legend in (*A*) applies to all panels.

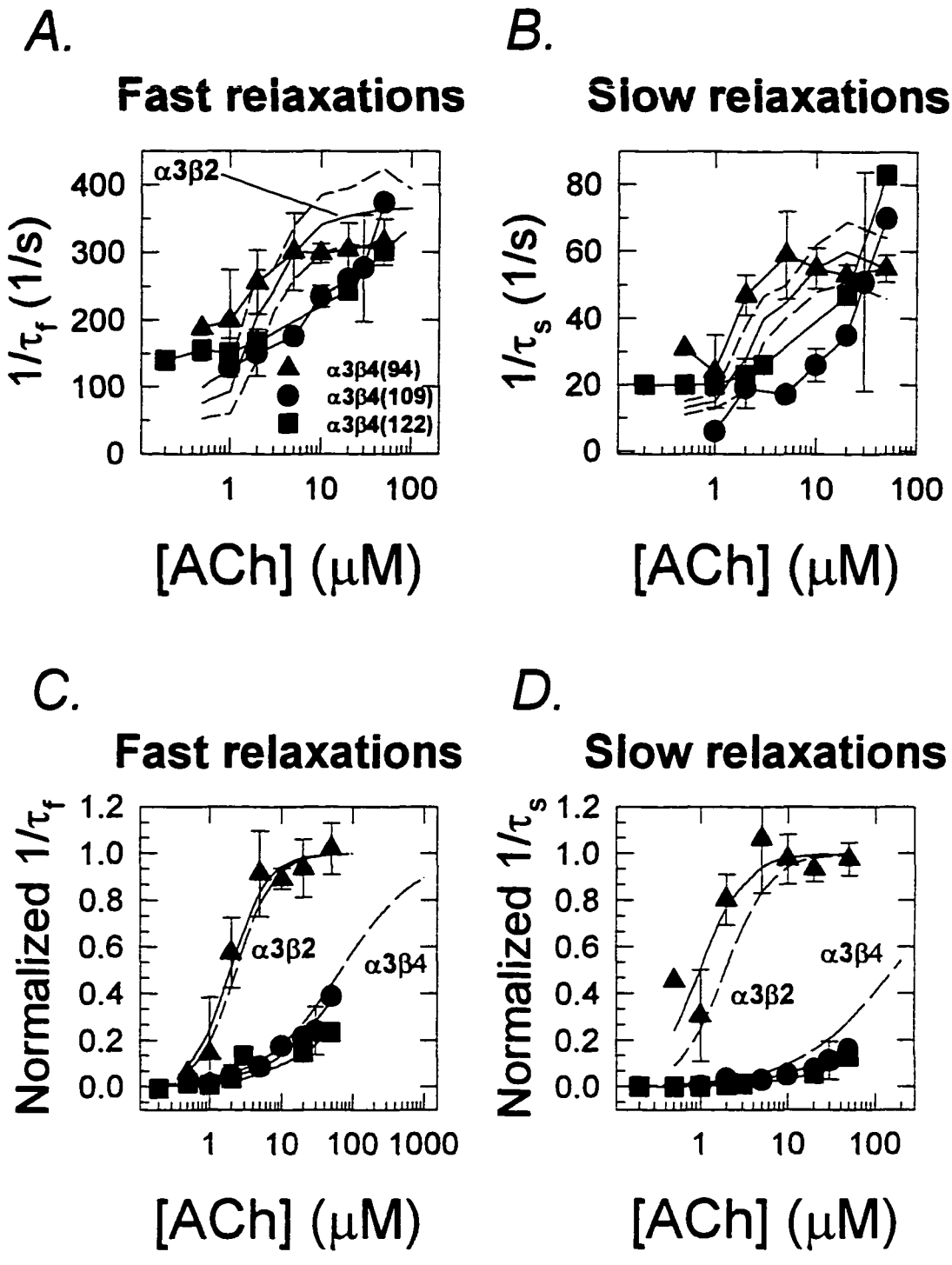
A.
Fast relaxations
α3β2
α3β4(94)
α3β4(109)
α3β4(122)
1/τf (1/s)
400
300
200
100
0
1
10
100
[ACh] (μM)
B.
Slow relaxations
1/τs (1/s)
80
60
40
20
0
1
10
100
[ACh] (μM)
C.
Fast relaxations
Normalized 1/τf
1.2
1.0
0.8
0.6
0.4
0.2
0.0
α3β2
α3β4
1
10
100
1000
[ACh] (μM)
D.
Slow relaxations
Normalized 1/τs
1.2
1.0
0.8
0.6
0.4
0.2
0.0
α3β4
α3β2
1
10
100
[ACh] (μM)

Figure 7. Voltage dependence for several chimeric β4/β2 receptors, as well as for the wild-type β4 and β2 subunits, expressed with the α3 subunit. Analyses as in the experiment of Fig. 1. Data have been pooled from concentrations ranging from 1 to 3 μM ACh. Data are averages of 2 to 10 cells per point. SEM's are shown where they exceed the size of the symbols.

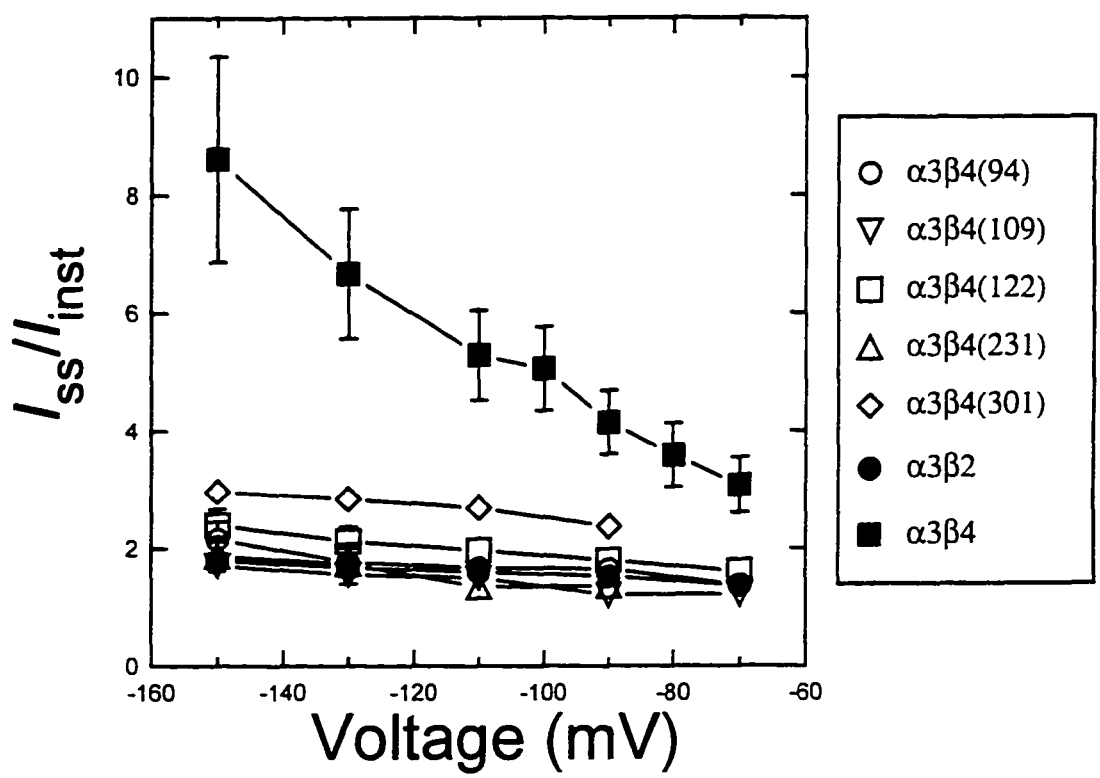
$I_{ss}/I_{inst}$
10
8
6
4
2
0
-160
-140
-120
-100
-80
-60
Voltage (mV)
α3β4(94)
α3β4(109)
α3β4(122)
α3β4(231)
α3β4(301)
α3β2
α3β4

Figure 8. Voltage-jump relaxations for α4β4 receptors. Rate constants are plotted versus [ACh], as in Fig. 4. (*A*) Exemplar traces of α3β4 relaxations at 2 μM ACh. After a 50 ms prepulse at +50 mV, a series of six 400 ms test pulses were applied between -120 and -70 mV in 10 mV increments. The line preceding the prepulse denotes the zero current level. (*B*) Traces for α3β4 relaxations at 2 μM ACh. After a 50 ms prepulse at +50 mV, the voltages were stepped as in panel (*A*) for 800 ms. Note the difference in horizontal calibration. (*C*) and (*D*) Concentration dependence of the fast and slow relaxation components of α4β4 receptors. Points show mean ± SD (n = 3 to 6 cells). The data are superimposed on the solid lines and dashed lines summarizing the dose-response relation for α3β2 receptors (mean and ± SD, respectively).

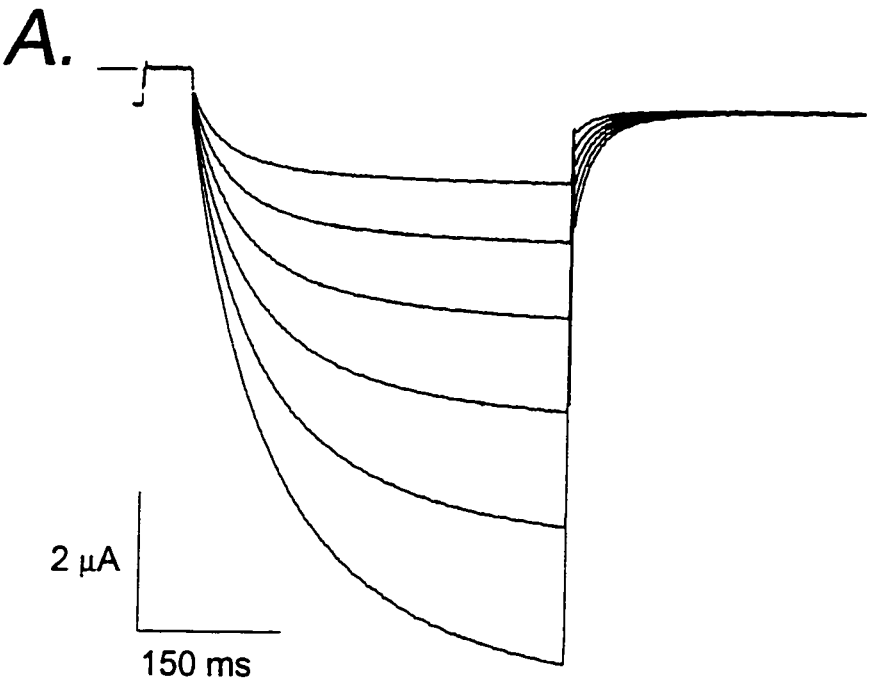


α4β4

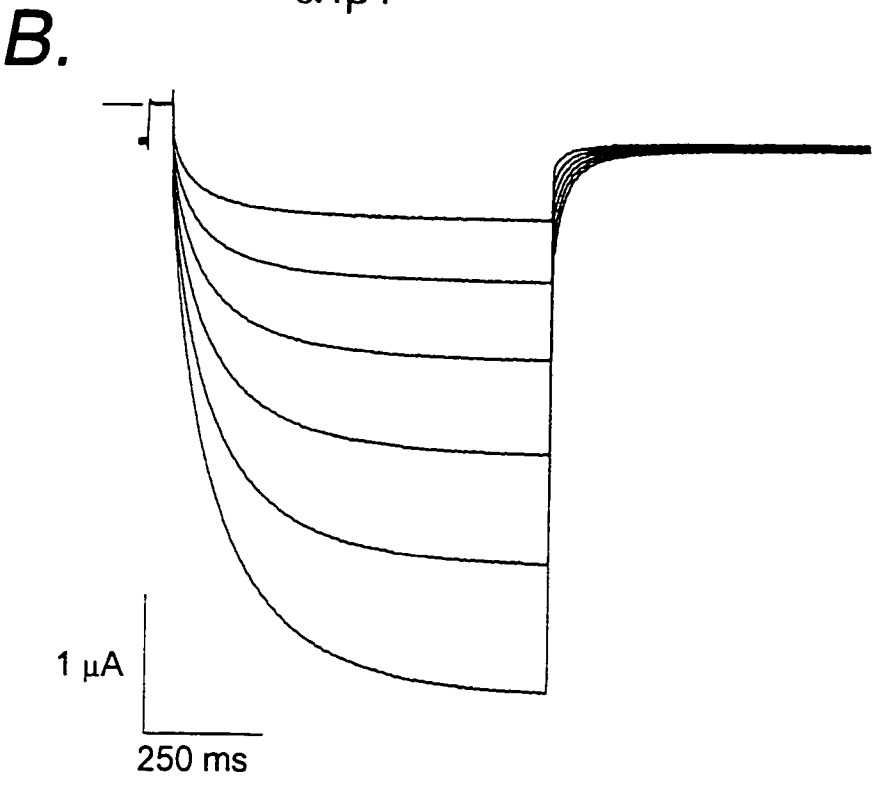

Figure 8 (part II)

C.

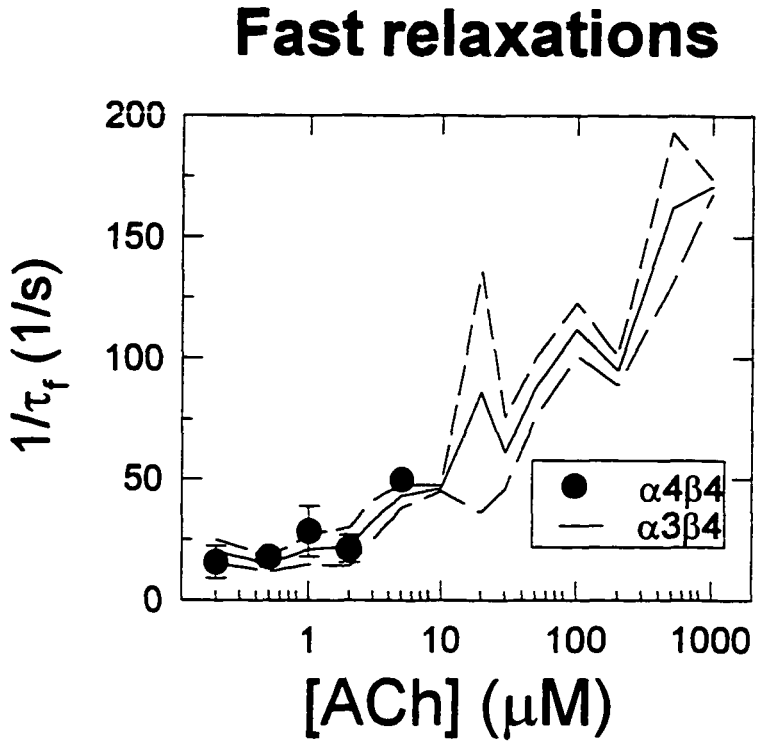


D.